DEPARTMENT OF INNOVATION IN BIOLOGY, AGRI-FOOD AND FOREST SYSTEMS - DIBAF

University of Tuscia

Via S. Camillo de Lellis ,01100 Viterbo

PhD in Sciences, Technologies and Biotechnologies for Sustainability – Curriculum: Food

XXXV cycle

PhD DISSERTATION

Academic Discipline

AGR/09 – Agricultural Machinery and Mechanization

"Use of non-destructive analysis techniques for the technological and chemical-physical characterization of fruit and vegetables and for monitoring of the drying process"

Tutor:
Prof. Roberto Moscetti

PhD Candidate:
M.Sc. Giacomo Bedini

PhD Coordinator:
Prof. Andrea Vannini

ACADEMIC YEAR 2022/2023

Acknowledgments

First of all, I want to sincerely thank my tutor Prof. Roberto Moscetti for giving me this precious opportunity and for his constant support and trust during all phases of my PhD. He inspired this work and teaching me every possible topic useful for my research activity.
I would like to thank Prof. Riccardo Massantini for his valuable tips and advice. He was a true point of reference, especially in terms of his humanity.
I am happy that I had the opportunity of working with these two Professors. These years have been crucial to my professional and especially personal growth. We spent also a lot of friendly moments building a great relationship and supporting each other.

Thanks to Mrs. Grazia Franco, PhD. Alessio Cimini and all the people who work and collaborate with the post-harvest laboratory of DIBAF for their availability and support.

I am grateful to C.C.OR.A.V. (Consorzio Cooperativo ORtofrutticolo Alto Viterbese), Cooperativa Centro Agricolo Alto Viterbese, and CO.P.A.VIT. (Consorzio Patata Alto Viterbese) for cofounding my scholarship, also providing me the samples, technical assistance and support.

Sincerely thanks to PhD Pietro Ibba and Prof. Luisa Petti and their all research group for hosting me at Free University of Bolzano. It has been a great occasion to meet a friend (Pietro), to know good people and to broaden my horizons from a research point of view.

Thanks to my colleagues Swathi Sirisha Nallan Chakravartula, Andrea Bandiera and Marco Nardella. We shared a lot of good moments and we worked a lot as a group, supporting and helping each other.

Thanks to my English teacher, Ms. Lesley Bowles. Her work has been crucial for learning and improving my English.

Thanks to my wonderful family, Mom, Dad, Brother, grandmothers and Alessia for their continuous support and trust. Thank you also to Gianni, Claudia, Elisa, Andrea, and little Ettore, the other great family that has become a part of my life.

Last but not least, a special thanks to my better half Ilaria. She is the most important person in my life, supporting and motivating me in every moment. It has been a long journey, but we accomplished it!

Ringraziamenti

Innanzitutto, desidero ringraziare sinceramente il mio tutor, il Prof. Roberto Moscetti, per avermi dato questa preziosa opportunità, per la fiducia e per il suo costante sostegno durante tutte le fasi del mio dottorato. È lui che ha ispirato questo lavoro e mi ha insegnato ogni possibile argomento utile per la mia attività di ricerca.
Desidero ringraziare il Prof. Riccardo Massantini per i suoi preziosi consigli e suggerimenti. È stato un vero punto di riferimento, soprattutto dal lato umano. Riesce sempre a toccare le corde giuste e i suoi consigli di vita sono sempre preziosi.
Sono felice di aver avuto l'opportunità di lavorare con questi due professori. Questi anni sono stati fondamentali per la mia crescita professionale e soprattutto personale. Abbiamo trascorso anche molti momenti di amicizia, costruendo un ottimo rapporto e sostenendoci a vicenda in questi anni non facili.

Grazie alla Sig.ra Grazia Franco, al Dott. Alessio Cimini e tutte le persone che lavorano e collaborano con il laboratorio di post-raccolta del DIBAF per la loro disponibilità e il loro supporto.

Sono grato al C.C.OR.A.V. (Consorzio Cooperativo ORtofrutticolo Alto Viterbese), alla Cooperativa Centro Agricolo Alto Viterbese e al CO.P.A.VIT. (Consorzio Patata Alto Viterbese) per aver cofinanziato la mia borsa di studio. Ringrazio soprattutto gli agronomi, i tecnici e gli operatori che hanno contribuito in maniera importante a questa tesi fornendomi i campioni, l'assistenza tecnica ed il supporto.

Un sincero ringraziamento al Dott. Pietro Ibba e alla Prof.ssa Luisa Petti e a tutto il loro gruppo di ricerca per avermi ospitato presso la Libera Università di Bolzano. È stata una grande occasione per incontrare un amico (Pietro), conoscere tante altre brave persone e ampliare i miei orizzonti dal punto di vista della ricerca.

Grazie ai miei colleghi Swathi Sirisha Nallan Chakravartula, Andrea Bandiera e Marco Nardella. Abbiamo condiviso molti bei momenti e abbiamo lavorato molto come gruppo, sostenendoci e aiutandoci sempre a vicenda.

Grazie alla mia insegnante di inglese, la signora Lesley Bowles. Il suo lavoro è stato fondamentale per migliorare il mio inglese.

Grazie alla mia meravigliosa famiglia, mamma, papà, fratello e nonna per il loro continuo sostegno e la loro fiducia. Grazie anche a Giovanni, Claudia, Elisa, Andrea ed il piccolo Ettore, l’altra splendida famiglia che è entrata a far parte della mia vita.

Infine, un ringraziamento speciale alla mia dolce metà Ilaria. È la persona più importante della mia vita, che mi sostiene e mi motiva in ogni momento. È stato un lungo viaggio, ma ce l'abbiamo fatta!

Abstract

Due to the increasing consumer knowledge, awareness and attention to food-quality and safety, farmers, processing industries and sellers of fruit and vegetables sector must ensure high standards, studying and monitoring many aspects from the farm to the shelf.

Nowadays, potato (*Solanum tuberosum* L.) ranks fourth as the most important crop in the world. In Italy, the Lazio region is the 6th largest producer. Approximately 70 % of the potato production of this region is grown in the north of Lazio. In this area, potato is a typical crop that is very important for the local economy. In fact, since 2014, the potato supply chain of this area has held the quality designation PGI ("Patata dell'Alto Viterbese PGI") from the European Community. In this context, potatoes are sold as a (i) fresh and raw product or as (ii) fresh-cut products in several format (slice, stick, cube, etc.). About 20 potato varieties are cultivated in this area and each of them is characterized by specific pre- (water demand, yield, resistance to disease, etc.) and post-harvest attributes (storability, dormancy, physico-chemical characteristics, etc.). In particular for post-harvest, physico-chemical characterization of potato cultivars is a crucial aspect of accurate varietal selection, identifying and selecting varieties for a specific destination of use. Moreover, considering that some important quality parameters significantly change during storage, monitoring the physico-chemical composition of tubers along months of storage is crucial to always offer the consumer a high-quality product and to avoid food losses. In this perspective, the development of novel fast, reliable, cost-effective and portable technologies (e.g., near infrared spectroscopy, NIR) is extremely important to provide operators of a solution and an end-user-friendly protocol for in situ multi-parametric analysis of potatoes. In addition, the Process Analytical Technologies (PATs) that involve the use of tools (e.g., computer vision and near infrared spectroscopy) and practices as for both real-time monitoring of food quality and dynamic control of product processing, are really promising for food sector.

The PhD thesis aimed to innovate the potato sector, with specific regards to the "Patata dell'Alto Viterbese PGI" consortiums (Viterbo, Italy), by developing solutions to improve its competitiveness at regional and national level. The doctoral study was divided in three research activity, identifying several counteracts to solve specific issues concerning local consortiums.

The first activity focused on physico-chemical and enzymatic characterization of four pre-selected potato cultivars. This activity aimed (i) to select the best potato cultivars for fresh-cut processing, increasing the shelf-life of final product, and (ii) to make a contingency table linking

storage status and optimal final use of the tubers allowing operators to schedule both production and sale. For this intended purpose the main physico-chemical and enzymatic attributes of four pre-selected potato cultivars (i.e., Constance, Fontane, Gaudi and Jelly) were analyzed at the harvest and every month for 6 months of storage. The analyses were performed for two production seasons (i.e., 2020 and 2021). The results revealed the best properties of Fontane for processing (especially for frying) followed by Jelly that showed good qualities for both domestic use and processing, especially for fresh-cut potato.

The second activity involved drying tests to evaluate the implementation of Process Analytical Technology (PAT) tools i.e., load cell and computer vision system in a cabinet dryer for drying of carrot and potato slices. Regarding potato drying, the cultivar selected during activity 1 (i.e., Fontane) was used for semi-drying test (i.e., up to 1.5 of dry basis moisture content). Several pre-treatments were pre-tested and two of them (i.e., dipping in citric acid and sodium metabisulphite solution, 3 % and 0.1 % w/v, respectively) were retained for semi-drying tests. For both tested products, the CV system and load cell were selected as in-line Process Analytical Technology tools within a proactive Quality-by-Design framework and embedded for, i) monitoring of product features (i.e., weight, color, and size); and ii) developing shrinkage-dependent moisture prediction models using linear regression. The evaluated shrinkage-dependent linear models showed superior performances benchmarked against selected thin-layer models of increasing complexity. The best models reported a Root Mean Square Error (RMSE) equal to 0.005-0.007 and this represents an interesting result because by predicting the residual moisture content, it's possible to stop the drying process at the optimal time, avoiding quality deterioration and reducing energy consumption.

Finally, the third activity concerned the development of NIR-based predictive model for the determination of an important quality parameter for potato such as dry matter (DM) content. The NIR-based DM prediction was evaluated for each different potato tissues: i) periderm, ii) cortex, iii) outer medulla and iv) inner medulla of 17 different cultivars sampled during three production seasons (i.e., 2020, 2021 and 2022). The DM prediction models developed using standard chemometrics approaches (i.e., partial least squares, PLS; and interval-PLS, iPLS) showed that among the evaluated tissues, the inner medulla was the most suitable reporting a RMSE and coefficient of determination (R^2) in prediction close to 1 % and 0.90, respectively. This information can be used to develop more advanced systems inclusive of portable tools and advanced technologies for in situ evaluation to support operators and ensure better pre- and post-harvest management of potatoes.

Keywords

Solanum tuberosum L., post-harvest storage, quality attributes, near-infrared spectroscopy, chemometrics, predictive models, Quality-by-Design

Sommario

La crescente conoscenza, consapevolezza e attenzione dei consumatori nei confronti della qualità e della sicurezza degli alimenti, obbliga agricoltori, industrie di trasformazione e venditori del settore ortofrutticolo a garantire standard elevati, analizzando e monitorando numerosi aspetti, dal campo agli scaffali di supermercati e negozi.

Oggi la patata (*Solanum tuberosum* L.) è al quarto posto tra le colture più importanti al mondo. In Italia, la regione Lazio è il sesto produttore e circa il 70% della produzione di patate di questa regione è coltivata nella zona settentrionale che comprende i comuni a nord del Lago di Bolsena. In questa zona, la patata è una coltura tipica molto importante per l'economia locale. Dal 2014, infatti, la filiera della patata di questa zona ha ottenuto la denominazione di qualità IGP dalla Comunità Europea ("Patata dell'Alto Viterbese IGP"). In questo contesto, le patate vengono commercializzate come (i) prodotto fresco o come (ii) prodotto di IV gamma di diversi formati (fetta, bastoncino, cubetto, ecc.). In quest'area si coltivano circa 20 varietà di patate, ognuna delle quali è caratterizzata da specifiche caratteristiche pre- (fabbisogno idrico, resa, resistenza alle malattie, ecc.) e post-raccolta (conservabilità, dormienza, caratteristiche fisico-chimiche, ecc.). In particolare, per quanto riguarda la post-raccolta, la caratterizzazione fisico-chimica delle cultivar di patata è un aspetto cruciale per un'accurata selezione varietale e nello specifico per identificare e selezionare le varietà per una determinata destinazione d'uso. Inoltre, considerando che alcuni importanti parametri qualitativi cambiano significativamente durante la conservazione, il monitoraggio della composizione fisico-chimica dei tuberi durante i mesi di stoccaggio è fondamentale per offrire sempre al consumatore un prodotto di alta qualità ed evitare perdite di prodotto lungo la filiera. In questa prospettiva, lo sviluppo di nuove tecnologie veloci, affidabili, economiche e portatili (ad esempio, la spettroscopia nel vicino infrarosso) è estremamente importante per fornire agli operatori una soluzione e un protocollo di facile utilizzo per un'analisi multi-parametrica in situ delle patate. Inoltre, le tecnologie analitiche di processo (Process Analytical Technologies, PAT), che prevedono l'uso di strumenti (ad esempio, la visione artificiale e la spettroscopia nel vicino infrarosso) e pratiche per il monitoraggio in tempo reale della qualità degli alimenti e per il controllo dinamico della lavorazione dei prodotti, sembrano essere davvero promettenti per il settore alimentare.

La presente tesi di dottorato si proponeva di innovare il settore della patata, con particolare riguardo ai consorzi e cooperative della "Patata dell'Alto Viterbese IGP" (Viterbo, Italia), sviluppando soluzioni per migliorarne la competitività a livello regionale e nazionale. Lo studio

di dottorato si è articolato in tre attività di ricerca, individuando diverse soluzioni per risolvere problematiche specifiche dei consorzi locali.

La prima attività si è concentrata sulla caratterizzazione fisico-chimica ed enzimatica di quattro cultivar di patata preselezionate. L'obiettivo è stato quello di selezionare le migliori cultivar di patata per la trasformazione in prodotto di IV gamma, aumentando la shelf-life del prodotto finale e soddisfare così le esigenze della Grande Distribuzione Organizzata (GDO). Il secondo obiettivo, ma non per importanza, è stato quello di realizzare una tabella di contingenza che metta in relazione lo stato di conservazione e l'uso finale ottimale dei tuberi, consentendo agli operatori di programmare sia la produzione che la vendita. A questo scopo sono stati analizzati i principali attributi fisico-chimici ed enzimatici delle quattro cultivar di patata preselezionate (Costance, Fontane, Gaudi e Jelly) al momento della raccolta e ogni mese per 6 mesi di conservazione. Le analisi sono state eseguite per due stagioni di produzione consecutive (2020 e 2021). I risultati hanno rivelato le migliori proprietà di Fontane per l'industria di trasformazione, in particolare per la frittura, seguita da Jelly che ha mostrato buone qualità soprattutto per la IV gamma.

La seconda attività ha riguardato prove di disidratazione per valutare l'implementazione di tecnologie analitiche di processo (PAT), quali celle di carico e sistemi di visione artificiale, in un disidratatore ad armadio per la disidratazione di fette di carota e di patata. Per quanto riguarda l'essiccazione delle patate, la cultivar selezionata durante l'attività 1 (Fontane) è stata utilizzata per il test di semi-disidratazione (cioè fino ad un contenuto di umidità pari a 1,5 su base secca). Sono stati testati inoltre diversi pretrattamenti e due di questi (immersione in soluzione di acido citrico e di metabisolfito di sodio, rispettivamente al 3 % e allo 0,1 % p/v) sono stati selezionati per i test di semi-disidratazione. Per entrambi i prodotti testati, il sistema di visione artificiale e la cella di carico sono stati scelti come strumenti di tecnologia analitica di processo in linea all'interno di un quadro proattivo di Quality-by-Design e sono stati integrati per: i) il monitoraggio delle caratteristiche del prodotto (ad esempio, peso, colore e dimensioni); e ii) lo sviluppo di modelli di previsione dell'umidità dipendenti dal restringimento utilizzando la regressione lineare. I modelli lineari dipendenti dal restringimento hanno mostrato prestazioni superiori rispetto ai modelli a strato sottile di complessità crescente. I modelli migliori hanno riportato un errore quadratico medio (RMSE) pari a 0,005-0,007 e questo rappresenta un risultato interessante perché, prevedendo il contenuto di umidità residua, è possibile interrompere il processo di disidratazione al momento ottimale, evitando il deterioramento della qualità e riducendo il consumo energetico.

Infine, la terza attività ha riguardato lo sviluppo di un modello predittivo basato sulla spettroscopia del vicino infrarosso (NIR) per la determinazione di un importante parametro qualitativo della patata, il contenuto di sostanza secca. Le prestazioni di predizione di questo parametro basata sulla spettroscopia NIR è stata valutata per ogni diverso tessuto della patata: i) periderma, ii) corteccia, iii) parenchima esterno e iv) parenchima interno di 17 cultivar differenti campionate durante tre stagioni di produzione (2020, 2021 e 2022). I modelli predittivi della sostanza secca sviluppati utilizzando approcci standard di chemometria (cioè, Partial Least Squares, PLS; e interval-PLS, iPLS) hanno mostrato che tra i tessuti valutati, il parenchima interno permetteva di ottenere misurazioni più precise e affidabili, con valori di RMSE e coefficiente di determinazione (R^2) in predizione vicini all'1% e allo 0,90, rispettivamente. Queste informazioni possono essere utilizzate per sviluppare sistemi più avanzati, comprendenti strumenti portatili e tecnologie avanzate per la valutazione in situ, al fine di supportare gli operatori e garantire una migliore gestione del pre- e post-raccolta delle patate.

Parole chiave

Solanum tuberosum L., conservazione post-raccolta, parametri di qualità, spettroscopia del vicino infrarosso, chemometria, modelli predittivi, approccio Quality-by-Design

Table of contents

CHAPTER 1 - THESIS SUMMARY

1.1 MOTIVATION

Potato (*Solanum tuberosum* L.) is globally considered one of the most important food crop behind wheat, maize and rice and consumed nearly daily by more than one billion people, representing a staple food in many developed and developing countries.

In Italy, one of the most suitable area for potato growing is located north of Lazio region. Specifically, this area includes the municipalities north of Lake Bolsena. Since 2014, the potato supply chain of this area has held the quality designation PGI ("Patata dell'Alto Viterbese PGI") from the European Community. Local consortiums sell potatoes as a raw (sorted, washed and packed) and fresh-cut product (washed, peeled and cut). In fact, in 2012, the consortiums inaugurated a new processing factory for the production of fresh-cut potatoes, in order to satisfy the increasing demand of consumers for high-convenience food.

In every processing process of fruit and vegetables (especially for fresh-cut elaboration) is essential to use a high-quality raw material, selecting varieties with specific characteristics. For this reason, a feature of the fresh produce industry is the constant need to study existing cultivars and introduce new ones as raw materials. The quality of a fresh-cut product is generally affected by preharvest and postharvest factors, including processing. Genotype is one of the most important preharvest factors, and the first to be evaluated in order to select cultivars to be processed as fresh-cut products. In fact, not all the varieties are adapted to fresh-cut elaboration and their improper use results in low-quality products that cause consumer dissatisfaction. Therefore, to ensure the quality of the final product, it is important to determine the suitability of such varieties for fresh-cut elaboration. Moreover, cultivar selection may be also important to extend the shelf-life of fresh-cut product. However, the high perishability that characterizes this type of product makes it difficult to store, handle and trasport. For this reason, for fresh-cut producers is often complicate to ensure the standards requested by large-scale retailers, both in terms of shelf-life and quality.

Among post-harvest operations, drying is one of the most effective preservation processes, preventing both food spoilage and decay through moisture removal due to simultaneous heat and mass transfer. This process is commonly used by food industry to store foods for long period at room temperature with minimal deterioration occurring and simplifying the handling of the products through their reduction of weight and packaging volume. However, hot-air drying may be responsible for quality degradation, with a reduction of consumer acceptance as a result of the undesirable changes in colour, texture, size and shape as well as the organoleptic, nutritional and functional properties. Moreover, the convection-based drying systems are criticised for their resource-intensiveness (energy, labour) and high environmental impact. To overcome the stated issues, the drying sector invests continuously in innovative solutions that consider the complex, nonlinear and dynamic nature of food drying while ensuring high-quality products, efficient processes, and sustainable production practices. Among the possible strategies, the implementation of sensors, and machine learning models for efficient product-process monitoring and control has been gaining considerable interest both in academia and industry.

In the potato sector, the suitability of cultivar for specific type of processing or for specific culinary uses is affected by their physico-chemical attributes. Moreover, in post-harvest, the quality parameters of potatoes can considerably change. The significance of these changes depends on storage conditions and genotype. Consequently, the quality assessment of potato cultivars is fundamental both at harvesting time and during months of storage. The information resulting from the analysis is useful for both fresh tubers sellers and processors as it allows them to schedule sales and processing, always offering the consumer a high-quality product. In addition, potato suppliers must provide more details on labels (e.g., best culinary use) according to potato cultivar and storage status. This could prevent improper use of the raw material, safeguarding consumer’s health and interests. The common methods employed to determine the main constituents of potatoes are often time-consuming, expensive, and involve the destruction of the sample subjected to study. These disadvantages have raised the interest in new technologies (e.g., near-infrared spectroscopy, NIR) that enable rapid, reliable, multi-parametric, and executable in-situ measurements through simple methods, avoiding the use of chemicals.

1.2 AIMS OF THE THESIS

Considering the motivations listed in section 1.1 and the study of the state of-the-art on this subject presented in chapter 2, the PhD thesis aimed to innovate the potato sector, with specific regards to the “Patata dell’Alto Viterbese PGI” consortiums (Viterbo, Italy), by developing solutions to improve its competitiveness at regional and national level through the resolution of the following specific issues: i.e., i) poor shelf-life of fresh-cut potatoes and subsequent limited acceptance by large-scale retailers; ii) scheduling failure in tuber processing during storage due to poor cultivar characteristics records; iii) lack of knowledge for the production of semi-dried potatoes; iv) slowness in decision-making due to the non-timely monitoring of the maturity stage (DM content) of tuber in pre- and post-harvest, carried out by slow standard methods (e.g., oven and gravimetric methods) that cannot be performed in-situ. In particular, for each specific issue, specific counteracts were identified dividing the work in three activities:

1. Cultivar characterization: to deeply analyse and monitor the main physico-chemical properties of some potato cultivars grown in the "Patata dell'Alto Viterbese PGI" area, the most important quality parameters of potato tubers were analysed at harvesting time and for the whole storage period. This activity aimed to identify the most suitable cultivars for fresh-cut processing, in order to increase the shelf-life of final product.
   In addition, through the systematic analysis carried out during storage, knowledge of the peculiarities of cultivars can be increased, enabling (i) improved post-harvest management, (ii) planning for the sale of fresh produce and processing of fresh cuts, and (iii) providing consumers with more details on the best culinary use.
2. Smart semi-drying tests: this acitivity aimed (i) to evaluate the implementation of Process Analytical Technology (PAT) tools i.e., load cell and computer vision system as part of smart monitoring and control systems (SMCS) in a cabinet dryer and (ii) to introduce to the consortiums a different post-harvest operation in order to obtain a more storable and handled potato product than fresh-cut potato. The implementation of PAT tools in the dryer aimed to avoid some criticalities of convection-based drying systems such as high environmental impact and food quality deterioration.
3. Development of NIR-based predictive models for dry matter (DM) determination: the third activity aimed to design a new reliable, fast, handled and end-user-friendly solution for in situ measurements of an important potato quality parameters (i.e., DM content). For the intended purpose, this study proposed a novel approach for predicting potato DM content considering the impact of the heterogeneous distribution of DM content among tuber tissues on model performance.

1.3 THESIS OUTLINE

The PhD thesis is structured into a total of 8 chapters. In chapter 2 a synthetic review of the state-of-the-art concerning the main topics of the research is reported. From chapter 3 to 5, the scientific publications listed in Table 1.1 are presented.

Table 1.1: Publications and corresponding chapters in the thesis.

Chapter	Publication	Status
3	Characterization of Local Potato Varieties (*Solanum tuberosum* L.) for their Optimal End-Use: Effect of Genotype and Storage Time on Quality Parameters *Giacomo Bedini, Andrea Bandiera, Swathi Sirisha Nallan Chakravartula, Riccardo Massantini, Roberto Moscetti*	In preparation
4	Computer Vision-based Smart Monitoring and Control System for Food Drying: A Study on Carrot *Swathi Sirisha Nallan Chakravartula, Andrea Bandiera, Marco Nardella, Giacomo Bedini, Pietro Ibba, Riccardo Massantini, Roberto Moscetti*	Accepted
5	Prediction of Potato Dry Matter Content by FT-NIR Spectroscopy: Impact of Tuber Tissue on Model Performance *Giacomo Bedini, Swathi Sirisha Nallan Chakravartula, Marco Nardella, Andrea Bandiera, Riccardo Massantini, Roberto Moscetti*	Submitted

Specifically, in the chapter 3 the scientific paper regarding the first activity (i.e., potato cultivar characterization) is reported. The study was conducted on four pre-selected potato cultivars. The results of analyses of major potato quality parameters are reported, showing the effect of genotype and storage time on tuber properties, which influence their suitability for specific end uses.

The chapter 4 is divided in two sections. The first (4.1) reports a publication concerning the implementation of Process Analytical Technology (PAT) tools based QbD framework as part of Smart monitoring and control system in a cabinet dryer for real-time monitoring and Computer Vision (CV)-based moisture prediction for drying of carrot slices. The smart drying unit tested for carrot slices was used to perform preliminary studies on potato slices. Several pre-drying treatments were tested to identify the one most effective in preventing browning processes. The real-time monitoring by load cell and CV system was used to select the best pretreatments and to develop moisture predictive models. The results are reported in the second section (4.2).

The results of the third activity are reported in chapter 5. The first section (5.1) refers to a publication concerning an investigation of the impact of potato tissue on performance of Near-Infrared Spectroscopy (NIRS) for dry matter (DM) determination. This study described how dry matter is distributed among the different potato tissues. Then, the effect of the heterogeneous distribution of DM on NIR spectral profile and on linear regression models computed was shown. Further studies are ongoing to improve the predictive performance and to make this technology suitable for in-situ applications. Moreover, in collaboration with the Free University of Bolzano, the combination of electrical impedance spectroscopy (EIS) and NIRS was tested. A brief description and the preliminary results of these activities are reported in section 5.2.

Chapter 6 concerns the general conclusions and future perspectives, reporting the impact of the research and any spin-offs from its applications.

Other scientific publications related to other contributions are listed in the chapter 7. Finally, in the chapter 8, the literature cited in the Introduction (chapter 2) is listed.

CHAPTER 2
INTRODUCTION

2.1 *Solanum tuberosum* L. – "PATATA DELL'ALTO VITERBESE PGI"

2.1.1 History, Product Description and Relevance for Local Economy

The Protected Geographical Indication product 'Patata dell'Alto Viterbese' is strongly dependent on the environmental (soil and climate) and socio-economic characteristics of the area. In fact, the soil and climate characteristics are such as to enhance the uniqueness of the qualitative aspects of the product, which is known on the market under the common name of 'Patata dell'Alto Viterbese', as can be seen from the numerous commercial documents (invoices, delivery notes, labels, etc.) and the well-established popular festivals.

The characteristics of the 'Patata dell'Alto Viterbese' PGI, such as its aroma, flavour and, above all, the intensity of its flesh colour (which is exclusively yellow), are determined not only by genetics but also by the production environment (soil, climate, cultivation techniques, type of storage), thus establishing a clear link between the 'Patata dell'Alto Viterbese' and the production area.

The soils of the area are of volcanic origin, with the presence of lava and pyroclastic formations, with a loamy-sandy texture, high permeability and low bulk density. The soils are subacid to subalkaline, with a pH of between 5.5 and 7.5 - to which the potato, as an acid-tolerant crop, adapts well - and are rich in potassium (between 600 and 1300 ppm).

The climatic conditions are influenced by the presence of Bolsena Lake, an imposing basin which, thanks to its mitigating effect, creates particularly favorable microclimatic conditions for the cultivation of the 'Patata dell'Alto Viterbese'. In fact, in spring (April/May), when the potato is at the stage of sprouting and the beginning of vegetative development, temperatures in the PGI area are between 12 and 14.5°C, which is optimal for this physiological stage of the plant. In summer, thanks to the influence of Bolsena Lake, average temperatures in the area tend to rise gradually from 17°C to around 24°C in July, during which time the potato completes the entire biological cycle up to the ripening stage. These optimal climatic conditions in the area (temperature below 24°C) determine a better translocation of carbohydrates and mineral elements to the plant tubers.

With regard to rainfall (annual average between 800 and 1200 mm/year) in August, the lack of rain, combined with high temperatures, with peaks of up to 33-35°C, favors the ripening or senescence phase. During this last physiological phase, there is a progressive yellowing of the leaves, loss of functionality, translocation of the products of photosynthesis and nutrients accumulated during growth into the tubers and thickening of the skin. This ripening phase is accelerated and favored by high temperatures and water stress: conditions that occur every year in the 'Patata dell'Alto Viterbese' area. In addition, the drought conditions at harvest time determine the quality characteristics of the 'Patata dell'Alto Viterbese', such as the uniform color of the skin and the general appearance of the tubers (rain causes skin discoloration and darkening).

There are numerous oral and written records from local elders that attest to the strong historical, cultural and social link between the product and the land. Potato cultivation began in the 1920s in the area known as "Alto Viterbese", although the decisive factor in its development was the abandonment of strawberry cultivation, which was widespread until the mid-1950s, when it was replaced by potatoes due to health problems. In fact, from the 1960s onwards, potatoes became the dominant crop in the area, and in the years that followed, and still today, they are the main source of income for the local agricultural economy, as well as for the workers involved in storage, packaging, marketing and transportation. In addition to related industries, the high concentration of potato production led some mechanical workshops to improve the tuber processing machines on the market, adapting them to the specific soil conditions and practices used in the area.

The importance of the product in local customs is also reflected in the tradition of festivals: from the “Gnocchi” festival, inaugurated in 1977 in San Lorenzo Nuovo, to the Potato Festival, which has been held in the municipality of Grotte di Castro since 1985 and involves the local population in the preparation of the events. The cultural link is also underlined by the extensive use of the potato in many traditional local recipes.

The designation 'Patata dell'Alto Viterbese' refers to mature tubers of the species *Solanum tuberosum* L. of the *Solanaceae* family, obtained from seed tubers of potato varieties listed in the Common Catalogue of Varieties of Agricultural Plants, grown in the defined area and having certain physical and chemical characteristics when released for consumption. The production area of the 'Patata dell'Alto Viterbese' PGI is located in the northernmost part of Lazio, in the province of Viterbo, between Bolsena Lake, Umbria and Tuscany.

Harvesting, by hand or machine, must take place between 15 June and 30 September each year, after careful assessment of the degree of ripeness of the tubers. The product may be marketed as a fresh product or stored in cold storage rooms, protected from light, at a temperature of 5-8 °C and a relative humidity of 88-93 %. Tubers may not be refrigerated for more than 9 months. The potatoes are subjected to a gas phase anti-sprouting treatment.
With regard to processing, the 'Patata dell'Alto Viterbese' PGI is also sold as a fresh-cut product. In fact, in 2012, the consortiums inaugurated a new processing factory for the production of fresh-cut potatoes, in order to satisfy the increasing demand of consumers for high-convenience food.

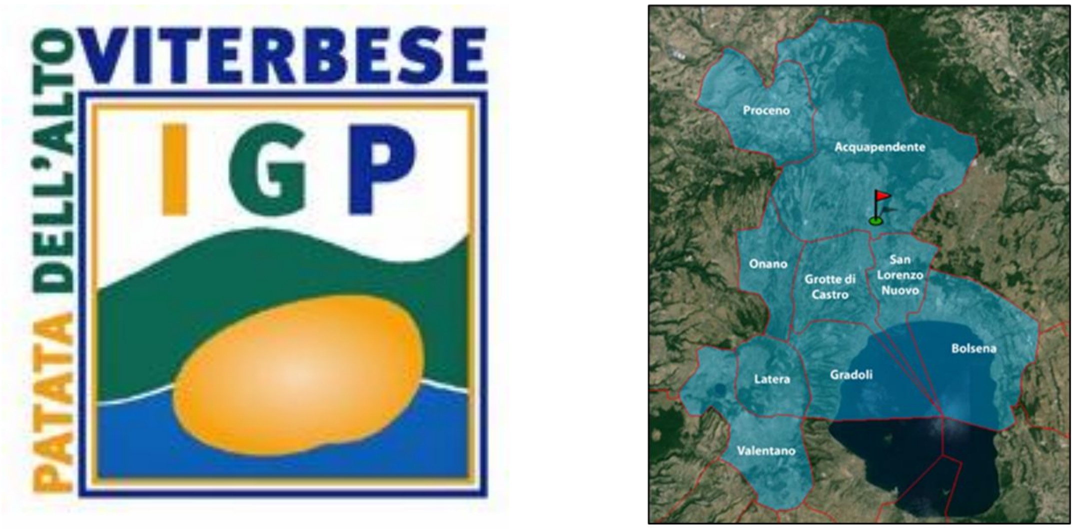

Figure 2.1: *Logo and geographic area of the 'Patata dell'Alto Viterbese' PGI*

2.1.2 Potato Quality and Attributes Influencing the Destination of Use

Potato (*Solanum tuberosum* L.) is one of the most widely grown crops in the world and it is a staple food in many developed and developing countries. Potatoes are sold as a fresh product (31%) or processed into frozen chips (30%) and crisps (12%), and dehydrated (12%). Pinhero and Yada, (2016) defined quality of potatoes as “the suitability for their intended use” and the key parameters affecting the destination of use are: (i) dry matter content, (ii) carbohydrates (reducing and nonreducing sugars), (ii) textural characteristics (e.g., firmness), and (iv) colour-related alterations (post-cut browning and after-cooking darkening) (Torres and Parreño, 2016). DM content is one of the most important attributes in processing qualities, which substantially affect the texture and the potato suitability for processing. Generally, potato varieties used for processing must have a DM content greater than 20 %. In contrast, a medium DM content (16-19 %), corresponding to medium-firm, slightly floury potatoes that do not disintegrate, is the most suitable for multipurpose and domestic use (i.e., boiling, steaming, soups). Textural characteristics influence quality and palatability of potato products. The sugar content (sucrose and reducing sugars) affects both taste and acceptability of fried or roasted potatoes. In fact, if the reducing sugar content is too high (>2%), the Maillard reaction causes unacceptable browning and the production of harmful amounts of acrylamide (Torres and Parreño, 2016). The other key quality parameters concern colour-related alterations. These undesirable processes are influenced by the phenol content and composition. Moreover, oxidative enzyme activity (e.g., polyphenol oxidase) plays a key role for enzymatic browning.

2.1.3 Factors Affecting Potato Quality

All the above-mentioned parameters are strongly influenced pre- and post-harvest factors (Figure 2.1). In general, the quality of the stored potato is primarily determined by the health and quality of the potato prior to storage. Good storage management cannot improve the quality of stored potatoes if the health of the tubers is compromised by pre-harvest conditions.

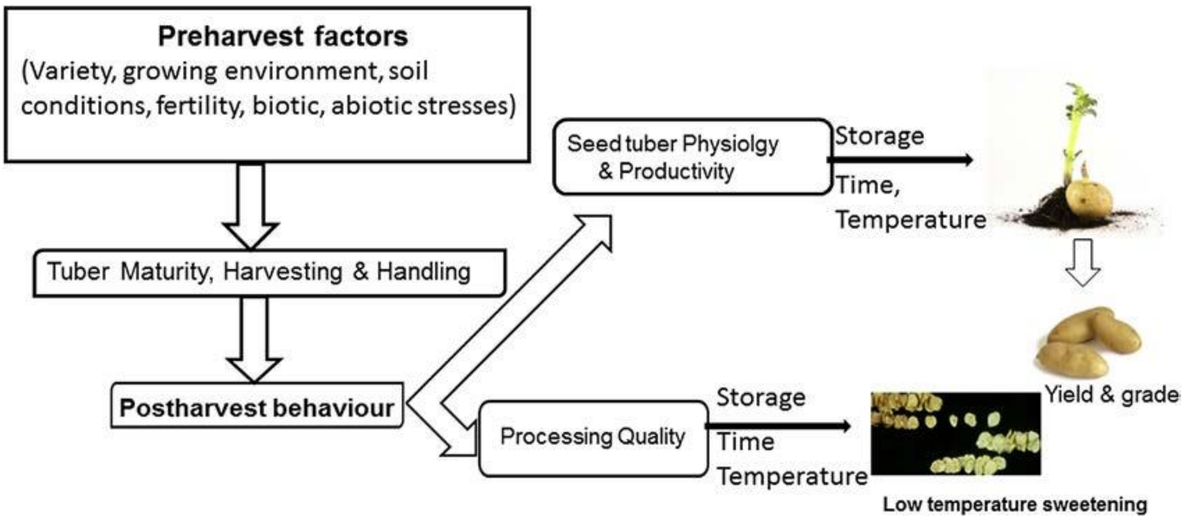

Figure 2.2: *Factors affecting the postharvest behavior and quality of potato tubers (Pinhero and Yada, 2016).*

Pre-harvest factors

Genotype is one of the most important preharvest factors, and the first to be evaluated in order to select cultivars for a specific final intended use (Cabezas-Serrano et al., 2009). In fact, a lot of pre- and post-harvest aspects are cultivar-dependent (e.g., water demand, resistance to pests and diseases, storability, dormancy, etc.)

The growing conditions such as biotic (pests and diseases) and abiotic factors (soil moisture and temperature) strongly affect the potato quality. Potatoes grow in most soil types, but deep, well-drained, light-to-medium soil is preferred. Regarding water requirements, potatoes need optimal water supply throughout their growth, and even moderate water stress affects the various stages of tuber development and will have an effect during storage. The water requirements of potatoes vary according to soil type, maturity, variety and intended use, whether for fresh consumption or processing. Lack of water at harvest can cause easy bruising of tubers, while clods of soil/clay promote mechanical damage, which can lead to disease development and the appearance of black spots during storage.

However, high soil moisture in excess of 90% available soil moisture can lead to storage rot and can favor the development of several foliage diseases such as late blight and white mold. Also the crop nutritional status influence the storage. For example, high nitrogen fertility increases yield but usually decreases storage quality (Pinhero and Yada, 2016).

The conditions and timing of harvesting, tuber health, and soil conditions can significantly affect tuber health and quality throughout storage. Optimal harvest conditions are 60–65% available soil moisture and tuber pulp temperatures of 10–18°C. Harvesting immature tubers when soil conditions are too wet or too dry, and when the weather conditions are too warm, can affect the quality of the tubers. If tubers are harvested in very warm conditions, the respiration rate of the tubers increases.

The maturity of tubers is another crucial aspect. Maturity is a complex physiological and morphological condition affected by various factors such as variety, climatic conditions (e.g., temperature, rainfall, light), and biological and environmental stressors. Potato tuber maturation as described by Heltoft et al. (2017), involves a variety of processes that include skin set (physical maturation), accumulation of dry matter (physiological maturation) and lowering of sucrose content (chemical maturation). Specifically, the physiological maturity of the tuber is indicated by the soluble sugar content reaching a minimum (chemical maturation) which usually coincides with the maximum of starch (peak of dry matter content). The maturity of tubers influences the skin thickness and the morphology of the periderm. Immature tubers result in easily removable skin, increasing the potential for damage or disease and the water loss during storage. However, the most important aspect of tuber maturity is its effect on the biochemical changes that occur during storage. Specifically, potato maturity influence the respiration rate, dormancy and Low-Temperature Sweetening (LTS). In fact, potatoes with sucrose content greater than 0.15% tuber fresh weight at harvest are prone to premature increase in reducing sugars such as glucose and fructose during storage, which causes darkened processed products. Consequently, potatoes should be harvested after reaching maturity in order to preserve quality and maximize the storability (Pinhero and Yada, 2016).

Post-harvest storage

For both growers and processors, it is essential to maintain potato quality based on end use. It is important to highlight that even the best storage can only maintain the quality of tubers placed in storage. In Europe, potatoes are generally stored in moveable pallet boxes inside dark buildings at 6-9 °C and 85-95 % of relative humidity, using different natural or chemical compounds as sprout inhibitors. These conditions aim to control the most important biochemical changes that occur during storage: i) respiration, ii) water loss, iii) sprouting, and iv) Low-Temperature Sweetening (LTS) (Pinhero and Yada, 2016).

As a living organism, potato tubers continue to respire during storage consuming sugars produced by starch hydrolysis. Due to this process, loss of dry matter content occurs, resulting in weight loss. At 10 °C, the dry matter loss by respiration represents approximately 1–2% of fresh weight during the first month and about 0.8% per month thereafter, but rises to about 1.5% per month when sprouting is well advanced. The respiration rate is affected by temperature and hence will vary depending on storage conditions and the end use of the tubers. For example, most varieties for processing chips and French fries should not be stored below 9 °C owing to LTS. The respiration rate is minimal at about 5°C and increases slowly up to about 15°C, at which point respiration starts to increase quickly. The respiration rate also increases rapidly when the temperature is lowered to 3°C, due to the high concentration of reducing sugars produced by the breakdown of starch. The heat generated by respiration during storage may increase the storage temperature. To maintain the temperature of the potatoes at a specific level, the heat generated by respiration of tubers must be removed by cooling. It is also important to have a constant supply of fresh air during storage to provide the oxygen required for respiration and to remove the CO_2 released during respiration (Pinhero and Yada, 2016).

Regarding the water loss, 98% of the moisture that leaves a tuber during storage is lost through its skin by evaporation. Only 2.4% leaves the tuber through the lenticels with the carbon dioxide produced by respiration. Tubers that have lost large amounts of water suffer to mechanical damage and a reduction in culinary quality leading to economic loss. Specifically, water loss is of focal interest as it compromises the marketability of the tubers when it is higher than 10 % of initial weight. Water loss depends on several factors such as i) heat production in potatoes, ii) temperature of the tubers, iii) relative humidity (RH), iv) quality of potato skin, v) variety, vi) sprout growth, and vii) duration of ventilation. The balance between dry matter loss through respiration and water loss through evaporation determines the changes in dry matter content and textural characteristics of potato tubers, also affecting weight loss. In general, storing potatoes at 6-9 °C and controlled relative humidity minimize both respiration rate and water loss, preserving the tuber weights and dry matter content, as confirmed by Gikundi et al., (2022).

Sprouting, the breaking of dormancy, affects the quality of the tubers during storage by remobilizing storage compounds, mainly starch and protein, and shrinking tubers owing to loss of water. Sprouting accelerates both respiration rate and water loss and reduces the quality and value of the crop because of increased levels of toxic glycoalkaloids, accelerated starch breakdown with concomitant accumulation of undesirable reducing sugars, and decreases in vitamin content. In general, it increases physiological aging and affects the appearance of the tuber. Sprout growth is mainly influenced by the temperature and storage atmosphere. For example, below 5°C, sprout growth is slow and increases up to an optimum temperature of 20°C, above which the growth rate decreases. Higher RH promotes sprout growth, which is more pronounced at higher temperatures. Higher CO_2 concentrations also increase sprout growth. Consequently, the use of anti-sprouting compounds or other successful management of sprout inhibition such as low temperature or controlled atmosphere (CA), are necessary to avoid quality deterioration of tubers during storage (Pinhero and Yada, 2016). Several chemicals are widely used for sprout control. Chlorpropham (isopropyl N-(3-chlorophenyl) carbamate; CIPC) is the most effective post-harvest sprout inhibitor registered for use in potato storage. This product has been used successfully as a sprout inhibitor for more than 40 years. However, in 2019, the European Union, following a report released by The European Food Safety Authority (EFSA), officially prohibit the use of this substance. Ethylene is also an effective sprout inhibitor, but its use may result in darkening of fry color (Daniels Lake et al., 2007). However, considering the increased awareness of environmental and health concerns, there is considerable interest in finding effective potato sprouting suppressants that have a negligible environmental impact. For example, Teper-Bamnolker et al., (2010) reported the efficacy of mint (*Mentha spicata* L.) essential oil in inhibiting sprouting in eight potato cultivars during large-volume 6-month storage.

After harvest, low-temperature storage between 4 and 7 °C can prolong dormancy and reduce shrinkage and diseases. However, temperatures below 9 °C can cause a negative process named Low-Temperature Sweetening, an often reversible accumulation of reducing sugars (glucose and fructose). The reducing sugars participate in the Maillard browning reaction with free amino acids (particularly asparagine) during frying, resulting in dark brown fries and chips. These darkened chips and fries are unacceptable to consumers and may result in greater amounts of acrylamide production. This compound and its active metabolite are characterized by clastogenic and mutagenic properties recently confirmed by EFSA (Benford et al., 2022). Specifically, the optimal reducing sugar content for industrial frying is 0.1% and it is considered unacceptable when over 0.5 % (Biedermann-Brem et al., 2003). Relative resistance or susceptibility to LTS can vary dramatically among cultivars with respect to carbohydrate and respiratory metabolism as reported by Zommick et al., (2014). It was also shown that reducing sugar content reflected the activity of acid invertase and its inhibitors, and the fructose/glucose ratio indicated the extent of cold sweetening. Genetic engineering can be used successfully to improve LTS tolerance in potato tubers (Pinhero and Yada, 2016). The development of potato varieties with a high tolerance to LTS can be important for processors to ensure a high quality end product and to avoid health issues for consumers.

The description of biochemical changes provides insight into the effect of storage on the nutritional quality of potatoes and their intended use. These aspects are crucial for growers, fresh sellers and processors to manage storage based on the final intended use.

2.1.4 Potato Management and Processing

Considering the impact of genotype on the quality attributes and storability of potatoes, the first step for productive associations such as consortiums or cooperatives is to select the best potato varieties based on environmental factors and their intended use. From a commercial point of view, it is possible to categorize potato varieties in four groups: i) early cultivars, ii) fresh-market cultivars, iii) dual-purpose cultivars and iv) cultivar for processing industry.

Early potatoes are harvested before they are fully mature and marketed immediately to obtain a premium price; their skins can be removed easily without peeling. Early potatoes are harvested to meet the demand for the fresh market, and some are used for chip processing. Because of the succulent nature and immature skin of early potatoes, they are easily bruised or damaged and the rate of respiration is about four to five times greater than mature potatoes. Early harvested potatoes are usually stored for only a short time (Pinhero and Yada, 2016). Cultivars intended for the fresh market must be able to be stored for at least 5 months with good nutritional quality. Potatoes used for processing are selected on the basis on specific characteristics (e.g., low reducing sugar content with high tolerance to the LTS, low susceptibility to post-cut browning, etc.). They are usually grown under contract, with the processing industry specifying the cultivar. The dual-purpose varieties can be processed or used for the fresh market.

Potatoes are a very popular product throughout Europe and the world, both as fresh tubers and as processed products. Focusing on processed potatoes, in Europe, the main product is frozen potatoes, including pre-fried, pre-cooked by steaming or boiling and uncooked potatoes. In fact, frozen potato products account for more than 65 % of all potatoes that are processed, followed by potato chips (or crisps) for ~25 % and dried potato for ~5 % (Eurostat, 2013). Regarding fresh cut potatoes, the market penetration of this product is limited due to its poor shelf-life. The main causes of quality loss are related to the enzymatic browning, dehydration and whitening, off-odors and exudation. However, with the increasing demand for high convenience foods such as fresh-cut fruit and vegetables, fresh-cut potatoes are an attractive product for consumers, foodservice, canteens and large-scale retail trade.

In general, the production of high-quality potato products depends on the initial quality of the raw tubers. Each type of potato processing requires a raw material with specific physico-chemical and enzymatic characteristics. For example, the most important attributes for frying are dry matter and reduced sugar content. It is therefore important to select and use potato varieties with high dry matter content and high tolerance to LTS. For both fresh cut and dried potatoes, the susceptibility to post-cut browning is a key factor. In this case, the selection of potato varieties must take this into account.

At this point, it is easy to see how important it is for the potato supply chain to analyze the quality of the raw material at harvest and during storage. Analyzing and monitoring the changes of the most interesting quality attributes, fresh sellers and processors can schedule sales and processing, always offering the consumer a high-quality product. Moreover, providing more details on labels (e.g., best culinary use) according to potato cultivar and storage status would prevent improper use of the raw material. This could avoid, for instance, excessive intake of acrylamide at domestic levels.

The common methods employed to determine the main constituents of potatoes are chemical analysis such as high-performance liquid chromatography (HPLC) or other chemical-based protocols that require a laboratory. These methods are time-consuming, expensive, involve the destruction of the sample and have a significant impact on the environment. For these reasons, the potato industry is increasingly interested in high-tech systems capable of rapidly measuring key quality parameters (López et al., 2013). Moreover, these technologies can be implemented in-line for real-time monitoring of food quality and dynamic control of processing such as drying (Moscetti et al., 2017).

2.2 NOVEL EMERGING TECHNOLOGIES FOR QUALITY ANALYSIS AND PROCESS MONITORING

2.2.1 A Paradigm Shift Towards Smart Industry: Industry 4.0/5.0

The Fourth Industrial Revolution (a.k.a. Industry 4.0) originated in 2011 from a project in the high-tech strategy of the German government. It advanced the concept of Cyber Physical Systems (CPS) into Cyber Physical Production Systems (CPPS). SmartFactory is one of the key associated initiatives of Industry 4.0. In the Industry 4.0 era, production systems, in the form of CPPS, can make intelligent decisions through real-time communication and cooperation between “manufacturing things”, enabling flexible production of high-quality products at mass efficiency (Xu et al., 2021). Industry 4.0 embraces advanced physical, digital, and biological technologies. It includes, but is not limited to, artificial intelligence (AI), machine learning, big data, the Cloud, the Internet of Thing (IoT), blockchain, smart sensors, robotics, cybersecurity, and digital twins and cyber-physical systems (CPS) (Hassoun et al., 2023).

As businesses started to embrace Industry 4.0, along came the Fifth Industrial Revolution (Industry 5.0). Industry 5.0 is understood to recognize the power of industry to achieve societal goals beyond jobs and growth, to become a resilient provider of prosperity, by making production respect the boundaries of our planet and placing the wellbeing of the industry worker at the center of the production process. The introduction of Industry 5.0 is based on the observation or assumption that Industry 4.0 focuses less on the original principles of social fairness and sustainability but more on digitalization and AI-driven technologies for increasing the efficiency and flexibility of production. The concept of Industry 5.0, therefore, provides a different focus and point of view and highlights the importance of research and innovation to support the industry in its long-term service to humanity within planetary boundaries (Xu et al., 2021).

Industry 4.0 and 5.0 are taking hold in the agricultural and industrial sectors, including the food industry. The applications in the food sector concern several interesting topics such as intelligent manufacturing, quality analysis and control, food traceability system and other functions commonly found in the food industry. Artificial intelligence (AI), machine learning, and big data are essential components of Industry 4.0 and 5.0 for this sector. Machine learning is a subset of AI, and it concern the development and application of algorithms used to find patterns in data to make classifications and predictions. The AI revolution has become one of the main drivers of Industry 4.0. The increase of digitalization creates a massive amount of data which is characterized by its Variety, Velocity, and Volume (the 3 Vs of big data) (Hassoun et al., 2023). Big data has thus become the new norm, enabling AI and ML to advance at an exponential rate. Big data analytics is also closely related to the emerging components of Industry 4.0, such as blockchain and IoT. The IoT includes a network of devices and other physical objects connected to the Internet through various technologies (e.g. sensors and software), enabling the exchange and collection of data. The data collected can be used to assess the status of a given system and then be used to optimize the performance of that system. Blockchain is another digital technology approach. In the food industry sector, it can be used to improve and ensure higher performance of different aspects of food value chain systems, such as those for food safety, food quality, and food traceability (Hassoun et al., 2023). Moreover, Industry 4.0 and 5.0 are characterized by highly autonomous intelligent systems in industrial processes due to the implementation of technologies such as smart sensors. Smart sensors are increasingly used in the food industry in various production equipment to smartly control, monitor, and optimize multiple manufacturing tasks in real-time, along with improving traceability and food quality (Hassoun et al., 2023). For example, optical sensors such as imaging systems with or without spectroscopy are increasingly being used to monitor food processing, quality and authenticity, including as Process Analytical Technology (PAT) tools (Nallan Chakravartula et al., 2022; Sirisha et al., 2023; Bedini et al., 2020). Implementing these sensors in-line for real-time monitoring of quality aspects can help to optimize the food processing using a Quality by Design (QbD) approach (Rathore and Kapoor, 2016).

2.2.2 Near Infrared Spectroscopy (NIRS)

Near infrared (NIR) radiation covers the range of the electromagnetic spectrum between 780 and 2500 nm. In NIR spectroscopy, the product is irradiated with NIR radiation, and the reflected or transmitted radiation is measured. While the radiation penetrates the product, its spectral characteristics change through wavelength dependent scattering and absorption processes. This change depends on the chemical composition of the product, as well as on its light scattering properties which are related to the microstructure (Nicolaï et al., 2007). The interaction between energy and matter follows the Beer−Lambert's Law. According to it, absorbance at any wavelength is proportional to the number or concentration of absorbing molecules present in the path of the radiation. Most absorption bands in the near infrared region are overtone or combination bands of the fundamental absorption bands in the infrared region of the electromagnetic spectrum which are due to vibrational and rotational transitions. In large molecules and in complex mixtures, such as foods, the multiple bands and the effect of peakbroadening result in NIR spectra that have a broad envelope with few sharp peaks. In general, the NIR spectra obtained for fruit and vegetables are very similar and are dominated by the water spectrum with overtone bands of the OH-bonds at 760, 970 and 1450 nm and a combination band at 1940 nm (Nicolaï et al., 2007). Consequently, advanced multivariate statistical techniques are essential to extract the required information from the usually convoluted spectra. For the calibration step, a mathematical relationship should be established between the two sets of data, spectra data and reference data, including physical or chemical information of the product. The most commonly used statistical techniques for this process are the multiple linear regression, principal component regression, and partial least squares (PLS) regression. These chemometric techniques establish a mathematical relationship between variations in the NIR spectra of samples with the variation in the parameter measured. This relationship can then be used to predict the parameter value in unknown samples . It should be noted that the main limitation of NIRS in the analysis of food products is that the initial phase of development of the calibrations depends on reference methods based on chemical analysis (López et al., 2013).

NIRS is considered as a technology with great potential to provide accurate and rapid predictions of the chemical composition and nutritional value of many foods. This technique has several advantages over reference methods. It is i) fast and easy to use, ii) environmentally friendly, iii) accurate and many applications are non-destructive (López et al., 2013).

Although the literature on NIR applications in potatoes is not as extensive as for other vegetables, NIR applications in this sector have mainly concerned the determination of the main quality parameters: dry matter, starch and reducing sugars. In this regard, López et al. (2013) summarized the results obtained by several authors in predicting the major and minor components of potatoes. Focusing on the prediction of DM content, several authors tested the application of NIRS on different states of potatoes such as whole (Helgerud et al., 2015), mashed (Haase, 2003) and fried (Shiroma and Rodriguez-Saona, 2009) samples. The best results ($R^2 > 0.95$) were observed when the sample was mashed and homogenized (Brunt and Drost, 2010; Haase, 2011); however, this sacrificed two of the strengths of NIR spectroscopy: minimum sample preparation and the possibility of in situ measurement (or portability of measure).

2.2.3 Computer Vision (CV)

Within a few decades, computer vision has fields such as pattern recognition, machine learning, computer graphics, 3D reconstruction, virtual reality and augmented reality. By 2010, computer vision was capable of performing high-end tasks such as object recognition, autonomous vehicle navigation, facial recognition, fingerprint recognition, fast computing image processing, and robotic navigation. Figure 2.2 illustrates the taxonomy of computer vision field and its inter-related branches such as science and technology, mathematics and geometry, physics and probability etc. (Kakani et al., 2020).

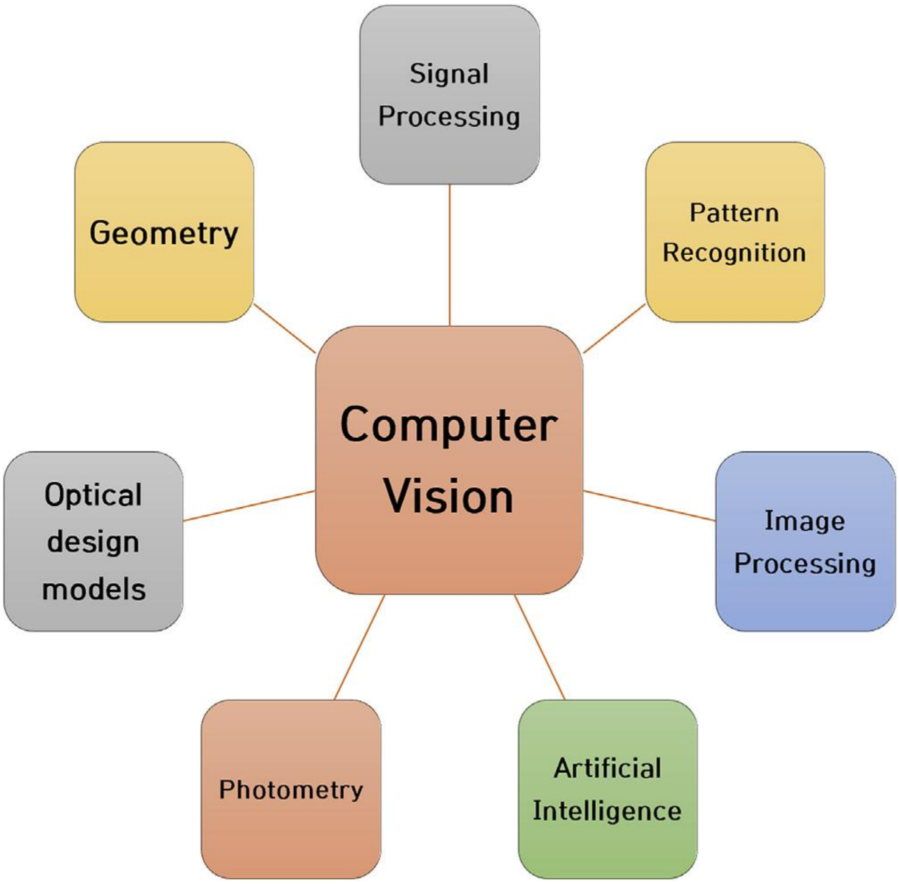

Figure 2.3: *Computer vision and its sub-concepts (Kakani et al., 2020).*

The combination of technologies such as CV and AI in various fields such as medicine, automobile, smart robotics, etc. seems intensively observable. One of the industries that has recently seen a huge impact from AI in its methods, tools and machinery is the food industry. Methods of growing, producing and processing crops have changed with the introduction of AI-driven methods and machines in both agriculture and the food industry. AI concepts such as machine learning and deep learning have made it possible to process images using CV system. Computers can now not only display images of food, but also identify and reveal facts about the nutritional information of that food (Kakani et al., 2020). CV systems have proven to be reliable in food processing, providing cost-effective and non-invasive solutions for various applications such as i) automated harvesting, ii) monitoring of product quality attributes like appearance, shape and texture, iii) picking and packing, and iv) sorting and grading (Figure 2.3).

Figure 2.4: *Examples of AI and CV applications in the food industry (Kakani et al., 2020).*

Further, CV systems can be implemented as real-time data acquirement tools in-line for quality monitoring, analyses, multivariate modelling, and feedback with the potential for proactively strengthening and/or replacing conventional offline methods. This also offers the advantage of comprehensive and precise quality monitoring from the start to the end of the process (Aghbashlo et al., 2014).

As showed in Figure 2.2, one of the “sub-concepts” of CV is image processing. It generally consists of the following five steps: i) image acquisition, ii) image pre-processing, iii) image segmentation, iv) measurement operations and v) classification (Du and Sun, 2004).

Image acquisition, i.e. the capture of an image in digital form, is obviously the first step in any image processing system. Over the last few decades, a considerable amount of research has been devoted to the development of image acquisition techniques. A very intensive area of research in image acquisition is the development of sensors and many different configurations of sensors are currently used to convert images into digital form. The two main types of digital image sensors are the charge-coupled device (CCD) and the active-pixel sensor (CMOS sensor).

Images captured by digital image sensors are subject to various types of noise. These noises can degrade the quality of an image and, as a result, it cannot provide correct information for subsequent image processing. In order to improve the quality of an image, it is necessary to perform operations on the image to remove or reduce the degradation suffered by the image during its acquisition. The purpose of preprocessing is to improve the image data by suppressing unwanted distortions or enhancing some of the image features that are important for further processing, and to produce an image that is more suitable than the original for a particular application. Two different types of image pre-processing approaches can be identified for food quality assessment: pixel pre-processing and local pre-processing, depending on the size of the pixel neighborhood used to calculate a new pixel (Du and Sun, 2004).

Image segmentation partitions an image into its constituent objects, which is a challenging task due to the richness of visual information in the image. The image segmentation techniques developed for food quality assessment can be divided into four different philosophical approaches, i.e. thresholding-based, region-based, gradient-based and classification-based segmentation. A recent literature review on image segmentation shows that thresholding and region-based methods have been used for segmentation in most applications (Du and Sun, 2004).

Once the image is successfully segmented into discrete objects of interest, the objects can be described and represented for further processing and analysis by measuring the individual features of each object. Measurements that can be performed on features in images for food quality assessment can be grouped into four classes: size, shape, color, and texture. For each class, a number of different specific measurements can be made, and there are a variety of different ways to perform the operations.

2.2.4 Other technologies for food quality analysis

As an alternative to optical techniques, there are several technologies that are commonly used to assess the quality of fruit and vegetables. Some of these methods are based on the interaction of the samples with an electromagnetic field, and are mostly used to obtain information about the internal structure of the fruit. Examples of such methods are represented by Magnetic Resonance Imaging (MRI) (Kirtil et al., 2017), Computer Tomography (CT) scan (Du et al., 2019), X-ray imaging (Arendse et al., 2018), acoustic impulse technique (Harker et al., 2019) and acoustical vibration technique (Baltazar et al., 2008).

Together with the above-mentioned techniques, electrical methods studying the interaction of a material and an applied electric field, are rapidly emerging as reliable alternatives for determining fruit quality. The most widely used method in this field is Electrical Impedance Spectroscopy (EIS), a technique of particular interest because of its simplicity (i.e. no need for sample pre-treatment and highly trained personnel), non-invasiveness, cost-effectiveness, rapid reproducibility on different samples and, most importantly, the ability to provide real-time results. EIS is also defined as bioimpedance when applied to a biological material such as fruit (Ibba et al., 2020).

2.4 Chemometrics and Predictive Modeling

The above-mentioned methods, based on diverse working principles (detailed hereafter), can produce a large amount of data with multiple variables, where multivariate analysis is utilized to identify key discriminatory variables that correlate with the quality status of a fruit to produce prediction models, enabling the non-destructive assessment of fruit quality. For example, the NIR spectrum is essentially composed of a large number of overtones and combination bands. This, combined with the complex chemical composition of a typical fruit or vegetable, causes the near infrared spectrum to be highly convoluted. The spectrum can be further complicated by wavelength dependent scattering effects, tissue heterogeneities, instrumental noise, environmental effects and other sources of variability. As a result, it is difficult to assign specific absorption bands to specific functional groups, let alone chemical constituents. Multivariate statistical techniques (also known as chemometrics) are therefore required to extract the quality attribute information buried in the NIR spectrum ('model calibration'). These are essentially regression techniques coupled with spectral pre-processing (Nicolaï et al., 2007).

2.3.1 Data Pretreatments

Spectral preprocessing techniques are used to remove any irrelevant information which cannot be handled properly by the regression techniques. The most common preprocessing steps are i) baseline correction, ii) noise reduction, iii) data normalization, and iv) resolution enhancement (Pierce et al., 2012).

Baseline correction is typically the first preprocessing step in the spectral data analysis. The most popular technique is Multiple Scatter Correction (MSC). It is used to compensate for additive (baseline shift) and multiplicative (tilt) effects in the spectral data caused by physical effects such as non-uniform scattering across the spectrum, since the amount of scattering depends on the wavelength of the radiation, particle size and refractive index. The method attempts to remove the effects of scattering by linearizing each spectrum to an 'ideal' spectrum of the sample, which in practice is the average spectrum. Another common method is called Standard Normal Variate (SNV) correction where each individual spectrum is normalized to zero mean and unit variance (Nicolaï et al., 2007).

Baseline correction procedures are usually designed to correct low frequency noise, but high frequency baseline correction procedures and smoothing techniques may be necessary to reduce high frequency variations and improve signal-to-noise ratio (Pierce et al., 2012). The Savitzky-Golay algorithm is typically applied for these intended purposes. The effectiveness of this algorithm varies according to the order of the polynomial function selected and the width of the smoothing window used. The operation of the Savitzky-Golay filter consists in replacing the signal assumed by each wavelength of the spectrum based on the signal of the wavelengths adjacent to the one under consideration. Finally, the value of the signal at each point is obtained by interpolating the points described by the polynomial function computed within the smoothing window. Noise reduction techniques are critical to successfully addressing a wide variety of analytical challenges (Pierce et al., 2012).

Data normalization is a basic step performed to correct between sample variations that are unavoidably introduced during sample preparation and measurements. Common scaling methods are autoscaling (where the mean of each spectrum is forced to be zero and each spectrum is forced to have unit standard deviation across all samples) or mean centering (where the average is subtracted from each variable). In NIR spectroscopy, the mean centering is more common. This operation is called mean centering and ensures that all results will be interpretable in terms of variation around the mean. It is recommended for all practical applications (Nicolaï et al., 2007).

2.3.2 Under-/Over-Fitting and Model Tuning

Under- and over-fitting is a concern for any predictive model regardless of research field. Several strategies exist to have confidence that the built model will predict new samples with a similar degree of accuracy on the set of data for which the model was evaluated. Without this confidence, the model’s predictions are useless. All modeling efforts are constrained by the available data. For many problems, the data may have a limited number of samples, may be of less than desirable quality, and/or may be unrepresentative of future samples. Almost all predictive modeling techniques have tuning parameters that allow the model to bend to find the structure in the data. Therefore, the existing data must be used to identify settings for the model parameters that will give the best and most realistic predictive performance (known as model tuning). Traditionally, this is achieved by splitting the existing data into training and test sets. The training set is used to build and tune the model, and the test set is used to estimate the model's predictive performance. The choice of data splitting method depends on characteristics of the existing data such as its size and structure. When the number of samples is not large, a strong case can be made that a test set should be avoided because every sample may be needed for model building. Additionally, the size of the test set may not have sufficient power or precision to make reasonable judgements. Resampling methods, such as cross-validation, can be used to produce appropriate estimates of model performance using the training set (Kuhn and Johnson, 2013). After model calibration, one major issue is the selection of the optimal number of Latent Variables (LVs), which is generally carried out on the basis of cross validation procedures. This should enable the optimization of the complexity of the multivariate model on the basis of the predictive ability of the model itself. Cross validation is usually performed by dividing samples in cross validation groups (also known as cancellation groups). Each cross validation group is removed from the training set, one at a time. Each time, the model is calibrated on the remaining training samples and then used to predict samples of the cross validation group. Samples are usually divided in cross validation groups on the basis of two procedures: venetian blinds or contiguous blocks. At this stage, only samples belonging to the training set are used to validate the model and select the optimal number of latent variables, while the samples previously randomly selected in the test set are not considered at all. There are also other procedures to internally validate a model. However, cross validation is commonly used because it is statistically founded, simple to implement and fast to run (Ballabio and Consonni, 2013). The selection of optimal number of LVs is performed on the basis of the trends of error rate in calibration and cross-validation (Figure 2.4). Choosing the correct number of LVs allows to find the optimal trade-off between under-fitting and over-fitting. Statistically comparing two models with a different number of selected LVs, if the performance are not significantly different, the model with fewer variables is preferable in terms of simplicity, interpretation and stability.

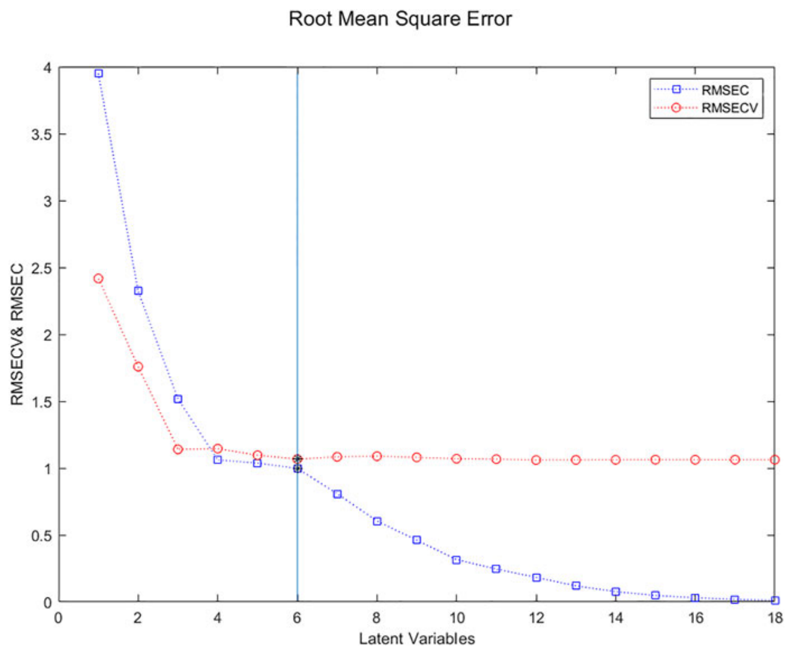

Figure 2.5: *Example of selection of LVs on the basis of cross-validation procedure.*

2.3.3 Quantitative Measurements – Linear Regression Models

Multivariate regression techniques aim at establishing a relationship between the n × 1 vector of observed response values y ('Y-variables'; quality attributes of interest, such as soluble solids content and dry matter content) and the n × N spectral matrix X ('X-variables'), with n the number of spectra (or samples) and N the number of wavelengths. The regression techniques can be linear (e.g., Partial Least Squares) or non-linear (e.g., Neural Networks, Support Vector Machines, K-Nearest Neighbors, etc.).

All linear models are akin to linear regression in that each can directly or indirectly be written in the form:

(2.1) $$y_i = b_0 + b_1 x_{i1} + b_2 x_{i2} + \cdots + b_P x_{iP} + e_i$$

where y_i represents the numeric response for the ith sample, b_0 represents the estimated intercept, b_j represents the estimated coefficient for the *j*th predictor, x_{ij} represents the value of the *j*th predictor for the *i*th sample, and e_i represents random error that cannot be explained by the model. When a model can be written in the form of Eq. 2.1, it is *"linear in the parameters"* (Kuhn and Johnson, 2013).

The objective of multiple linear regression (MLR) is to find the plane that minimizes the sum-of-squared errors (SSE) between the observed and predicted response:

(2.2) $$SSE = \sum_{i=n}^{n} (y_i - \hat{y}_i)^2$$

Hence, in the case of NIR spectroscopy, y is approximated by a linear combination of the spectral values at every single wavelength. A stepwise multiple linear regression (SMLR) technique may be applied to select a number of variables for the equation. SMLR selects first the variable with the largest correlation with the Y-data, then a second variable that results in the best improvement of the accuracy of the prediction, then a third variable and so on until no further significant improvement can be obtained. For development of NIR-based predictive models, MLR typically do not perform well because of the often high co-linearity of the spectra and easily lead to overfitting and loss of robustness of the calibration models (Nicolaï et al., 2007).

Principal component regression is a two-step procedure, which first decomposes the X by a principal component analysis (PCA) and then fits a MLR model, using a small number of principal components (PCs) (or latent variables) instead of the original variables as predictors. The advantage with respect to MLR is that the X-variables (PCs) are uncorrelated, and that the noise is filtered. Also, usually a small number of PCs is sufficient. A drawback is that the principal components are ordered according to decreasing explained variance of the spectral matrix, and the first principal components used in the regression model are not necessarily the most informative with respect to the response variable (Nicolaï et al., 2007).

The Partial Least Squares regression was introduced by Wold in 1966 and then, the same authors, adapted this technique in 1983 (Wold et al., 1966, 1982 and 1983). The PLS algorithm iteratively tries to find underlying or latent relationships between the predictors that are highly correlated with the response. For a univariate response, each iteration of the algorithm assesses the relationship between the predictors (X) and the response (y) and numerically summarizes this relationship with a vector of weights (w); this vector is also known as the direction. The predictor data are then orthogonally projected onto the direction to produce scores (t). The scores are then used to generate loadings (p), which measure the correlation of the score vector with the original predictors. At the end of each iteration, the predictors and response are "deflated" by subtracting the current estimate of the predictor and response structure, respectively. The new “deflated” predictor and response information is then used to generate the next set of weights, scores and loadings. These quantities are stored sequentially in matrices W, T and P, respectively, and are used to predict new samples and calculate predictor importance. A schematic of the PLS relationship between predictors and response is shown in Figure 2.5 (Kuhn and Johnson, 2013).

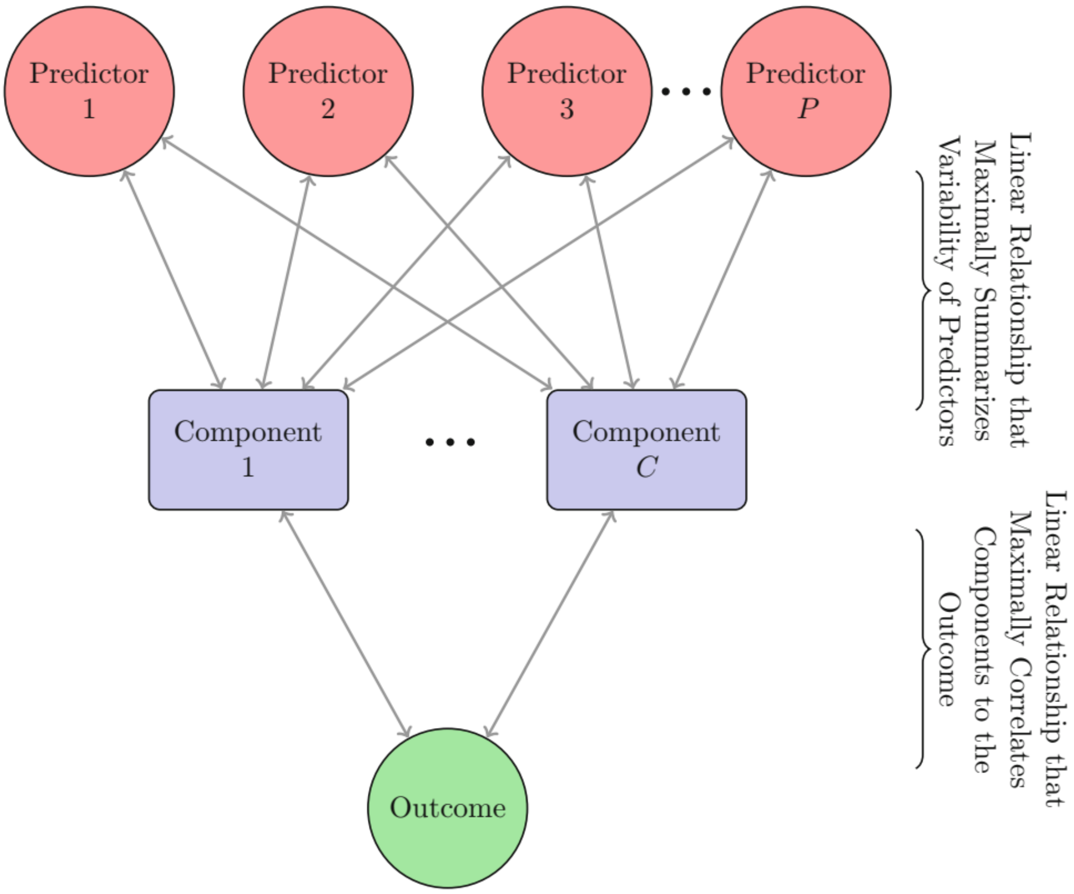

Figure 2.6: *A diagram depicting the structure of a PLS model. PLS finds components that simultaneously summarize variation of the predictors while being optimally correlated with the outcome (Kuhn and Johnson, 2013).*

Prior to performing PLS, the predictors should be centered and scaled, especially if the predictors are on scales of differing magnitude. Once the predictors have been preprocessed, the PLS model can be computed. PLS has one tuning parameter: the number of components to retain. Resampling techniques, such as cross-validation (section 2.3.2), are necessary to determine the optimal number of components (LVs).

2.3.4 Model Performances Evaluation

When the outcome is a number (quantitative analysis), the most common method for characterizing a model predictive capabilities is to use the root mean squared error (RMSE). This metric is a function of the model residuals, which are the observed values minus the model predictions. The mean squared error (MSE) is calculated by squaring the residuals, summing them and dividing by the number of samples. The RMSE is then calculated by taking the square root of the MSE so that it is in the same units as the original data. The value is usually interpreted as either how far (on average) the residuals are from zero or as the average distance between the observed values and the model predictions. Another common metric is the coefficient of determination, commonly written as R^2. This value can be interpreted as the proportion of the information in the data that is explained by the model. Thus, an R^2 value of 0.75 implies that the model can explain three-quarters of the variation in the outcome. There are multiple formulas for calculating this quantity, although the simplest version finds the correlation coefficient between the observed and predicted values (usually denoted by R) and squares it. While this is an easily interpretable statistic, the practitioner must remember that R^2 is a measure of correlation, not accuracy (Kuhn and Johnson, 2013).

The MSE can be decomposed into more specific pieces. Formally, the MSE of a model is equal to:

$$MSE = \frac{1}{n}\sum_{i=1}^{n}(y_i - \hat{y}_i)^2 \quad (2.3)$$

where y_i is the outcome and is $\hat{y}_i$the model prediction of that sample outcome. If we assume that the data points are statistically independent and that the residuals have a theoretical mean of zero and a constant variance of σ^2, then:

$$E[MSE] = \sigma^2 + (Model\ BIAS)^2 + Model\ Variance \quad (2.4)$$

where E is the expected value. The first part (σ^2) is usually called "irreducible noise" and cannot be eliminated by modeling. The second term is the squared BIAS of the model. The BIAS correspond to the difference of the mean of the predicted versus the mean of the measured *y* values. It is also called the error of means. The BIAS comes from systematic errors (e.g., due to the instrument, methodology of analysis, and even discrepancies in the reference analysis). Most of these sources of errors can be mitigated (instrument, methodology, reference analysis), but others (e.g., the lack of fit of model) really depend on the robustness of the model with regard to these new conditions. In other words, it reflects how close the functional form of the model can get to the true relationship between the predictors and the outcome and it represents another parameters commonly used to evaluate the model performance (Kuhn and Johnson, 2013; Bellon-Maurel et al., 2010).

2.4 References

Aghbashlo, M., Hosseinpour, S., Ghasemi-Varnamkhasti, M., 2014. Computer vision technology for real-time food quality assurance during drying process. Trends Food Sci. Technol. https://doi.org/10.1016/j.tifs.2014.06.003

Arendse, E., Fawole, O. A., Magwaza, L. S. and Opara, U. L. (2018). Non-destructive prediction of internal and external quality attributes of fruit with thick rind: A review. *Journal of Food Engineering* 217, 11–23. URL: *http://dx.doi.org/10.1016/j.jfoodeng.2017.08.009*

Ballabio, D., Consonni, V., 2013. Classification tools in chemistry. Part 1: Linear models. PLS-DA. Analytical Methods. https://doi.org/10.1039/c3ay40582f

Baltazar, A., Aranda, J. I. and González-Aguilar, G. (2008). Bayesian classification of ripening stages of tomato fruit using acoustic impact and colorimeter sensor data. *Computers and Electronics in Agriculture* 60(2), 113–121. URL: *http://www.sciencedirect.com/science/article/pii/S0168169907001627*

Bedini, G., Nallan Chakravartula, S.S., Bastianelli, G., Caccia, R., Contarini, M., Morales-Rodríguez, C., Rossini, L., Speranza, S., Vannini, A., Moscetti, R., Massantini, R., 2020. Feasibility of ft-nir spectroscopy and vis/nir hyperspectral imaging for sorting unsound chestnuts. Italus Hortus 27, 3–18. https://doi.org/10.26353/j.itahort/2020.1.0318

Bellon-Maurel, V., Fernandez-Ahumada, E., Palagos, B., Roger, J.M., McBratney, A., 2010. Critical review of chemometric indicators commonly used for assessing the quality of the prediction of soil attributes by NIR spectroscopy. TrAC - Trends in Analytical Chemistry. https://doi.org/10.1016/j.trac.2010.05.006

Benford, D., Bignami, M., Chipman, J.K., Ramos Bordajandi, L., 2022. Assessment of the genotoxicity of acrylamide. EFSA Journal 20. https://doi.org/10.2903/j.efsa.2022.7293

Biedermann-Brem, S., Noti, A., Grob, K., Imhof, D., Bazzocco, D., Pfefferle, A., 2003. How much reducing sugar may potatoes contain to avoid excessive acrylamide formation during roasting and baking? Eur. Food Res. Technol. 217, 369–373. https://doi.org/10.1007/s00217-003-0779-z

Brunt K, Drost WC (2010) Design, construction, and testing of an automated NIR in-line analysis system for potatoes. Part I: Off-line NIR feasibility study for the characterization of potato composition. Potato Res 53:25–39. doi: 10.1007/s11540-010-9149-y

Cabezas-Serrano, A.B., Amodio, M.L., Cornacchia, R., Rinaldi, R., Colelli, G., 2009. Suitability of five different potato cultivars (Solanum tuberosum L.) to be processed as fresh-cut products. Postharvest Biol. Technol. 53, 138–144. https://doi.org/10.1016/j.postharvbio.2009.03.009

Daniels-Lake, B.J., Prange, R.K., Kalt, W., Walsh, J.R., 2007. Methods to minimize the effect of ethylene sprout inhibitor on potato fry color. Potato Research 49, 303–326.

Du, C.J., Sun, D.W., 2004. Recent developments in the applications of image processing techniques for food quality evaluation. Trends Food Sci Technol 15, 230–249. https://doi.org/10.1016/j.tifs.2003.10.006

Du, Z., Hu, Y., Ali Buttar, N. and Mahmood, A. (2019). X-ray computed tomography for quality inspection of agricultural products: A review. *Food Science and Nutrition* **7**(10), 3146–3160.

Eurostat, 2013. http://ec.europa.eu/eurostat (Copyright © Eurostat).

Gikundi, E.N., Buzera, A.K., Orina, I.N., Sila, D.N., 2022. Storability of Irish Potato (Solanum tuberosum L.) Varieties Grown in Kenya, Under Different Storage Conditions. Potato Res. https://doi.org/10.1007/s11540-022-09575-8

Haase NU (2003) Estimation of dry matter and starch concentration in potatoes by determination of under-water weight and near infrared spectroscopy. Potato Res 46:117–127. doi: 10.1007/BF02736081

Haase NU (2011) Prediction of potato processing quality by near infrared reflectance spectroscopy of ground raw tubers. J Near Infrared Spectrosc 19:37–45. doi: 10.1255/jnirs.919

Harker, F. R., Feng, J., Johnston, J. W., Gamble, J., Alavi, M., Hall, M. and Chheang, S. L. (2019). Influence of postharvest water loss on apple quality: The use of a sensory panel to verify destructive and non-destructive instrumental measurements of texture. *Postharvest*

Biology and Technology 148 (October 2018), 32–37. URL: *https://doi.org/10.1016/j.postharvbio.2018.10.008*

Hassoun, A., Aït-Kaddour, A., Abu-, A.M., Bhojraj Rathod, N., Bader, F., Barba, F.J., Biancolillo, A., Cropotova, J., Galanakis, C.M., Jambrak, R., Lorenzo, J.M., Måge, I., Ozogul, F., n.d. The fourth industrial revolution in the food industry-Part I: Industry 4.0 technologies 2.

Helgerud T, Wold JP, Pedersen MB, et al (2015) Towards on-line prediction of dry matter content in whole unpeeled potatoes using near-infrared spectroscopy. Talanta 143:138–144. doi: 10.1016/j.talanta.2015.05.037

Heltoft P, Wold AB, Molteberg EL (2017) Maturity indicators for prediction of potato (Solanum tuberosum L.) quality during storage. Postharvest Biol Technol 129:97–106. doi: 10.1016/j.postharvbio.2017.03.011

Ibba, P., Falco, A., Abera, B.D., Cantarella, G., Petti, L., Lugli, P., 2020. Bio-impedance and circuit parameters: An analysis for tracking fruit ripening. Postharvest Biol Technol 159. https://doi.org/10.1016/j.postharvbio.2019.110978

Kakani, V., Nguyen, V.H., Kumar, B.P., Kim, H., Pasupuleti, V.R., 2020. A critical review on computer vision and artificial intelligence in food industry. J Agric Food Res. https://doi.org/10.1016/j.jafr.2020.100033

Kirtil, E., Cikrikci, S., McCarthy, M. J. and Oztop, M. H. (2017). Recent advances in time domain NMR & MRI sensors and their food applications. *Current Opinion in Food Science* 17, 9–15. URL: *http://dx.doi.org/10.1016/j.cofs.2017.07.005*

Kuhn, M., Johnson, K., 2013. Applied Predictive Modeling. Springer. Chapter 4, pp 61–92

López A, Arazuri S, García I, et al (2013) A review of the application of near-infrared spectroscopy for the analysis of potatoes. J Agric Food Chem 61:5413–5424. doi: 10.1021/jf401292j

Moscetti, R., Haff, R.P., Ferri, S., Raponi, F., Monarca, D., Liang, P., Massantini, R., 2017. Real-Time Monitoring of Organic Carrot (var. Romance) During Hot-Air Drying Using Near-Infrared Spectroscopy. Food Bioprocess Technol. 10, 2046–2059. https://doi.org/10.1007/s11947-017-1975-3

Nallan Chakravartula, S.S., Moscetti, R., Bedini, G., Nardella, M., Massantini, R., 2022. Use of convolutional neural network (CNN) combined with FT-NIR spectroscopy to predict food adulteration: A case study on coffee. Food Control 135. https://doi.org/10.1016/j.foodcont.2022.108816

Nicolaï BM, Beullens K, Bobelyn E, et al (2007) Nondestructive measurement of fruit and vegetable quality by means of NIR spectroscopy: A review. Postharvest Biol Technol 46:99–118. doi: 10.1016/j.postharvbio.2007.06.024

Pierce, K.M., Kehimkar, B., Marney, L.C., Hoggard, J.C., Synovec, R.E., 2012. Review of chemometric analysis techniques for comprehensive two dimensional separations data. J. Chrom. A 1255, 3-11.

Pinhero R.G., Yada R.Y., 2016. Postharvest Storage of Potatoes. In: Singh J, Kaur L., Advances in potato chemistry and technology, Second edi. Academic Press, Chapter 10, pp 283–309

Rathore, A.S., Kapoor, G., 2016. Implementation of Quality by Design for processing of food products and biotherapeutics. Food Bioprod. Process. https://doi.org/10.1016/j.fbp.2016.05.009

Shiroma C, Rodriguez-Saona L (2009) Application of NIR and MIR spectroscopy in quality control of potato chips. J Food Compos Anal 22:596–605. doi: 10.1016/j.jfca.2008.09.003

Sirisha, S., Chakravartula, N., Bandiera, A., Nardella, M., Bedini, G., Ibba, P., Massantini, R., Moscetti, R. (2023). Computer vision-based smart monitoring and control system for food drying: a study on carrot slices.

Teper-Bamnolker, P., Dudai, N., Fischer, R., Belausov, E., Zemach, H., Shoseyov, O., Eshel, D., 2010. Mint essential oil can induce or inhibit potato sprouting by differential alteration of apical meristem. Planta 232, 179–186. https://doi.org/10.1007/s00425-010-1154-5

Torres, M.D.Á., Parreño, W.C., 2016. Thermal Processing of Potatoes, in: Singh, J., Kaur, L., Advances in Potato Chemistry and Technology. Academic Press, Chapter 14, pp. 403–457.

Wold H (1966). “Estimation of Principal Components and Related Models by Iterative Least Squares.” In P Krishnaiah (ed.), “Multivariate Analyses,” pp. 391–420. Academic Press, New York.

Wold H (1982). “Soft Modeling: The Basic Design and Some Extensions.” In K Joreskog, H Wold (eds.), “Systems Under Indirect Observation: Causality, Structure, Prediction,” pt. 2, pp. 1–54. North–Holland, Amsterdam.

Wold S, Martens H, Wold H (1983). “The Multivariate Calibration Problem in Chemistry Solved by the PLS Method.” In “Proceedings from the Conference on Matrix Pencils,” Springer–Verlag, Heidelberg.

Xu, X., Lu, Y., Vogel-Heuser, B., Wang, L., 2021. Industry 4.0 and Industry 5.0—Inception, conception and perception. J Manuf Syst 61, 530–535. https://doi.org/10.1016/j.jmsy.2021.10.006

Zommick, D.H., Knowles, L.O., Knowles, N.R., 2014. Tuber respiratory profiles during low temperature sweetening (LTS) and reconditioning of LTS-resistant and susceptible potato (Solanum tuberosum L.) cultivars. Postharvest Biol. Technol. 92, 128–138. https://doi.org/10.1016/j.postharvbio.2014.01.020

CHAPTER 3

POTATO CULTIVAR CHARACTERIZATION

3.1 CHARACTERIZATION OF LOCAL POTATO VARIETIES (*Solanum tuberosum* L.) FOR THEIR OPTIMAL END-USE: EFFECT OF GENOTYPE AND STORAGE TIME ON QUALITY PARAMETERS

Giacomo Bedini, Andrea Bandiera, Swathi Sirisha Nallan Chakravartula,
Riccardo Massantini, Roberto Moscetti*
Department of Innovation in Biology, Agri-food and Forest systems,
University of Tuscia, Italy
** Corresponding author*

INDEX

KEYWORDS: *Solanum tuberosum L.; quality assessment, post-harvest storage, cultivar properties, processing scheduling*

ABSTRACT

Four pre-selected potato cultivars (*Solanum tuberosum* L.) from "Patata dell'Alto Viterbese PGI" area were subjected to a physico-chemical and enzymatic characterization in order to evaluate their suitability for specific destination of use. The most important chemical, physical, physico-chemical and enzymatic parameters were analyzed at harvest and every month during a 6-months storage period along two production seasons (i.e., 2020 and 2021). The one-way within subject ANOVA results as well as the Principal Component Analysis showed the best properties of Fontane cultivar for processing industry, especially for frying (e.g., chips, French fries, etc.). Compared with the other tested cultivars, Fontane reported i) the highest DM content

(> 20 %), ii) the lowest TPC and RSC, iii) the highest firmness, (iv) a low susceptibility to browning and a high tolerance to the Low-Temperature Sweetening (LTS). The Jelly cultivar showed suitable properties for multipurpose use, both for domestic (i.e., roasting, homemade "gnocchi", etc.) and industrial purposes (i.e., fresh-cut or dried potato). It reported high DM content (~ 20 %) and firmness, the lowest PPO activity, a good TPC but RSC higher than Fontane. This latter attribute makes Jelly a variety poorly suited to industrial frying. Constance and Gaudi cultivars showed good properties for domestic use like boiling and steaming, reporting a medium-low DM content and firmness. However, both cultivars reported a low tolerance to the LTS and Gaudi cultivar showed the worst properties for processing, reveling the highest susceptibility to browning.

INTRODUCTION

Due to the increasing consumer knowledge, awareness and attention to food-quality and safety, farmers, processing industries and sellers must ensure high standards, studying and monitoring many aspects from the farm to the shelf. Even in the potato supply-chain, awareness of the relevance of the biochemical composition of tubers for the quality and safety of the final product has been growing in the last years.

Nowadays, potato (*Solanum tuberosum* L.) ranks fourth as the most important crop in the world after maize, wheat and rice in terms of area covered and production (Gikundi et al., 2022) with a total of 359 million tons produced in 2020 (FAOSTAT, 2022). Potatoes are cultivated in 160 countries with over 4000 known cultivars. In Italy, the potato production in 2022 was 1.38 million tons. The Lazio region is the 6th largest producer with ~64k tons of which ~45k tons (70 % approx.) are produced in the north of Lazio (ISTAT, 2022). In this area, since 2014, the potato supply chain has held the quality designation PGI ("Patata IGP dell'Alto Viterbese") from the European Community. About 20 potato varieties are cultivated in this area, but in the last few years, some local varieties have been replaced with high-yielding cultivars, without considering other important aspects such as their physico-chemical qualities and their link to the specific environment. This represents one factor contributing to the reduction of the crop's biodiversity in contrast with the 15th Sustainable Development Goal, where halting the loss of biodiversity is one of the most important targets (United Nations, 2022). The physico-chemical and enzymatic characterization of potato cultivars is a crucial aspect of accurate varietal selection, considering not only yield and other agronomic and economic aspects (resistance to diseases, water demand, etc.), but also the final product quality and certain parameters related to consumer health.

Potatoes are processed to obtain different types of products (dried, pre-cooked, frozen, snacks, etc.) or they are sold as a raw product. At home, potatoes can be cooked (fried, roasted or boiled) or can be used for other preparations (e.g., dumplings). For each different destination of use, there are suitable and unsuitable varieties, depending on their physico-chemical and enzymatic parameters. In fact, the most appropriate definition of quality for potatoes is "the suitability for their intended use" (Pinhero and Yada, 2016). Potatoes used for processing must possess certain quality characteristics, and as a result some potato varieties have been developed specifically for the purpose of processing. Regarding home cooking, there is still limited consumer knowledge and poor communication by companies on the influence of the chemical and physical composition of raw potatoes on the quality and safety of the final product. Specifically, the dry matter (DM) content, carbohydrates (reducing and nonreducing sugars), textural characteristics (e.g., firmness), and color-related alterations (post-cut browning and after-cooking darkening) are the key quality parameters influencing the destination of use (Torres and Parreño, 2016). DM content is one of the most important attributes in processing qualities, which substantially affect the texture and the potato suitability for processing. Generally, potato varieties used for processing must have a DM content greater than 20 %. In contrast, a medium DM content (16-19 %), corresponding to medium-firm, slightly floury potatoes that do not disintegrate, is the most suitable for multipurpose and domestic use. DM content of tubers is affected by the location of production, the year, cultivar, and storage conditions (Pritchard and Scanlon, 1997). Textural characteristics influence quality and palatability of potato products (Torres and Parreño, 2016). Another important quality parameter is the sugar content (sucrose and reducing sugars). The sugar content of potatoes is affected by the genotype (varieties with low dry matter content tend to accumulate more sugar) and by several pre- and post-harvest factors (e.g., tubers maturity and storage conditions) (Kumar et al., 2004). Potatoes containing more than 2 % of reducing sugars (dry weight) are unacceptable for processing and for specific domestic uses (Torres and Parreño, 2016). In fact, the high temperatures required during frying or baking result in the nonenzymatic reaction of free amino acids, particularly asparagine, with the reducing sugars in the Maillard reaction. If reducing sugar content is too high, this results in unacceptable rates of browning and also acrylamide production (McKenzie and Corrigan, 2016). Specifically, in order to minimize consumer health risks associated with the excessive acrylamide production it is recommended to use potatoes with a reducing sugar content ranging from 0.1 to 0.5 % (dry weight) (Biedermann-Brem et al., 2003; EFSA, 2015). Other important aspects concern color-related alterations. Both post-cut browning and after-cooking darkening (ACD) are influenced by the phenol content and composition. Moreover, oxidative enzyme activity (e.g., polyphenol oxidase) plays a key role for enzymatic browning. Consequently, susceptibility to browning depends on physico-chemical and enzymatic composition, varying between different cultivars (Cabezas-Serrano et al., 2009; Wang-Pruski and Nowak, 2004).

In post-harvest, the above-mentioned quality parameters, are influenced by storage conditions. It is imperative for both growers and processors to maintain quality based on end use. Potatoes are generally stored in moveable pallet boxes inside dark buildings at 6-8 °C and 90-95 % of relative humidity, using different natural or chemical compounds as sprout inhibitors (Gómez-Castillo et al., 2013). At storage temperatures below 10 °C, one of the most important biochemical changes to monitor is the accumulation of reducing sugars, known as Low-Temperature Sweetening (LTS), especially for cultivars with low tolerance to this process (Zommick et al., 2014).

Considering these aspects, studying the physico-chemical composition of potato cultivars at harvest is not sufficient. In order to identify and select varieties for a specific destination of use, it is fundamental to consider also how tubers maintain their quality attributes during the months of storage. With this information available, producers and processors can schedule sales and processing, always offering the consumer a high-quality product. Moreover, providing more details on labels (e.g., best culinary use) according to potato cultivar and storage status would prevent improper use of the raw material. This could avoid, for instance, excessive intake of acrylamide at domestic levels.

Although several researches were performed to investigate the effect of genotype and storage time on suitability for specific destination of use (Cabezas-Serrano et al., 2009; Silveira et al., 2017), to the best of our knowledge, there are few studies comparing the trends of the main quality parameters of different cultivars for each months of storage with the aim to elaborate a schedule where the best destination of use are reported for each cultivar, considering also domestic uses. This study was performed on four cultivars, and it will form the basis for further investigations to be conducted on all the varieties grown in the "Patata dell'Alto Viterbese" PGI area. Specifically, the investigation aimed at providing local consortiums with useful information (i) to identify the best cultivar for a specific intended end use, (ii) to know how the most important quality parameters change during storage, (iii) to schedule sales and processing, and (iv) to provide more details to the consumer.

MATERIAL AND METHODS

Raw material and storage conditions

The study was conducted on potato tubers (*Solanum tuberosum* L.) provided by the "Patata dell'Alto Viterbese" PGI consortia (C.C.OR.A.V. and Coop. Centro Agricolo Alto Viterbese, Viterbo, Italy). Four potato cultivars were selected through preliminary tests conducted on thirteen cultivars grown in this area. The selection was carried out analyzing their DM content and susceptibility to post-cut browning, but also considering the information collected by surveys at the consortia, studying literature and by consulting websites of seed tubers sellers or specific databases like the European Cultivated Potato Database. Constance, Fontane and Jelly were selected as their DM content ranged from medium to high (18-22 % approx.) and they also showed low susceptibility to post-cut browning. Moreover, they are medium/late-cultivars, and the suggested destination of use is for industrial or domestic frying (especially Fontane and Jelly) and all culinary uses (especially Jelly and Constance). Differently, Gaudi was selected as a "control", as it reported a high susceptibility to post-cut color changes and a medium-low DM content (~17 %). Moreover, Gaudi is an early variety, and it is suggested for domestic use such as boiling or steaming. The time of harvesting was decided by the farmers according to the guidelines of the consortia. Gaudi and Constance were harvested in the first half of August, while Jelly and Fontane were harvested in the first ten days of September. At harvest time and every month for six months of storage until February or March (when some tubers started to sprout), a batch of approximately five kilograms per variety of raw potato tubers were sampled and analyzed. The samples were stored inside the same storage room of the consortium in four different pallet boxes, one for each cultivar. The storage temperature was 7 ± 1 °C, the relative humidity ranged from 88 to 93 % and an anti-sprouting system based on ethylene gas (Restrain Company Ltd, Breda, Netherlands) was applied. The analyses were repeated along two production seasons (i.e., 2020 and 2021).

Sample preparation

Tubers were washed in tap water in order to remove traces of soil and other impurities. After this, every batch was split in two sub-batches (Fig. 3.1). One sub-batch (10 tubers) was used for the analysis of firmness; the other sub-batch (15 tubers) was destined to all other analyses. Both dry matter content and color assessment were determined on fresh samples and during these analyses, a slice from each potato tuber was sampled, cut in cubes and freeze dried to be stored until other physico-chemical and enzymatic analyses.

Potato cultivars characterization

Firmness

Firmness was measured cutting two slices for each tuber (~ 1-cm thick) and puncturing each slice on five points (four measurements on the outer medulla and one on the inner medulla) with an Instron Universal Testing Instrument (Model 4301, Instron Corporation, Norwood, MA, USA). The crosshead speed was 10 mm/min. An 8-mm diameter convex tip Magness-Taylor type probe was used. The penetration depth was set at 6 mm. This test measured individual tuber firmness based on the resistance of the potato flesh to penetration by the probe. A total of 100 measurements were acquired for each potato cultivar (5 puncture × 2 slices × 10 tubers).

Colorimetric assessment

Each potato tuber was cut in half and the change in color on the exposed surface to air at ambient temperature was measured (at CIE Standard Illuminant D65 with a 10° standard observer) by using a Konica Minolta colorimeter (Model CM-2600d). For each half of tuber, five measurements were performed (four measurements on the outer medulla and one on the inner medulla). Colorimetric coordinates (L*, a*, b*) were measured at four different times of air exposure (0, 30, 60 and 120 min). The CIELab color difference (ΔE*) was calculated with respect to time 0, based on the following equation (3.1):

$$\Delta E^* = \sqrt{\Delta \mathrm{L}^2 + \Delta \mathrm{a}^2 + \Delta \mathrm{b}^2} \tag{3.1}$$

ΔE* values reported in the results and discussion section refer to CIELab color difference after 120 min of air exposure.

Dry matter content

Potato tubers were peeled and homogenized and ~ 10 g were dried at 65 °C for 72 h. DM content was expressed as a percentage by mass (grams per 100 grams). The dry matter determination was performed in triplicate.

Total Phenol Content (TPC)

One gram of freeze-dried potato powder was homogenized with 20 ml of methanol:water solution (80:20 v/v) in an orbital shaker (mod. 711, Tecnochimica Moderna S.r.l., Italy) in dark at ambient temperature for 24 h. The extract was centrifuged (mod. PK121R, ALC, Italy) at approx. 3400 g for 10 min at 18 °C, filtered and stored at 4 ± 1 °C prior to the assay.

Total phenol content (TPC) was determined by the Folin–Ciocâlteu method with slight modifications (Singleton and Rossi, 1965). The assay was conducted by mixing 1.44 ml of deionized water, 0.16 ml of extract, 0.1 ml of Folin–Ciocâlteu reagent, and 0.3 ml of sodium carbonate solution (7.5 % w/v). The mixture was stored in dark at room temperature for 2 h. The absorbance was read at 760 nm using a UV-Vis spectrophotometer (ONDA UV-20, Giorgio Bormac s.r.l, Carpi, Italy) against a blank prepared by mixing 1.44 ml of deionized water, 0.16 ml of methanol:water solution (80:20 v/v), 0.1 ml of Folin–Ciocâlteu reagent, and 0.3 ml of sodium carbonate solution (7.5 % w/v).

The total phenol content was calculated on the basis of the calibration curves of gallic acid and was expressed as mg of Gallic Acid Equivalents per 100 g of dry weight (mg GAE 100 g^{-1}). The TPC was measured in triplicate.

Reducing Sugar Content (RSC)

One gram of freeze-dried potato powder was homogenized with 20 ml of distillated water in an orbital shaker (mod. 711, Tecnochimica Moderna S.r. l, Italy) at ambient temperature for 15 min. The extract was centrifuged (mod. PK121R, ALC, Italy) at approx. 3400 g for 10 min at 18 °C and stored at 4 ± 1 °C prior to the assay.

Reducing sugar content (RSC) was determined by using the 3,5-Dinitrosalicylic acid (DNS) reagent according to Lindsay (1973), with slight modifications. The DNS reagent was prepared dissolving at room temperature 1 g of DNS, 0.05 g of sodium sulphite and 20 g of sodium potassium tartrate (Rochelle salt) in 50 ml of NaOH (2 % w/v). The volume was then made up to 100 ml with distilled water. The assay was conducted by mixing in the tubes 1.5 ml of DNS reagent and 0.75 ml of each extract. The DNS:extract ratio was case by case adapted on the basis of the estimated concentration in reducing sugar of sample. The tubes were placed in a thermoblock (TD 200 P1, Falc Intruments s.r.l., Treviglio, Italy) set at 135 °C for 15 min, transferred to ice for 10 min to rapidly cool down and then brought to room temperature. Prior to the readings, all samples were diluted with 5 ml of distilled water. The absorbance was read at 540 nm in a UV-Vis spectrophotometer (ONDA UV-20, Giorgio Bormac s.r.l, Carpi, Italy) against a blank prepared by mixing 1.5 ml of DNS reagent and 0.75 ml of distilled water.

The reducing sugar content was calculated on the basis of the calibration curves of glucose and was expressed as g of glucose equivalents per 100 g of dry weight (g GluE 100 g^{-1}). The reducing sugar content was measured in triplicate.

Polyphenol oxidase (PPO) activity

Enzyme activity was determined in accordance with Moscetti et al. (2019) with several modifications. One point five grams of freeze-dried potato powder was homogenized with 15 ml of PBS (Phosphate Buffer Saline 0.1 M, pH 6.5) containing 2 % (w/v) of polyvinylpolypyrrolidone (PVPP). The mixture was centrifuged at approx. 6300 g for 20 min at 4 ± 0.5 °C; the supernatant was collected and stored at 4 ± 1 °C prior to the enzymatic assay. The assay was performed using an UV-Vis spectrophotometer (ONDA UV-20, Giorgio Bormac s.r.l, Carpi, Italy) at 420 nm for 2 min. Before enzymatic assays, PBS was placed in a water bath at 27 ± 0.5 °C, whose temperature was controlled by a refrigerated/heated bath circulator (HAAKE K10, Thermo Fisher Scientific, Waltham, MA). The final reaction mixture contained 0.6 ml of crude enzyme, 2.2 ml of PBS (0.1 M, pH 6.5) and 0.2 ml of catechol (2 mmol).

One unit of enzyme activity (U) was defined as an increase in absorbance of 0.001 min-1. PPO enzymatic activity was expressed on dry weight basis (U mg^{-1}). Enzyme activity was measured in triplicate.

Statistical analysis

Data handling and statistical analyses were performed using R software v4.2.2 coupled with the ‘Agricolae’, ‘Hmisc’ and ‘Rtsne’ packages, v1.3.5, v4.7.2 and v0.16, respectively.

For each time of storage, data were subject to One-Way within-subject ANOVA in order to evaluate differences among cultivars. The One-Way within-subject ANOVA was also performed for each cultivar to evaluate its compositional changes during storage. The analysis of variance was carried out for the two production seasons considering the season as within-subject factor. The Fisher’s pairwise comparison method was performed, and the Least Significant Difference (LSD) was calculated at an appropriate level of interaction ($p \leq 0.05$).

Pearson’s linear correlation test was computed to detect significant bivariate correlations between the measured features. The linear correlation test was evaluated for the whole dataset (i.e., data from all cultivars) as well as separately for each cultivar. The values of the Pearson correlation coefficient (r) between the parameters analyzed was considered as satisfactory when $r \geq 0.70$. Specifically, the strength of correlation was classified as follows: $0.95 \leq r \leq 1$, excellent; $0.90 \leq r < 0.95$, very good; $0.80 \leq r < 0.90$, good; $0.70 \leq r < 0.80$, weak.

Moreover, both Principal Component Analysis (PCA) and t-distributed Stochastic Neighbour Embedding (t-SNE) algorithms were individually applied to have a graphical overview of differences among cultivars developed during 6-months of storage. Regarding PCA, the original data was converted into score and loading vectors, and the screen-plot criterion was used to select the required number of principal components (PCs). The t-SNE is a non-linear FEA (Feature Extraction Algorithm) based on manifold learning with usually better performance than PCA for its capability to capture global and local structures of high-dimensional data, as well as to identify the presence of clusters at various scales (Luo et al., 2021). The algorithm initially reduces high-dimensional Euclidean distances using similarities between two data points into conditional probabilities. Subsequently, the Student's t-distribution is used to further transform the probabilities into a low-dimensional space, using a single degree of freedom. Dimensionality reduction through t-SNE was performed by setting the 'perplexity' at 18 and the 'output dimensionality' at 2. Specifically, the 'perplexity' parameter refers to the effective number of neighbours used in the t-SNE algorithm; it may affect data visualization if outside the limit of 5-50 (Luo et al., 2021). The 'output dimensionality' corresponds to the number of dimensions of the lowdimensional space in which data are "compressed".

RESULTS AND DISCUSSION

Cultivars characterization at harvest

The four potato cultivars showed a great variability in terms of physico-chemical and enzymatic composition at the harvest, as reported in Table 3.1. The DM content ranged from 17.13 % in Gaudi to 19.70 % in Fontane. Gaudi showed the highest TPC (106.58 mg GAE 100 g^{-1}) and RSC (2.71 g GluE 100 g^{-1}), but this latter value was not significantly different from that of Jelly (2.17 g GluE 100 g^{-1}). Differently, Fontane revealed both the lowest TPC (55.79 mg GAE 100 g^{-1}) and RSC (0.28 g GluE 100 g^{-1}), also reporting the highest firmness (92.51 N), followed by Jelly and Gaudi (77.82 and 75.01 N, respectively), while Constance showed the statistically lowest value (64.51 N). Regarding CIELab colour difference, Gaudi was characterized by the highest susceptibility to post-cut browning reporting a ΔE^* value (5.75) higher than the perceptibility threshold ($\Delta E^* = 3.5$) after 120 min of air exposure (Mokrzycki and Tatol, 2011). Gaudi also showed the highest PPO activity (0.93 U mg^{-1}), suggesting a likely positive correlation with the colorimetric parameter ΔE^* for this cultivar. Finally, Jelly was characterized by the lowest PPO activity. The analyses performed at the harvest confirmed the excellent aptitude of Fontane for processing, especially for frying (e.g., French fries), as specified on the European Cultivated Potato Database and as reported by Biedermann-Brem et al., (2003). In fact, its high DM content (~20 %) and firmness, the low susceptibility to browning and the low RSC are key attributes for the processing industry. Moreover, its floury structure makes it perfect for homemade or industrial "gnocchi".

Jelly showed good attributes for both processing and domestic use, thus it is possible to classify this cultivar as a dual-purpose variety. Considering its low susceptibility to post-cut browning, the lowest PPO activity and a good TPC. Jelly, at harvest, revealed good properties for fresh-cut processing. Moreover, its medium-high DM content, corresponding to good firmness and slightly floury structure, make it suitable for multipurpose and domestic use (e.g., dumplings). However, in contrast to information collected by surveys and by consulting websites of seed-tuber sellers, the Jelly cultivar appeared to be a suboptimal cultivar for processing processes such as frying (e.g., crisps or French fries). In fact, at harvest, it reported the RSC slightly higher than the suitability threshold mentioned by Torres and Parreño, (2016) for processing (2% approx.). Even for domestic use, it must be fried carefully to avoid excessive amounts of acrylamide in the final product (Biedermann-Brem et al., 2003). These results were in accordance to Ingallina et al., (2020), who performed a study on potato cultivars grown in Piedmont reporting high levels of monosaccharides (glucose and fructose) for Jelly.

Constance showed good properties for domestic use, reporting a medium DM content, good TPC, and low RSC. However, due to its low firmness, it seemed to be more suitable for boiling or steaming. Regarding processing, Constance reported good characteristics for the fresh-cut industry, showing a low susceptibility to post-cut browning.

Gaudi revealed unsuitable characteristics for processing: medium-low DM content, high RSC and high susceptibility to post-cut colour changes. The latter attribute seemed to be related to its high TPC and high PPO activity, that are directly involved in the enzymatic browning reaction (Moscetti et al., 2019). The results confirmed the suitability of Gaudi only for domestic uses, except for frying. Moreover, its high phenol content makes this cultivar nutritionally rich. In fact, potato phenolic compounds have beneficial effects for human health (Singh et al., 2020).

Cultivars characterization during storage

DM content (Fig. 3.2a) and firmness (Fig. 3.2b) showed no considerable changes during storage. Fontane always showed the highest DM (20-21 %). Only in three months, Fontane returned values not statistically different from those of Jelly, which showed medium/high DM content (19-20 %). Whereas Constance and Gaudi reported a DM content always lower than 18 %, with no significant differences between them, but significantly different from Fontane and Jelly. DM content influences the resistance to disintegration during cooking. Specifically, “waxy” potato cultivars with a low DM content (15-17 %) are characterized by moist appearance and disintegrate less. They are suitable for boiled or steamed potato (e.g., potato salad). In contrast, “mealy” potato cultivars, characterized by higher starch and DM content (>

20 %), have higher water uptake and loss during cooking than those with lower starch content. Consequently, when "mealy" potatoes are cooked, they result in dry-appearing tissue that crumbles readily. These cultivars are preferred by consumers and industry for baking and frying (McComber et al., 1988). For processing industry, the DM content also has an impact of process yield. Moreover, for dried potatoes, a low DM content lengthens the drying time, increasing the cost and the environmental impact of the process.

Regarding the firmness, Fontane always showed the highest values. Gaudi and Jelly reported intermediate values, whereas Constance was characterized by being less firm. The results confirmed that the DM content has a strong impact on textural properties like the firmness, but it is not the only factor influencing this parameter. In fact, this attribute is affected by several factors such as starch content and distribution, cell size and cell wall structure (Taylor et al., 2007). Consequently, a good cell wall structure often leads to a good firmness. Furthermore, as suggested by Cabezas-Serrano et al., (2009), a high membrane stability may contribute to the good performance of Fontane and Jelly in terms of susceptibility to browning, delaying the contact between the PPO enzyme and substrates.

The trends of DM content and firmness during storage are mainly related to two biochemical changes: respiration and water loss. Potato tubers continue to respire during storage using sugars produced by starch hydrolysis. Consequently, loss of DM content occurs during starch hydrolysis, resulting in weight loss. The other important biochemical change occurring during potato storage is the water loss. Ninety-eight percent of the moisture that leaves a tuber during storage is lost through its skin by evaporation. Both these processes are affected by storage conditions (temperature and relative humidity) and variety. Moreover, water loss also depends on other factors like heat production in potatoes, the quality of the potato skin, the sprout growth, and the duration of ventilation. The balance between DM loss through respiration and water loss through evaporation determines the changes in DM content and firmness of potato tubers, also affecting weight loss. The results showed that storing potatoes at 7 °C and controlled relative humidity stabilized DM and firmness, probably preserving the tuber weights, as confirmed by Gikundi et al., (2022).

The trends of RSC and TPC (Fig. 3.3a and 3.3b, respectively) revealed significant differences between cultivars during the storage period. The RSC of Fontane significantly increased, but it remained at an acceptable level (0.8-1.5 %), demonstrating the high tolerance to the LTS of this cultivar, as reported by Elmore et al., (2015). Differently, other cultivars largely exceeded the acceptability threshold for processing (2 %) after only one month of storage. In the last two months of storage, Constance and Gaudi reported the statistically highest RSC (~9 % and ~12 %, respectively). On the other hand, Jelly showed values statistically comparable to those of Fontane for the last three months of storage. Specifically, the RSC of Jelly increased significantly only in the first month of storage, and then stabilized (4-5 %), demonstrating a good tolerance of this variety to the LTS. The results confirmed the suitability of the Fontane cultivar for the crisps or French-fries industry not only at harvest, but also throughout all the months of storage. In fact, its RSC stabilized to value slightly higher than 0.5 % (0.8-1 %). Consequently, frying these tubers leads to low acrylamide levels in the final product, as demonstrated by Biedermann-Brem et al., (2003) and Elmore et al., (2015). Jelly is not recommended for industrial frying. However, its good tolerance to the LTS makes this variety good for domestic use, avoiding excessive sweetness in the final product which is historically regarded as an undesirable trait for potato (Burton, 1969). Moreover, also after a few months of storage, Jelly can be roasted or fried at home, following some cooking tips listed by the EFSA such as: (i) using hot-air fryers instead of conventional deep oil fryers (Zaghi et al., 2019), and (ii) frying at temperatures below 175 °C. Regarding Gaudi and Constance, these varieties showed a low tolerance to LTS. Especially in the last months of storage, the high levels of RSC reached can lead to a sweet taste even for boiled or steamed potatoes. Gaudi and Constance were definitely unsuitable for frying and roasting. In fact, these levels of glucose and fructose result in unacceptable darkening of finished fried or roasted potatoes, increasing the acrylamide production.

TPC (Fig. 3.3b) showed no clear trends, except for Gaudi, where it notably increased starting from the first month of storage (from ~95 to ~150 mg GAE 100 g^{-1}). Moreover, Gaudi always reported the highest phenol content. Jelly often showed a TPC statistically higher than Constance (from ~76 to ~94 and from ~65 to ~84 mg GAE 100 g^{-1}, respectively), while Fontane always reported the lowest values (from ~49 to ~59 mg GAE 100 g^{-1}). In addition to their nutritional value, the phenol content can also be useful in explaining the susceptibility to browning of some varieties compared to others. In fact, as reported by Brecht et al., (2004), vegetable products with higher TPC are more susceptible to browning. The effect of storage on potatoes at 4 °C and 20 °C for 110 days on phenolic content was studied by Blessington et al., (2010). No significant differences in TPC were observed after storage at 4 °C or 20 °C, confirming the trends observed for Constance, Fontane and Jelly. However, another study reported by Hasegawa et al., (1966), showed that the chlorogenic acid, the principal phenolic compound in the inner tissue of tubers, was the only compound which increased significantly during the storage of the potatoes at 4 °C. The authors postulated that the increase in chlorogenic acid during cold storage is due to the accumulation of sugars. In accordance with this statement, Gaudi showed a significant increase for both RSC and TPC starting after the first month of storage. Further investigations are also needed to study the chlorogenic acid/citric acid ratio in the potato tubers. The oxidation of the ferri-chlorogenic acid in the boiled or fried potatoes cause the negative process named after-cooking darkening (Wang-Pruski and Nowak, 2004). This browning process concern both processing industry (crisps, dried or pre-cooked potato) and domestic use (frying, boiling, etc.). The authors reported that the severity of the darkening is always higher in the cortex tissue, where the highest concentration of chlorogenic acid was detected. In fact, higher chlorogenic acid/citric acid ratio results in a darker potato product.

Figure 3.4a reports the trends of the parameter used to evaluate the post-cut browning susceptibility of tubers (CIELab color differences after 120 min of air exposure). Gaudi always showed the highest susceptibility to color changes, reporting the highest ΔE^* values except for the last month of storage, where a strong decrease was noticed. According to the classification of ΔE^* proposed by Mokrzycki and Tatol, (2011), until the 5th month, the ΔE^* values of Gaudi always were higher than the perceptibility threshold ($\Delta E^* > 3.5$) corresponding to a "clear difference" and reaching a peak at the month #3, where ΔE^* value was 8.75, corresponding to "different colors". The other cultivars showed some fluctuation without a clear pattern, reporting ΔE^* values that always ranged between "minor" (detectable by a trained observer) and "just perceptible" color differences (detectable by an untrained observer).

The PPO activity (Fig. 3.4b) showed a similar trend to ΔE^*. In other words, Gaudi showed the highest PPO activity up to the last two months of storage. Subsequently, the enzyme activity dropped to the same level of other cultivars. The PPO and ΔE^* trends of Gaudi confirm the effect of PPO activity on post-cut browning susceptibility. In fact, when PPO activity dropped, also the color difference after 120 min of air exposure became "just perceptible", despite the increase of TPC. These results allowed speculation that the drop of PPO activity could be associated with increased phenol content, particularly of the chlorogenic acid, the main phenolic compound of potato. The chlorogenic acid has good affinity with PPO activity (Thybo et al., 2006), but if it is above a certain threshold, it probably becomes an inhibiting factor. In fact, Cheng et al., (2020) reported that the relative PPO activity of fresh-cut potato slices remarkably reduced with increasing concentration of chlorogenic acid. Another possible explanation for the drop of the enzyme activity could be related to start of sprouting. In fact, the sprouting modifies the physico-chemical and nutritional properties of potatoes and can lead to the production of toxic compounds in the potato flesh, such as solanine and chaconine (Visse-Mansiaux et al., 2021). These changes could have an impact on protein components (e.g., enzymes) by altering their structure and denaturing them.

Jelly showed the lowest PPO activity, with no significant changes during storage. Fontane revealed a more stable trend than Constance, which showed a significant increase from month #3 to month #5 and then decreased in the last month. Despite a PPO activity of Constance and Fontane significantly higher than Jelly, these cultivars showed the same susceptibility to post-cut browning. This can be explained by referring to phenol content and composition. In fact, both cultivars (especially Fontane) reported a TPC lower than Jelly, thus a lower amount of substrate for the enzyme. Moreover, as reported by Thybo et al., (2006), not all the potato phenols have the same affinity with PPO enzymes. Specifically, the authors reported a good correlation of enzymatic browning and PPO activity with tyrosine and chlorogenic acid, and a negative correlation with caffeic acid. Another factor affecting the enzymatic browning is the citric acid content. Ingallina et al., (2020) reported that potato cultivars characterized by high levels of citric acid involved in the inhibition of the enzymatic browning in fresh-cut potato.

Considering that the susceptibility to browning is an important aspect for potato processing, especially for fresh-cut and dried potato, Constance, Fontane and Jelly confirmed their suitability for the whole storage period. Regarding Gaudi, there are several chemical browning inhibitors (e.g., citric acid, ascorbic acid, L-cysteine, sulfites, etc.) to control the enzymatic reactions, and also new anti-browning agents have been tested in recent studies (Feng et al., 2022; Ru et al., 2020). It should be pointed out that the use of these substances influences the quality and composition of the fresh-cut product (Rocculi et al., 2007). Furthermore, the impact on consumers' health must be considered. For example, the allergenic effect of sulfites on hypersensitive individuals is well-known (Taylor et al., 1986). Consequently, the selection and use of varieties with low susceptibility to browning is the basis for producing a quality product, also considering cost savings on the purchase of chemicals.

Results overview using PCA and t-SNE

The results showed in sections 3.1 and 3.2 are summarized in Fig. 3.5, which shows results from linear and non-linear feature extraction algorithm (PCA and t-SNE, respectively) computed on data from the physico-chemical and enzymatical analyses of the four potato cultivars for both seasons. In general, both methods confirmed the ANOVA results (data not shown), offering a clear visualization of the different properties of the four potato cultivars, at harvest and during storage. The graphical output was useful for the understanding of (i) cultivar potential for processing and of (ii) changes of quality attributes during storage.

Regarding PCA (Fig. 3.5a), the two main principal components explained the 80.38 % of total variance. Principal Components 1 and 2 (PC1 and PC2) accounted for 54.91 and 25.43 % of total variance, respectively. Despite of some overlaps especially due to the high variability of Gaudi, the score plot allows to approximately identify a cluster for each cultivar. In particular, Fontane clusters were positively correlated with both DM and firmness, and negatively correlated with both RSC and TPC. Moreover, especially in the season 2020 (○), Fontane showed a tight cluster, confirming the highest stability of this cultivar during storage. By contrast with Fontane, Constance showed a positive correlation for RSC and TPC and a negative correlation for DM and firmness. Gaudi showed a strong positive correlation with post-cut browning factors up to the 5th and 4th month of storage in the first (○) and second season (•), respectively. In addition, the scores of Gaudi were positive correlated with RSC and TPC, especially in the last months of storage, where it reported similar physico-chemical and enzymatic properties of Constance. Jelly was the only variety with a strong negative correlation with the susceptibility to browning, although it was positively correlated with RSC. As for the quality parameters included in the PCA, PPO activity and CIELab color difference (ΔE^*) were positively correlated with each other, both being in the fourth quadrant of the PCA plot. TPC showed a positive correlation with both PPO activity and ΔE^*, as well as with RSC. These results were in accordance with the PCA performed by Cabezas-Serrano et al., (2009). DM content and firmness were both in the third quadrant, demonstrating a positive correlation between them. In addition, DM content and RSC were negatively correlated with each other, confirming what Iritani, (1981) observed during the last weeks of tuber maturation.

In addition, the t-SNE analysis was also tested as non-linear method for visualizing data from the cultivar characterization (Fig. 3.5b). The improved clustering capability of this technique was already appreciable in the two-dimensional space. Finally, both t-SNE plots confirmed the goodness of data in characterizing the four selected cultivars. Anyway, t-SNE outperformed PCA in terms of cluster visualization for further analyses, as already observed by Luo et al., (2021).

Linear correlation test

The correlations showed in the PCA plot and described in previous section were statistically confirmed by the results of the Pearson's linear correlation test performed for each cultivar (Table 3.2). In general, good correlation metrics ($0.80 \leq r < 0.90$) were obtained for cultivars with medium/high variability during storage months. In fact, Fontane showed only a few unsatisfactory ($r < 0.70$) and uninteresting correlation coefficients. Constance reported good negative correlation between ΔE* and DM ($r = -0.84$) and good positive correlation between PPO activity and RSC ($r = 0.81$). This can be explained observing the trends of these parameters for this cultivar. In fact, a decreasing trend in DM coincided to an increase of ΔE*, PPO activity and RSC. Specifically, the unsatisfactory ($r = -0.67$) but significant negative correlation between DM and RSC confirmed what PCA and Iritani, (1981) had previously showed. Gaudi, the most susceptible to browning cultivar, revealed good positive correlation ($r = 0.84$) between ΔE* and PPO activity confirming that the post-cut browning of potato is mainly affected by PPO activity (Bøjer Rasmussen et al., 2021). However, this result contrasts with that of Cantos et al., (2002), who found no significant correlation between the rate of browning and any of the other biochemical and physiological attributes analyzed, including PPO activity. The Jelly cultivar showed a good positive correlation between the DM and firmness ($r = 0.81$), confirming that potato DM, predominantly consisting of starch, contributes to the textural properties (Taylor et al., 2007). Weak positive correlations resulted between ΔE* and TPC and between PPO activity and TPC ($r = 0.77$ and 0.78, respectively). These coefficients confirmed the impact of phenol content (especially the concentration of tyrosine) on enzymatic browning and PPO activity (Thybo et al., 2006).

Example of sales and production schedule

An example schedule was developed using the results of the physico-chemical and enzymatic analysis (Table 3.3). The schedule was developed on the basis of specific characteristics such as dry matter content, susceptibility to LTS and post-cut browning. This schedule recommends the monthly destination of use of each cultivar both for the processing industry and domestic use. Greater stability of potato cultivar during storage is optimal, as it guarantees the industry to process a suitable product for the whole storage period. Moreover, potatoes that retain approximately the same qualities as a freshly harvested product gives a positive image of the company (or consortium), also safeguarding the consumer’s interests and health. In this respect, Fontane represents an optimal variety, stable during storage and suitable for several domestic uses (e.g., frying, roasting or gnocchi) and for all most important industrial processing. Also Jelly showed a good stability during storage and good attitude for processing. Specifically for fresh-cut product, Jelly reported better characteristics than Fontane in terms of nutritional property (phenol content), PPO activity and susceptibility to browning. The latter aspect is important as it allows the shelf life of the product to be extended, minimizing the use of anti-browning pre-treatments. However, considering that fresh-cut potatoes can be used by consumers in different ways (frying, baking, salads, etc.), it is important to declare in the label the optimal final use, including any tips and precautions for proper use. In this respect, Fontane can be suggested for frying, while Jelly is suitable for multipurpose use, specifying the tips to reduce acrylamide production during frying. Moreover, the effect of reconditioning on this cultivar will have to be investigated. In fact, Zommick et al., (2014) reported that after a reconditioning of tubers at 16 °C for 21 days their color after frying improved due to the reduction in RSC. This process can make Jelly more suitable and safer for frying.

Constance is suitable cultivar for boiling and steaming and can be also used to be processed as fresh-cut product. However, selling and consuming this variety by December is preferable due to its low tolerance to LTS. Gaudi is only saleable as raw product by November, specifying boiling or steaming as optimal destination of use. For selling Constance and Gaudi after January and December, respectively, the effect of reconditioning will have to be investigated. In fact, the reduction of RSC tends to be more appreciable for LTS-susceptible potato cultivars (Zommick et al., 2014). Furthermore, a sensorial analysis should be performed to investigate the level of reducing sugars which corresponds to an unacceptable sweetness for consumers.

As for other end uses, such as mashed potatoes, the suitability of potato cultivars is also affected by consumers' preferences and habits. In fact, for creamy and dense mashed potatoes, varieties with medium DM-content are suggested (e.g., Constance and Gaudi). Instead, for “featherlight” mashed potatoes, cultivars with high starch content and low in moisture are the best (e.g., Fontane and Jelly). This type of potato tubers makes a light, soft mash because it absorbs more water during cooking.

CONCLUSIONS

The potato processing industry needs to identify and select different raw materials depending on the type of final product. Regarding domestic consumption, providing more details on the labels of potato bags is necessary so as to inform consumers of the optimal use of fresh tubers, avoiding improper cooking and possible health issues.

Generally, the description of potato cultivars concerns both pre- and post-harvest aspects. This study focused on the most important quality parameters concerning post-harvest. The in-depth analysis of the physico-chemical and enzymatic characteristics of four potato cultivars, analyzed at harvest and during storage, highlighted strong cultivar-dependent differences. In detail, among the potato cultivars analyzed in this experiment, Fontane showed the best properties for processing, especially for frying (e.g., crisps and French-fries). It reported low

RSC with high tolerance to LTS, DM greater than 20 %, good firmness and low susceptibility to post-cut browning. In the home, Fontane is suggested for frying, roasting and to make “homemade gnocchi”. Jelly, already at harvesting, showed a high RSC, making this variety not optimal for frying. However, Jelly is a suitable cultivar for both processing (e.g., for fresh cut or dried potato) and multipurpose domestic use due to its medium/high DM content, low susceptibility to browning and good tolerance to LTS. Constance and Gaudi reported good characteristics for domestic use, especially for boiling or steaming. In contrast with Gaudi, Constance also showed good qualities for processing as a fresh-cut product, reporting low susceptibility to enzymatic browning. However, the low tolerance to LTS reported from these cultivars made them unsuitable for both processing and domestic use as a raw product starting from December for Gaudi and January for Constance.

These results confirmed the extreme differences among potato cultivars in terms of post-harvest performance. Further investigations are needed to test other important varieties grown in the "Patata dell'Alto Viterbese" PGI area, and to analyze other important aspects and quality parameters such as: i) water loss of tuber, ii) phenol composition, iii) antioxidant activity, iv) phenylalanine ammonia-lyase (PAL) and v) peroxidase (POD) activity, vii) effect of the reconditioning process, viii) effect of frying in terms of acrylamide production and color changes. Moreover, a sensory analysis could be performed to understand the impact of LTS on potato flavor and to evaluate potato varieties, considering their organoleptic characteristics.

Table 3.1

Chemical, physico-chemical, physical and enzymatic characteristics of four potato cultivars at the harvest. Within the same row, values followed by the same letter are not significantly different (LSD test, $p \leq 0.05$).

Physico-chemical and enzymatic parameters	**Constance**		**Fontane**		**Gaudi**		**Jelly**	
Dry matter content (%)	17.77	c	19.70	a	17.13	c	18.63	b
Total Phenol Content (TPC, mg GAE 100 g^{-1})	80.25	b	55.79	c	106.58	a	77.26	b
Reducing Sugar Content (RSC, g GluE 100 g^{-1})	1.16	b	0.28	c	2.71	a	2.17	a
Firmness (N)	64.51	c	92.51	a	75.01	b	77.82	b
CIELab colour difference (ΔE^*)	2.31	b	2.12	b	5.75	a	2.23	b
PPO activity (U mg^{-1})	0.46	b	0.50	b	0.93	a	0.27	c

Table 3.2

Correlation matrix for physical, chemical, physicochemical and enzymatic parameters using data of each potato cultivars along 6-months of storage at 7 ± 1 °C and ~90 % of RH for two production seasons.

Cultivar		ΔE*		DM		Firmness		PPO		RSC		TPC
Constance	**ΔE***	-		-		-		-		-		-
	DM	-0.84	***	-		-		-		-		-
	Firmness	0.12		0.11		-		-		-		-
	PPO	0.70	**	-0.62	*	-0.02		-		-		-
	RSC	0.55	*	-0.67	**	-0.08		0.81	***	-		-
	TPC	0.61	*	-0.52		0.43		0.27		0.24		-
Fontane	**ΔE***	-		-		-		-		-		-
	DM	0.52		-		-		-		-		-
	Firmness	0.66	**	0.54	*	-		-		-		-
	PPO	0.61	*	0.64	*	0.65	*	-		-		-
	RSC	-0.23		-0.14		-0.51		-0.14		-		-
	TPC	0.01		-0.33		0.34		0.13		-0.47		-
Gaudi	**ΔE***	-		-		-		-		-		-
	DM	-0.09		-		-		-		-		-
	Firmness	0.13		-0.03		-		-		-		-
	PPO	0.84	***	-0.15		-0.03		-		-		-
	RSC	-0.26		-0.15		0.05		-0.26		-		-
	TPC	-0.23		-0.42		0.31		-0.31		0.78	**	-
Jelly	**ΔE***	-		-		-		-		-		-
	DM	-0.66	*	-		-		-		-		-
	Firmness	-0.56	*	0.81	***	-		-		-		-
	PPO	0.68	**	-0.51		-0.40		-		-		-
	RSC	0.08		0.02		0.10		0.49		-		-
	TPC	0.77	**	-0.64	*	-0.55	*	0.78	**	0.49		-

*** P ≤ 0.001, ** P ≤ 0.01, * P ≤ 0.05

Table 3.3

Example of a schedule showing the best use destination of each analyzed potato cultivar for each month of storage at 7 ± 1 °C and ~90 % of RH. Superscripts were used to rank the cultivars for each final use and for each month.

Recommended destination of use	Aug	Sep	Oct	Nov	Dec	Jan	Feb	Mar
Domestic use								
Frying or roasting	C^3 F^1 J^2	F^1 J^2	F^1 J^2	F^1 J^2	F^1 J^2	F^1 J^2	F^1 J^2	F^1 J^2
Steaming or boiling	C^1 G^2 J^3	C^1 G^2 J^3	C^1 G^2 J^3	C^1 G^3 J^2	C^2 J^1	J^1	J^1	J^1
Homemade gnocchi	F^1 J^2	F^1 J^2	F^1 J^2	F^1 J^2	F^1 J^2	F^1 J^2	F^1 J^2	F^1 J^2
Processing industry								
Snacks (e.g., crisps)	F^1	F^1	F^1	F^1	F^1	F^1	F^1	F^1
Pre-cooked or pre-fried	F^1	F^1	F^1	F^1	F^1	F^1	F^1	F^1
Fresh-cut	C^3 F^1 J^1	C^3 F^1 J^1	C^3 F^1 J^1	C^3 F^1 J^1	C^3 F^1 J^1	F^1 J^1	F^1 J^1	F^1 J^1
Dried	F^1 J^2	F^1 J^2	F^1 J^2	F^1 J^2	F^1 J^2	F^1 J^2	F^1 J^2	F^1 J^2
Gnocchi	F^1	F^1	F^1	F^1	F^1	F^1	F^1	F^1

***C**: Constance; **F**: Fontane; **G**: Gaudi; **J**: Jelly*

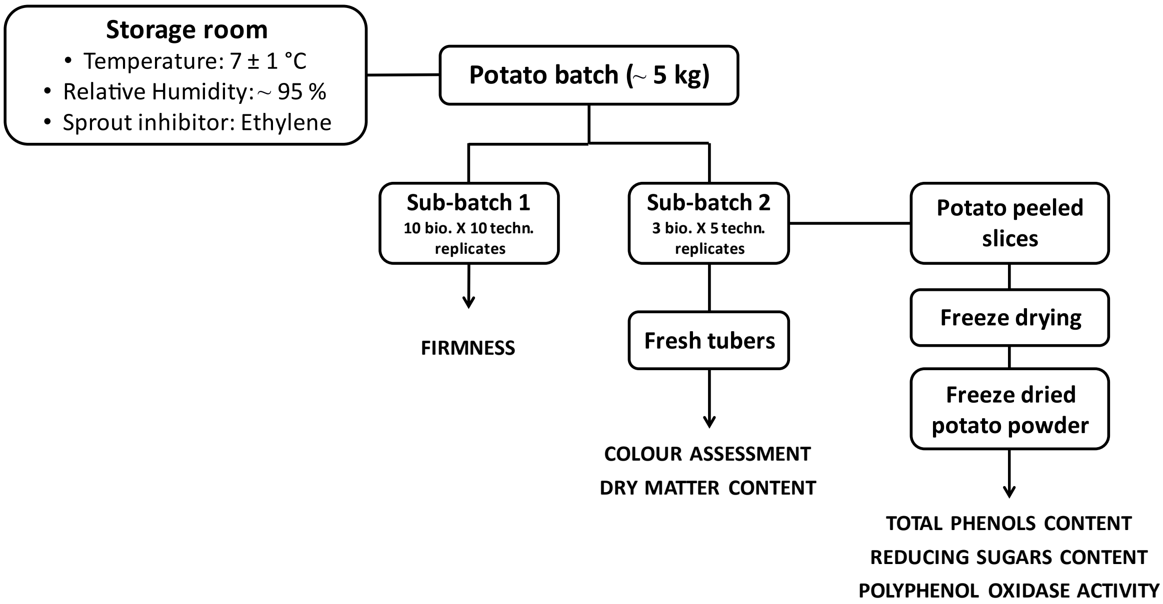

Figure 3.1

Flow chart of sample preparation.

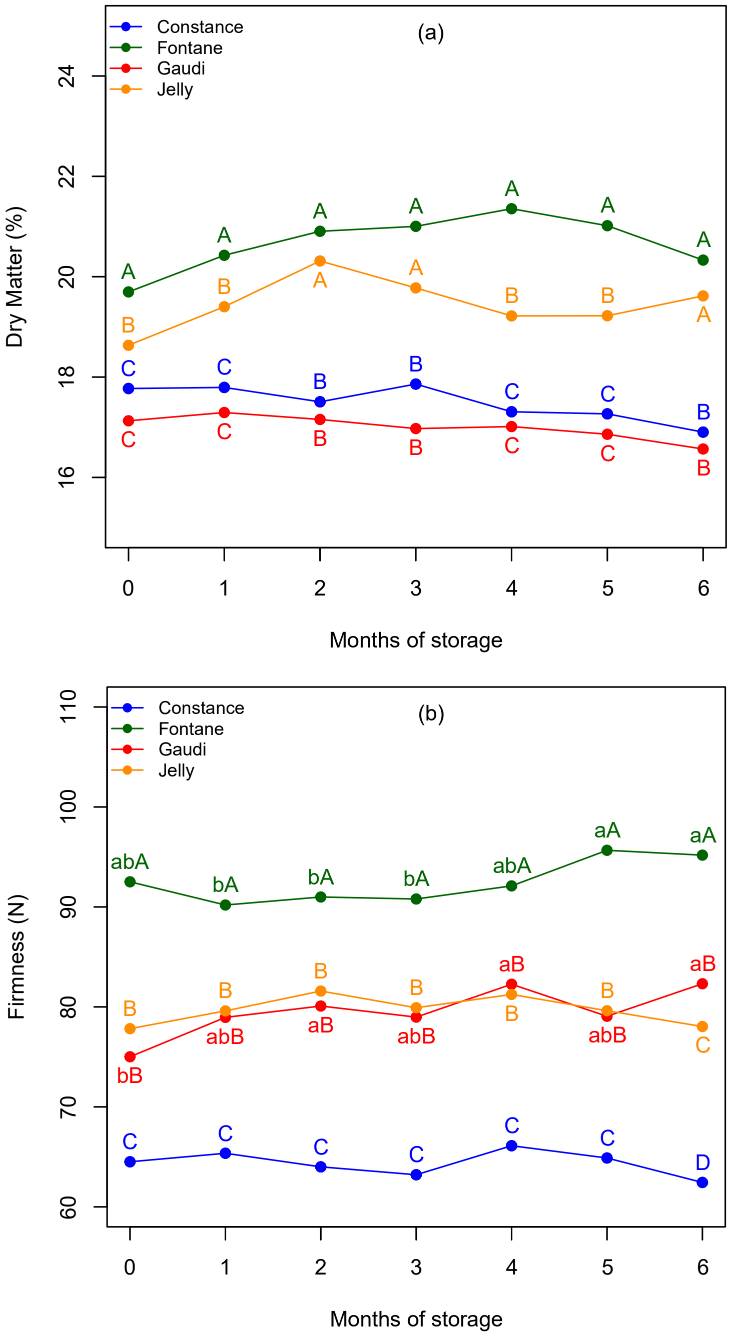

Figure 3.2

Trends in dry matter content (a) and firmness (b) of four potato cultivars towards 6 months of storage at 7 ± 1 °C and ~90 % of RH. Lower-case letters of significance refer to within-cultivar variations during the 6 months of storage, while capital letters of significance refer to between-cultivar variations within each month of storage (LSD test, $p \leq 0.05$). Points sharing the same letter are not significantly different.

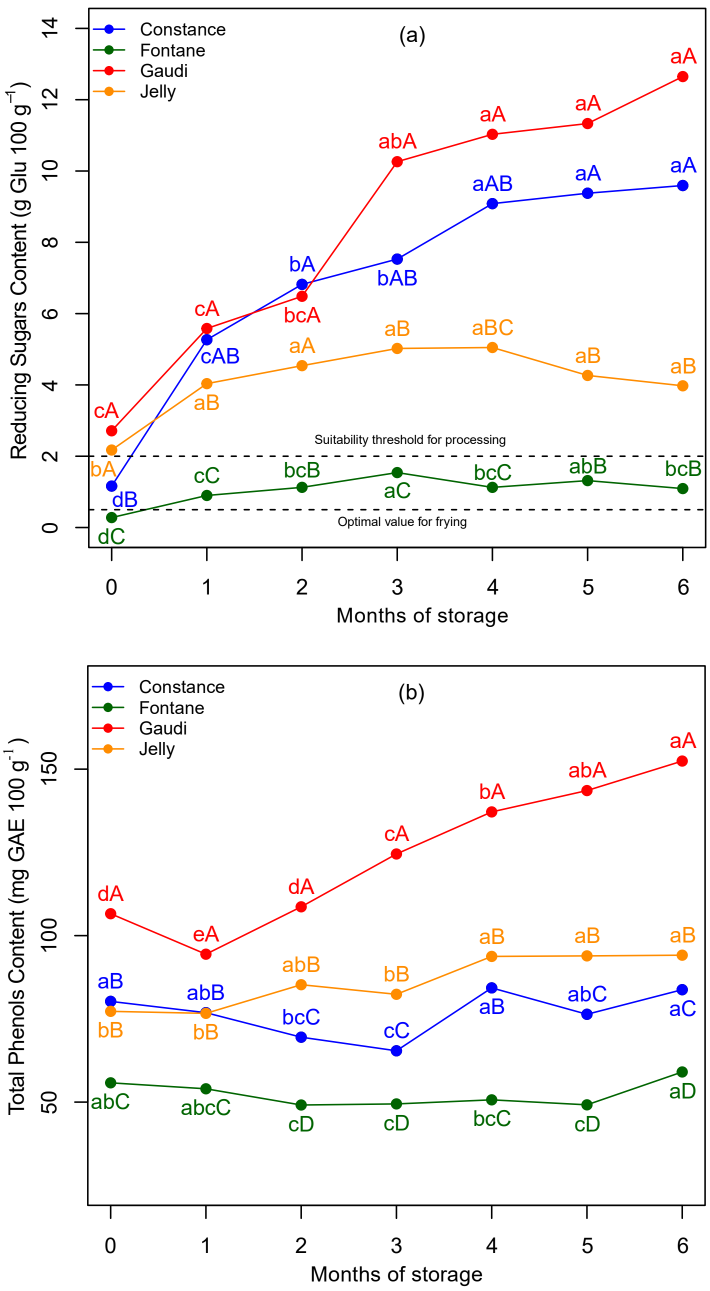

Figure 3.3

Trends in reducing sugar content (a) and total phenol content (b) of four potato cultivars towards 6 months of storage at 7 ± 1 °C and ~90 % of RH. Lower-case letters of significance refer to within-cultivar variations during the 6 months of storage, while capital letters of significance refer to between-cultivar variations within each month of storage (LSD test, $p \leq 0.05$). Points sharing the same letter are not significantly different.

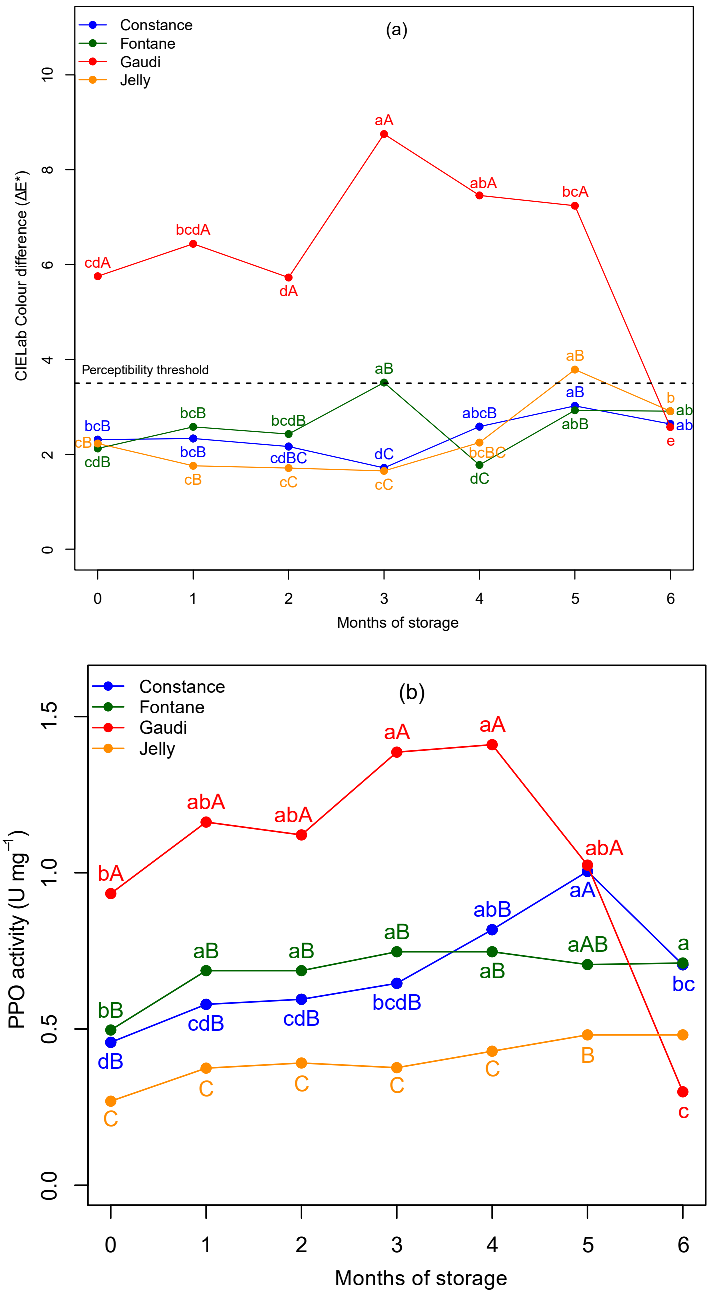

Figure 3.4

Trends in CIELab colour difference (a) and PPO activity (b) of four potato cultivars towards 6 months of storage at 7 ± 1 °C and ~90 % of RH. In the CIELab Colour difference plot, the horizontal-dotted line specifies the perceptibility threshold. Lower-case letters of significance refer to within-cultivar variations during the 6 months of storage, while capital letters of significance refer to between-cultivar variations within each month of storage (LSD test, $p \leq 0.05$). Points sharing the same letter are not significantly different.

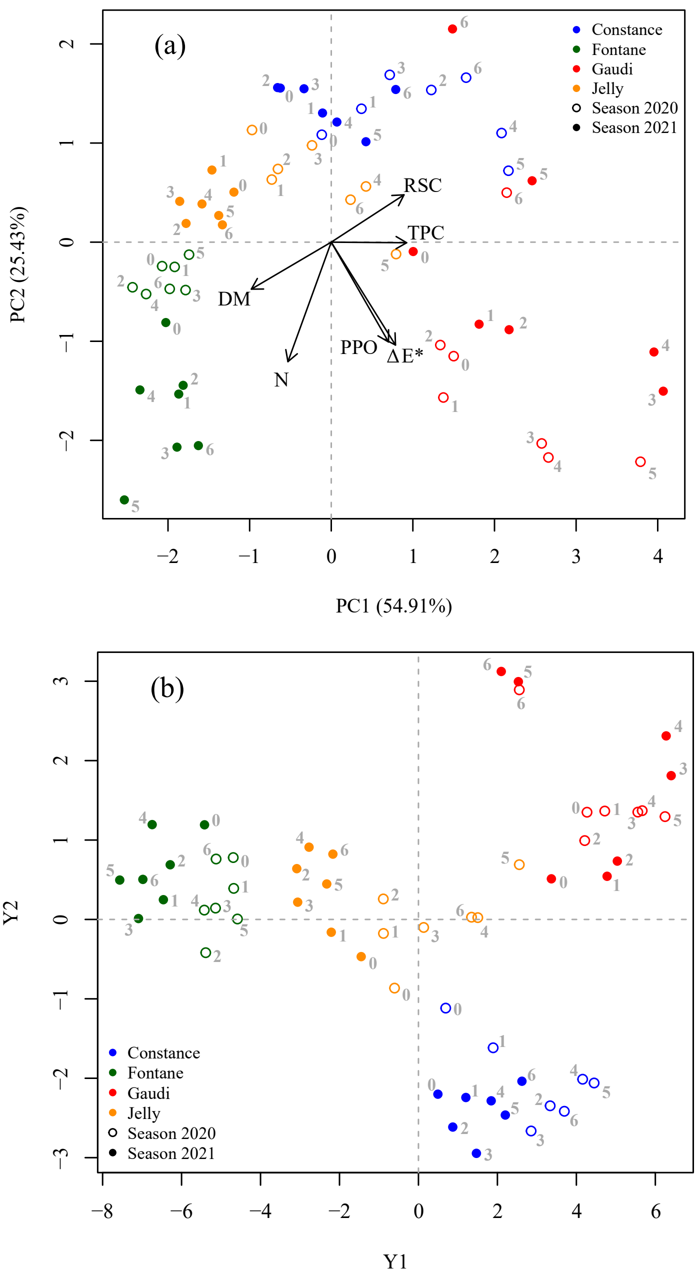

Figure 3.5

Principal Component Analysis (a) and t-Distributed Stochastic Neighbor Embedding (b) bi-plots computed using data from physicochemical and enzymatic analyses of four potato cultivars performed during 6 months of storage at 7 ± 1 °C and ~90 % of RH for the two production seasons. For PCA, the total variance explained by two principal components was 80.38 %. For t-SNE, the value of parameter "perplexity" was 18. The empty (○) and full (•) dots distinguish the two seasons (2020 and 2021, respectively) and the numbers close to the points correspond to the months of storage.

REFERENCES

Biedermann-Brem, S., Noti, A., Grob, K., Imhof, D., Bazzocco, D., Pfefferle, A., 2003. How much reducing sugar may potatoes contain to avoid excessive acrylamide formation during roasting and baking? Eur. Food Res. Technol. 217, 369–373. https://doi.org/10.1007/s00217-003-0779-z

Blessington, T., Nzaramba, M.N., Scheuring, D.C., Hale, A.L., Reddivari, L., Miller, J.C., 2010. Cooking Methods and Storage Treatments of Potato: Effects on Carotenoids, Antioxidant Activity, and Phenolics. Am. J. Potato Res. 87, 479–491. https://doi.org/10.1007/s12230-010-9150-7

Bøjer Rasmussen, C., Enghild, J.J., Scavenius, C., 2021. Identification of polyphenol oxidases in potato tuber (*Solanum tuberosum* L.) and purification and characterization of the major polyphenol oxidases. Food Chem. 365. https://doi.org/10.1016/j.foodchem.2021.130454

Brecht, J.K., Saltveit, M.E., Talcott, S.T., Schneider, K.R., Felkey, K., Bartz, J.A., 2004. Fresh-cut vegetables and fruits. Hortic. Rev. 30, 185–250

Burton, W.G., 1969. The sugar balance in some British potato varieties during storage. II. The effects of tuber age, previous storage temperature, and intermittent refrigeration upon low-temperature sweetening. Eur. Potato J. 12, 81–95. https://doi.org/10.1007/BF02364726

Cabezas-Serrano, A.B., Amodio, M.L., Cornacchia, R., Rinaldi, R., Colelli, G., 2009. Suitability of five different potato cultivars (*Solanum tuberosum* L.) to be processed as fresh-cut products. Postharvest Biol. Technol. 53, 138–144. https://doi.org/10.1016/j.postharvbio.2009.03.009

Cantos, E., Tudela, J.A., Gil, M.I., Espín, J.C., 2002. Phenolic compounds and related enzymes are not rate-limiting in browning development of fresh-cut potatoes. J. Agric. Food Chem. 50, 3015–3023. https://doi.org/10.1021/jf0116350

Cheng, D., Wang, G., Tang, J., Yao, C., Li, P., Song, Q., Wang, C., 2020. Inhibitory effect of chlorogenic acid on polyphenol oxidase and browning of fresh-cut potatoes. Postharvest Biol. Technol. 168, 111282. https://doi.org/10.1016/j.postharvbio.2020.111282

EFSA, 2015. Acrylamide in Food. EFSA Explains Risk Assessment. 2015 4.

Elmore, J.S., Briddon, A., Dodson, A.T., Muttucumaru, N., Halford, N.G., Mottram, D.S., 2015. Acrylamide in potato crisps prepared from 20 UK-grown varieties: Effects of variety and tuber storage time. Food Chem. 182, 1–8. https://doi.org/10.1016/j.foodchem.2015.02.103

FAOSTAT (2022) Food and Agriculture Organization of the United Nations. https://www.fao.org/faostat/en/#data/QCL/visualize. Accessed 21 Nov 2022

Feng, Y., Zhang, D., Sun, Y., Meng, Z., Malik, A.U., Zhang, S., Yan, H., Wang, Q., 2022. A novel anti-browning agent S-furfuryl thioacetate for fresh-cut potato screened from food-derived sulfur compounds. Postharvest Biol. Technol. 192, 112007. https://doi.org/10.1016/j.postharvbio.2022.112007

Gikundi, E.N., Buzera, A.K., Orina, I.N., Sila, D.N., 2022. Storability of Irish Potato (*Solanum tuberosum* L.) Varieties Grown in Kenya, Under Different Storage Conditions. Potato Res. https://doi.org/10.1007/s11540-022-09575-8

Gómez-Castillo, D., Cruz, E., Iguaz, A., Arroqui, C., Vírseda, P., 2013. Effects of essential oils on sprout suppression and quality of potato cultivars. Postharvest Biol. Technol. 82, 15–21. https://doi.org/10.1016/j.postharvbio.2013.02.017

Hasegawa, S., Johnson, R.M., Gould, W.A., 1966. Effect of Cold Storage on Chlorogenic Acid Content of Potatoes. J. Agric. Food Chem. 14, 165–169. https://doi.org/10.1021/jf60144a020

Ingallina, C., Spano, M., Sobolev, A.P., Esposito, C., Santarcangelo, C., Baldi, A., Daglia, M., Mannina, L., 2020. Characterization of local products for their industrial use: The case of Italian potato cultivars analyzed by untargeted and targeted methodologies. Foods 9, 1–15. https://doi.org/10.3390/foods9091216

Iritani, W.M., 1981. Growth and preharvest stress and processing quality of potatoes. Am. Potato J. 58, 71–80. https://doi.org/10.1007/BF02855381

ISTAT (2022). Istituto Nazionale di Statistica. http://dati.istat.it/Index.aspx?DataSetCode=DCSP_COLTIVAZIONI#. Accessed 21 Nov 2022

Kumar, D., Singh, B.P., Kumar, P., 2004. An overview of the factors affecting sugar content of potatoes. Ann. Appl. Biol. 145, 247–256. https://doi.org/10.1111/j.1744-7348.2004.tb00380.x

Lindsay, H., 1973. A colorimetric estimation of reducing sugars in potatoes with 3,5-dinitrosalicylic acid. Potato Res. 16, 176–179. https://doi.org/10.1007/BF02356048

Luo, N., Yang, X., Sun, C., Xing, B., Han, J., Zhao, C., 2021. Visualization of vibrational spectroscopy for agro-food samples using t-Distributed Stochastic Neighbor Embedding. Food Control 126, 107812. https://doi.org/10.1016/j.foodcont.2020.107812

McCOMBER, D.R., OSMAN, E.M., LOHNES, R.A., 1988. Factors Related to Potato Mealiness. J. Food Sci. 53, 1423–1425. https://doi.org/10.1111/j.1365-2621.1988.tb09291.x

McKenzie M., Corrigan V., 2016. Potato flavor. In: Singh J, Kaur L., Advances in potato chemistry and technology, Second edi. Academic Press, Chapter 12, pp 339–367

Mokrzycki, W.S., Tatol, M., 2011. Colour difference ΔE - A survey Mokrzycki. Mach. Graph. Vis. 20, 383–411.

Moscetti, R., Raponi, F., Monarca, D., Bedini, G., Ferri, S., Massantini, R., 2019. Effects of hot-water and steam blanching of sliced potato on polyphenol oxidase activity. Int. J. Food Sci. Technol. 54, 403–411. https://doi.org/10.1111/ijfs.13951

Pinhero R.G., Yada R.Y., 2016. Postharvest Storage of Potatoes. In: Singh J, Kaur L., Advances in potato chemistry and technology, Second edi. Academic Press, Chapter 10, pp 283–309

Pritchard, M.K., Scanlon, M.G., 1997. Mapping dry matter and sugars in potato tubers for prediction of whole tuber process quality. Can. J. Plant Sci. 77, 461–467. https://doi.org/10.4141/P96-111

Rocculi, P., Federico, G., Mendoza, F., Wads, L., Romani, S., Dalla, M., Sj, I., 2007. Effects of the application of anti-browning substances on the metabolic activity and sugar composition of fresh-cut potatoes 43, 151–157. https://doi.org/10.1016/j.postharvbio.2006.08.002

Ru, X., Tao, N., Feng, Y., Li, Q., Wang, Q., 2020. A novel anti-browning agent 3-mercapto-2-butanol for inhibition of fresh-cut potato browning. Postharvest Biol. Technol. 170, 111324. https://doi.org/10.1016/j.postharvbio.2020.111324

Silveira, A.C., Oyarzún, D., Sepúlveda, A., Escalona, V., 2017. Effect of genotype, raw-material storage time and cut type on native potato suitability for fresh-cut elaboration. Postharvest Biol. Technol. 128, 1–10. https://doi.org/10.1016/j.postharvbio.2017.01.011

Singh, B., Singh, J., Singh, J.P., Kaur, A., Singh, N., 2020. Phenolic compounds in potato (*Solanum tuberosum* L.) peel and their health-promoting activities. Int. J. Food Sci. Technol. 55, 2273–2281. https://doi.org/10.1111/ijfs.14361

Singleton, V.L.; Rossi, J.A. Colorimetry of total phenolics with phosphomolybdic-phosphotungstic acid reagents. Am. J. Enol. Vitic. 1965, 16, 144–158.

Taylor, M.A., McDougall, G.J., Stewart, D., 2007. Potato flavour and texture, Potato Biology and Biotechnology: Advances and Perspectives. Elsevier B.V. https://doi.org/10.1016/B978-044451018-1/50066-X

Taylor, S.L., Higley, N.A., Bush, R.K., 1986. Sulfites in foods: uses, analytical methods, residues, fate, exposure assessment, metabolism, toxicity, and hypersensitivity 1–76.

Thybo, A.K., Christiansen, J., Kaack, K., Petersen, M.A., 2006. Effect of cultivars , wound healing and storage on sensory quality and chemical components in pre-peeled potatoes 39, 166–176. https://doi.org/10.1016/j.lwt.2004.11.010

Torres, M.D.Á., Parreño, W.C., 2016. Thermal Processing of Potatoes, in: Singh, J., Kaur, L., Advances in Potato Chemistry and Technology. Academic Press, Chapter 14, pp. 403–457.

United Nations (2022) Sustainable Development Goals. https://sdgs.un.org/goals. Accessed 21 Nov 2022.

Visse-Mansiaux, M., Tallant, M., Brostaux, Y., Delaplace, P., Vanderschuren, H., Dupuis, B., 2021. Assessment of pre- and post-harvest anti-sprouting treatments to replace CIPC for potato storage. Postharvest Biol. Technol. 178. https://doi.org/10.1016/j.postharvbio.2021.111540

Wang-Pruski, G., Nowak, J., 2004. Potato after-cooking darkening. Am. J. Potato Res. 81, 7–16. https://doi.org/10.1007/BF02853831

Zaghi, A.N., Barbalho, S.M., Guiguer, E.L., Otoboni, A.M., 2019. Frying Process: From Conventional to Air Frying Technology. Food Rev. Int. 35, 763–777. https://doi.org/10.1080/87559129.2019.1600541

Zommick, D.H., Knowles, L.O., Knowles, N.R., 2014. Tuber respiratory profiles during low temperature sweetening (LTS) and reconditioning of LTS-resistant and susceptible potato

(*Solanum tuberosum* L.) cultivars. Postharvest Biol. Technol. 92, 128–138. https://doi.org/10.1016/j.postharvbio.2014.01.020

CHAPTER 4

SMART MONITORING AND CONTROL SYSTEM FOR FOOD DRYING

4.1 COMPUTER VISION-BASED SMART MONITORING AND CONTROL SYSTEM FOR FOOD DRYING: A STUDY ON CARROT

Swathi Sirisha Nallan Chakravartula[a], Andrea Bandiera[a], Marco Nardella[a], Giacomo Bedini[a], Pietro Ibba[b], Riccardo Massantini[a*], Roberto Moscetti[a*]

[a]Department of Innovation in Biology, Agri-food and Forest systems, University of Tuscia, Italy

[b]Faculty of Science and Technology, Free University of Bolzano-Bozen, Italy

** Corresponding authors*

INDEX

KEYWORDS: *Process Analytical Technology; Quality-by-Design; computer vision; Daucus Carota L.; segmented-linear model*

ABSTRACT

Convective dryer embedded with computer vision (CV) system and load cell was used to continuously monitor carrot slices that are either unblanched or blanched (90 °C for 2 min) during product drying (35 °C, 35 % R.H., 3 m s^{-1} airflow). The CV system and load cell were selected as in-line Process Analytical Technology tools within a proactive Quality-by-Design framework and embedded for, i) monitoring of product features (i.e., weight, colour, and size); and ii) developing shrinkage-dependent moisture prediction models using linear regression. The evaluated shrinkage-dependent linear models showed superior performances (RMSE, 0.005-0.007) benchmarked against selected thin-layer models of increasing complexity. The study

tested a smart-enabled prototype dryer with the potential for automation and integrating proactive quality strategies.

INTRODUCTION

A key element of food security is the uninterrupted availability of safe and quality products ensured by the agro-food sector through pre- and post-production processes like drying. Consequently, the agro-food industry is critical to the global greenhouse gas emissions contributing up to one-third of the emissions, more than half of which are related to drying operations (Crippa et al., 2021). Industrially, convection-based drying is the most viable process for extending the shelf-life of foods by minimising physicochemical changes and microbial spoilage (Mayor and Sereno, 2004; Moscetti et al., 2017). However, these drying systems are criticised for their resource-intensiveness (energy, labour), high environmental impact, and food quality issues that can be related to the (i) dominance of fossil fuel-based dryers (~85 %) that contribute to approx. 12-25 % of the total energy consumption; (ii) heavy reliance on the operator's experience in process control; and (iii) conventional reactive approaches of analyses for product testing which cause product quality failures i.e., under or over-drying (Aghbashlo et al., 2014; Raponi et al., 2017) and thereby low energy efficiency (Menon et al., 2020; Raponi et al., 2021).

To overcome the stated issues, the drying sector invests continuously in innovative solutions that consider the complex, nonlinear and dynamic nature of food drying while ensuring high-quality products, efficient processes, and sustainable production practices to meet the 12th sustainable development goal of 'Responsible production and consumption, SDG 12 (UN Report, 2019). As such, alternate strategies have been developed to improve drying systems that can be divided into two broad categories: (i) heat recovery, renewable energy-based and/or hybrid-drying technologies for improved energy efficiency; and (ii) implementation of sensors, and machine learning models for efficient product-process monitoring and control (Khan et al., 2020; Moses et al., 2014; Zhang et al., 2017). Among these, the second strategy has been gaining considerable interest both in academia and industry due to its feasibility of implementation with minimal efforts compared to the scaling-up required in implementing new systems as in the first category. However, these technologies are yet to have explosive industrial acceptance and implementation due to major roadblocks like the uncertainty of application for a wide range of products-processes, innovation and financial lags, and long technological gestation periods among others.

In this context, it is of interest to investigate further the use of real-time optical tools like imaging systems with or without spectroscopy (Aghbashlo et al., 2014; Bedini et al., 2020; Liu et al., 2017; Raponi et al., 2021) falling under the umbrella of Process Analytical Technology (PAT) tools as monitoring and control systems (MCS). Specifically, computer vision (CV) systems have been found to be reliable in the context of food processing offering cost-effective, non-invasive solutions for monitoring product's attributes like appearance, shape, and texture quantifiable into relevant quality parameters (colour, shrinkage, texture) (Aghbashlo et al., 2014; Moscetti et al., 2021; Raponi et al., 2021, 2017). Further, CV systems can be implemented as real-time data acquirement tools in-line for quality monitoring, analyses, multivariate modelling, and feedback with the potential for proactively strengthening and/or replacing conventional offline methods. This also offers the advantage of comprehensive and precise quality monitoring from the start to the end of the process (Ghasemi-Varnamkhasti and Aghbashlo, 2014). However, in practice, PAT tools alone might not completely render the process efficient due to the inherent variability of food matrices and the dynamic nature of food drying, thereby necessitating strategic approaches that can allow for establishing pro-active and robust quality systems (Moscetti et al., 2019; Rathore and Kapoor, 2016).

Quality-by-Design (QbD) is one such approach that integrates product quality as a part of the process design by a systematic and dynamic understanding of the product-process spaces and related changes along the production line (Rathore and Kapoor, 2016; van den Berg et al., 2013). However, this integration is highly complex owing to the simultaneous heat, mass, and momentum transport that occurs within drying at different scales, phases, and physical states that are preceded and/or followed by physiological and biochemical changes (Defraeye, 2014; Moscetti et al., 2019). These drying transitions although can be generalised are considered highly product-process specific within a QbD approach. Therefore, the desired product quality and the relevant quality characteristics, i.e., physical, chemical, or microbiological attributes within a given product design space should be identified, defined, and monitored (Rathore and Kapoor, 2016; van den Berg et al., 2013).

In fact, within the drying process, the product's quality characteristics and drying behaviour to ensure optimal process-end point as well as the overall design and operations can be estimated with a wide range of macroscopic and microscopic measures. Among these, drying curve-based approaches, particularly thin-layer drying models, remain to be the most popular owing to their simplicity of use and implementation for model-based prediction (Buzrul, 2022; Defraeye, 2014; Erbay and Icier, 2010). Most of these are time-dependent models with time as independent variable and their robustness is affected by process parameters and physical product characteristics such as shrinkage, bending, case hardening, and surface cracking. Alternately, the use of product deformation as a model factor can allow for estimation of the drying behaviour considering product's physical changes as evidenced in our recent findings (Raponi et al., 2021) as well as by other researchers by use of imaging systems (Gulati and Datta, 2015; Purlis et al., 2021; Seyedabadi et al., 2019).

In this context, the CV system was used within the dryer as a component of the smart MCS (SMCS) that can allow for real-time data measurements and subsequent model-based monitoring for process end-point determination as well as product quality control. For testing the set-up, convective drying of carrots (*Daucus carota* L.) was identified as a suitable product-process matrix owing to the wide industrial use of hot-air dryers as well as the importance of carrot as a vegetable in the drying sector. Thus, the objective of this work was to lay the foundation for a PAT-based QbD approach for carrot drying by (i) implementing a CV system as a component of SMCS in a prototype drier for real-time monitoring of product changes; (ii) to develop linear models utilising the in-line product changes (shrinkage) in predicting drying behaviour of samples subjected to common industrial pre-treatments like blanching; and (iii) to evaluate the performance and robustness advantages of the CV-based shrinkage-dependent solutions benchmarked against classical thin-layer methods for real-time drying monitoring and control.

MATERIALS AND METHODS

Sample preparation

Carrots (*Daucus carota* L.) of the same maturity (~18-cm length) were purchased from a local market (Ipercoop, Viterbo, Italy) and immediately stored at 4 ± 1 °C until further processing. Carrots free of blemishes and defects were tempered to room temperature for 12 h, washed, peeled, and cut into 5-mm thick slices. Samples were split into batches of 350 g of fresh weight before processing (~70 carrot slices). One batch of samples (BL) were blanched in water at 90 °C for 2 min (Klarstein Slowcooker 550W, Germany) to reduce the residual peroxidase (POD) activity to less than 10 % based on our previous study (Moscetti et al., 2017). The control (CNT) batch was dipped in water at room temperature for 2 min. Immediately after the treatment, the samples were cooled using an ice bath, rested on a cotton cloth for 2 min to remove excess surface moisture, re-weighed, and subjected to drying tests.

'Smart cabinet dryer' set-up

The prototype smart-enabled cabinet dryer set-up depicted in figure 4.1 used in the drying tests consisted of (i) a prototype temperature-controlled cabinet dryer developed by Innotech (Germany) with a drying chamber of 91-L holding a drying tray of 45x45-cm dimension; (ii) a monitoring and control system (MCS) for temperature and relative humidity (mod. DICON touch, JUMO, Germany); (iii) a digital balance (mod. HT1500, NHU, Germany), placed on the bottom of the drying tray used during the tests connected with a RS232 cable pinout to an external personal computer; and (iv) a computer vision (CV) system placed in a black box on the top of the drying chamber.

Specifically, the CV system consisted of (i) a CMOS camera (mod. DFK 33UX264, The Imaging Source Europe GmbH, Germany) equipped with a C1/1.2"-8 mm-F/2.4 optical lens; (ii) an illumination source consisting of four 4200K light-emitting diode strips or LEDs (mod. LBRX-00-200-3-W-24V, TMS Lite, Malaysia); and (iii) a DC 24V power supply controller (mod. ANG-4000-CH4-24V-A1, TMS Lite, Malaysia). The camera was mounted inside a black box to be insulated from external light and placed on the top of the dryer chamber. The four LED strips were arranged on the bottom of the black box and along the top side of the drying chamber at 90° angle to the product to improve the intensity and uniformity of the light along the field of view, and the response of the camera.

Drying process and real-time data acquisition

The hot-air drying experiments were performed at 35 °C, 35 % R.H and 3 m s^{-1} air flow based on preliminary trials. Each drying trial consisted of about 350 g of carrot slices dried for 36 h. Each treatment was replicated 4 times. The samples were subjected to offline analysis of moisture content at the end of the drying process according to AOAC 934.06 official method.

Weight loss and images as pre-selected product characteristics were monitored and recorded in real-time i.e., when the drying process is in progress. The in-line data was recorded in pre-set time intervals and relayed to the connected computer with minimal time lag (5 min) between data recording and relaying. The in-line acquisition of weight loss and images of the product was performed every 5 min by using in combination an ad-hoc Python3 script and the IC Capture software v.2.4 (The Imaging Source Europe GmbH, Germany). The weight measurements were stored as Comma-Separated-Values (CSV) files, while sample images were saved as Tagged Image File Format (TIFF). The resolution of the digital image was 2192×1888 pixels with a color depth of 24 bits, corresponding to 8 bits per RGB channel. The schematic for the process flow for monitoring the carrot drying with the use of selected PAT tools is presented in figure 4.2.

Data handling and features extraction

The changes in dry-basis moisture content (MC_{db}) during drying were computed by combining data from the in-line acquisitions (i.e., the fresh mass of the sample before drying; and mass changes during drying); and the off-line measurement of moisture content after drying. Thus, the moisture ratio (MR) was computed by applying a min-max data normalization to the MC_{db}, i.e., scaling values of moisture content to a common 0-1 scale, without distorting differences among the treatments (Raponi et al., 2021). Additionally, the drying rate at each instance and for the overall process was computed and expressed as rate of moisture removed per gram of dry matter per hour (i.e., $gH_2O\ gDW^{-1}\ h^{-1}$).

As for the in-line images acquired, they were utilized for features extraction (i.e., color and size information over time from samples). Prior to feature extraction, the camera was (i) calibrated, to remove the lens distortion on the image; (ii) profiled, to correct color distortion due to the camera sensor; and the images were (iii) flat-field corrected, to remove shading distortion due to uneven illumination; (iv) and segmented, to separate the true image of each sample (i.e., foreground) from its background (i.e., non-sample data) (Figure 4.3).

Firstly, the camera calibration was performed using the 'Camera Calibrator' app in the 'ComputerVision' toolbox of Matlab 2019b (MathWorks, CA, USA) by acquiring multiple images of a checkerboard calibration pattern randomly placed on the top tray of the dryer. Subsequently, images were color corrected using the 'makecform()' and 'applycform()' functions of Matlab 2019b fed with the ICC camera profile computed through the Colorchecker Passport kit (X-Rite Ltd., UK). Subsequently, the flat-field correction was applied using the eq. 1:

$$I = (I_0 - D) / (F - D) \quad (1)$$

where,

'I' is the corrected image, 'I_0' is the raw image, 'D' is the dark image and 'F' is the flat-field image, respectively. The 'D' image corresponds to the 'dark' current acquired by covering the camera lens with a non-reflective opaque black cap. The 'F' image was acquired by scanning a white-reference tile of 43x40-cm (H x W), used to capture unevenness in color and brightness on the top tray of the dryer due to the illumination system.

Further, the image segmentation was performed as a last stage of the image post-processing using an HSV filter ($0.0 \leq H \leq 0.1$; $0.3 \leq S \leq 1.0$; $0.5 \leq V \leq 1.0$) written in Matlab. Finally, the features extraction (i.e., color and spatial data extraction) was performed using a script written in Python v3.6.9 coupled with the OpenCV 3.4.2 library. Specifically, the Python script was used to extract from each carrot slice (i) the average color in terms of lightness (L^*), redness (a^*), yellowness (b^*), hue angle (h) and chroma (C^*) (Moscetti et al., 2017); (ii) the shape (i.e., minor and major axis lengths, and eccentricity); (iii) the surface area (in pixels); and (iv) the relative area shrinkage (AS), computed by dividing each surface area value over time by its initial value (Raponi et al., 2021).

Computer Vision-based moisture prediction models

Moisture ratio (MR) prediction models were computed for each treatment (i.e., CNT and BL), evaluating two different mathematical approaches (Table 4.1): (i) time- dependent models i.e., thin-layer models using changes in MR as a function of drying time (t); and (ii) shrinkage-dependent models i.e., the linear and segmented-linear models using changes in MR as a function of area shrinkage (AS). Specifically, considering diffusion as the dominant mechanism of moisture removal in carrots with drying predominantly taking place in the falling rate period (Aghbashlo et al., 2009; Erenturk and Erenturk, 2007; Krokida et al., 2003; Planinić et al., 2005) the four most frequently used thin-layer drying models of increasing complexity levels were chosen for the time-dependent approach (Onwude et al., 2016). Although frequently used to describe the moisture changes in food drying, thin layer drying models have boundary conditions which depend on the drying method, process condition, and product dimensions and geometry. Among them the critical ones are that the shrinkage effect during drying should be negligible, and the product size should be homogeneous and isotropic (Onwude et al., 2016). These requirements are difficult to fulfil in most food matrices, including carrots due to the obvious product deformation and heterogeneity in drying.

To circumvent the stated issues, dynamic shrinkage-dependent models specifically, linear, and segmented linear models which use product deformation as predictor instead of time were tested as an alternative approach. The segmented linear approach allows a predictive model to be optimized by identifying a breakpoint (BP) at an abrupt change between the response (y) and the explanatory variable (x) (Lyndgaard et al., 2012). This was considered advantageous in the case of area shrinkage (AS), as the partitioning of the influential factor into intervals helps describe its relationship to MR during drying. In detail, the BP was identified using the *segmented()* function of the Segmented R-package to fit the standard linear model with segmented relationships between MR and AS; for the intended purpose, the 'npsi' attribute of function (i.e., number of BR to be identified) was set equal to 1.

The model's goodness of fit was evaluated in terms of Root Mean Square Error (RMSE), Mean Absolute Error (MAE), systematic error (BIAS), reduced chi-square (red. χ^2), and adjusted coefficient of determination (adj-R^2).

Data handling and statistical analysis

One-way analysis of variance (ANOVA) was performed to evaluate and compare the main effect of the treatment factor (CNT and BL) on parameters and performance metrics of each model, as well as to identify the best model in terms of performances. Tukey's pairwise comparison method was performed, and the Honestly Significant Difference (HSD) was calculated for an appropriate level of interaction ($P \leq 0.05$). Scripts for data handling, breakpoint identification for the development of linear-segmented models, modelling and ANOVA were prepared using the R software v3.6.9 in combination with 'dplyr', 'segment', and 'Agricolae' R-packages.

RESULTS AND DISCUSSION

In-line quality parameters

Moisture content and drying rates

Figure 4.4a shows the change in moisture content (dry basis, MC_{db}) along the experimental drying times for control (CNT) and blanched (BL) carrot slices determined by the in-line weight changes.

The initial MC_{db} for either BL or CNT treatments ranged from 8.90 to 9.10 g g^{-1} which decreased to a final equilibrium moisture content (MC_e) of 0.13 g g^{-1} along 36 h of drying. The loss in moisture followed a pseudo first-order kinetic, irrespective of the pre-treatment. In detail, the moisture content decreased rapidly at the initial stages up to ~ 8 h to MC_{db} values of 1.60 (BL) to 2.06 (CNT) g g^{-1} followed by a slower and consistent moisture loss moving towards equilibrium. Interestingly, a significant difference in moisture loss was observed after 7-8 h between CNT and BL samples. This can be attributed to the blanching effects, as the samples were cut to the same thickness and dried under similar conditions. In fact, it is well known that blanching leads to damage of the cell membranes thereby influencing the cell wall permeability as well as the effective moisture diffusivity resulting in lower moisture content as observed in carrots and other fruits and vegetables (Fellows and Fellows, 2017; Planinić et al., 2005).

Further, the average drying rates as shown in Figure 4.4b rose rapidly as expected to 1.35 and 1.39 g H_2O g DW^{-1} h^{-1} in CNT and BL, respectively, within the first hour of drying due to the initial warm-up period and consequent increase in the product's surface temperature

(Raponi et al., 2021; Wu et al., 2014). Subsequently, up to approx. 11 h of processing the drying rate decreased sharply registering only a falling rate period and reached a plateau after about 24 h with the MC_{db} tending towards MC_e. No constant rate drying period was observed, regardless of treatment. This behaviour confirms that moisture diffusion was the predominant mechanism for moisture removal which further limits the drying rate, as is the case for most porous, cellular structured agro-food materials. These observations on drying behaviour were found to be consistent with other studies on convective as well as infrared or microwave drying of carrots in form of cubes and/or slices (Aghbashlo et al., 2009; Moscetti et al., 2017; Toğrul, 2006; Wu et al., 2014) as well as in other fruits and vegetables (Lahsasni et al., 2004; Raponi et al., 2021). As for the different treatments, there were no significant differences between the drying rates of CNT and BL, even though blanching treatment tended to have a slightly higher rate of moisture loss due to its well-known effects on the cellular structure.

Shrinkage

Figure 4.4c shows the general tendency of the relative area shrinkage (AS) of carrot slices along the drying time with significant differences between CNT and BL samples. The grey and red shaded areas along each response line in graph represent the experimental dispersion of measurements for CNT and BL samples respectively. Both samples exhibited pseudo first-order kinetics similar to that of MC_{db} (Fig. 4.4a) with rapid decrease in AS from an initial value of 1.00 to about 0.50 in CNT and 0.36 in BL samples within 8 h of drying time. Subsequently, the decrease in AS values gradually slowed, reaching a plateau around 24 h, generally proportional to the loss of MC_{db}. In fact, previous studies showed that carrots similar to that of potato and apple tissues had the ideal shrinkage behaviour with the shrinkage being linearly related to that of moisture loss (Dhall and Datta, 2011; Raponi et al., 2021). This proportionality has been attributed to the stress created due to loss of moisture and other contributing factors like sample dimensions, porosity, and material state (Madiouli et al., 2012; Mayor and Sereno, 2004; Nguyen et al., 2018). However, it is necessary to note that the linearity of the shrinkage at very low moisture contents might be disrupted due to the continuing change in the tissue's material state and mechanical characteristics. In particular, the transition of material state from rubbery to glassy states was evidenced to result in formation of relatively rigid structure which was evidenced to limit the rate and degree of shrinkage (Mayor and Sereno, 2004; Nguyen et al., 2018).

Furthermore, it is known that the shrinkage behavior is also affected by various factors like pre-treatments and drying conditions, which eventually influence the moisture diffusivity and drying rates. As previously noted, BL samples registered steeper shrinkage values significantly different from the CNT after 2 h of drying (marked with green vertical line and asterisk in figure 3c) up to the final drying of 36 h with the final relative area shrinkage being 0.208 for BL compared to 0.260 for CNT samples. These differences observed in BL samples can be attributed to the modifications caused by blanching in the cellular construct and the gas expulsion from the carrot tissue. The cell membrane and cell wall breakages because of blanching create pores (i.e., improved porosity) which improves moisture diffusivity and thereby the drying rates resulting in a higher tissue contraction (González-Fésler et al., 2008; Madiouli et al., 2012). Also, the gas expulsion decreases the instances of intercellular spaces causing the matrix to collapse which was more evident in BL than CNT samples even under mild drying conditions (Aprajeeta et al., 2015). In fact, it was observed by Lemmens et al., (2009) that high temperature blanching can result in weaker cellular structure susceptible to damage during subsequent thermal treatments due to further chemical demethoxylation compared to that of unblanched or mildly blanched (60 ° C or less) samples.

Surface color changes

Colorimetric parameters (CIELab), as an important visual aspect for dried food products critically impacting the purchase decisions, were monitored along the drying process by the CV system. The samples as expected exhibited changes in the CIELab coordinates (*L**, luminance; *a**, redness; *b**, yellowness) along the drying time represented by luminance (*L**) and hue angle (*h*) in figures 4.5a and 4.5b, respectively. In general, these colour changes in vegetal matrices can be attributed to the extensively studied multifaceted effects of drying as well as the pre-treatment (blanching) on the material state and properties like water activity and phase transition, cellular shrinkage and/ or disruption, enzymatic and/or non-enzymatic reactions as well as pigment degradation and/or concentration.

In terms of luminance (*L**), the values were observed to initially increase and then continuously decrease, concurrent to the loss of MC_{db} along the drying time (*t*, shown in Fig. 4.5a) for both CNT and BL samples. The observed initial increase in *L** values can be attributed mainly to the 'white blush/ bloom' i.e., surface whitening due to surface dehydration, which when intense might be irreversible due to the collapsing of superficial cells changing their structure (Simões et al., 2010). Some authors also attributed the white blush to coinciding enzyme activity post-cut, particularly those of phenylalanine ammonia-lyase (PAL) which can cause phenol accumulation as precursor for lignin biosynthesis (Rocha et al., 2007), although other authors evidenced that this effect is unrelated (Simões et al., 2010). Within the tested samples, BL evidenced significantly lower *L** values than CNT samples from time ‘0’ as indicated by the green-dashed area in the figure. This can be attributed to blanching which could have limited the stated enzyme activity as well as improved the surface homogeneity by gas expulsion as observed in other studies on drying (Moscetti et al., 2017; Rocha et al., 2007). As for the general decrease in the *L** value, it can be considered as a direct consequence of moisture loss during drying (Fig 4.5b) which resulted in lower refractive indices similar to dried apple and potato slices (Moscetti et al., 2018; Onwude et al., 2018; Raponi et al., 2021).

Regarding the hue angle (*h*), a continuous decrease in values was observed (Fig. 4.5b) for CNT from 53.35 to 42.35 and BL samples from 52.52 to 37.47 during 36 h of drying. The initial values reflected orange-red hues for both evaluated samples, whereas those of dried carrots tended towards intense red-orange hues with significant differences between the CNT and BL samples. This decrease in hue values can be attributed to the moisture loss and carotenoid degradation during drying (Liu et al., 2016; Moscetti et al., 2017). Interestingly after 6 h of drying when the relative MC_{db} reached approx. value of 4.57 g g^{-1}, the BL samples registered a drastic drop in the hue values and continued to be significantly lower than CNT samples all through the drying. This observation was in concurrence with the trends of MC_{db} (Fig 4.4a) and AS (Fig. 4.4c), with the critical drop being closer to the time frame at which the BL samples registered significantly smaller shrinkage values. This is indicative of the effect of physical changes i.e., shrinkage on the reflective characteristics and consequently the hue values which is known to be impacted by the differential light absorbance at different wavelengths (Pathare et al., 2013). The observations are similar to those of Liu et al. (2016) and Udomkun et al., (2016) in carrot and papaya evaluated using multi-spectra and laser imaging systems who noted that increase in shrinkage caused higher density of cells due to their closely packed structure leading to lower light reflection and diffusion.

Computer Vision-based moisture prediction models

As explained in the methodology section, two types of moisture prediction models, time-dependent models using drying time (*t*) and shrinkage-dependent models using relative area shrinkage (AS) as predictors were fitted. The selected time-dependent models were used as benchmarks despite their boundary conditions like product homogeneity and negligible shrinkage which are challenges for continually evolving product-process spaces like food drying.

Among the tested non-linear thin-layer models, figure 4.6a represents the logarithmic model for an individual replica of CNT samples visually showing a precise fit which was also the case in BL samples (figure not shown). This can be attributed to the use of multiple model parameters (3 or more), which contrarily can also result in insignificant model parameters (principle of parsimony) and data heteroscedasticity due to logarithmic transformation. In consideration of the stated concerns, simple non-linear models like Newton Lewis and Henderson-Pabis have also been evaluated. However, these models (figures not shown) have exhibited visibly evident under and/or over-estimation, which significantly affected the model performances. Moreover, like the logarithmic model, one and two-parameter thin layer models use time as an input model factor, and do not consider spatial changes in the product and its subsequent effects on the drying rate eventually resulting in less resilient and robust models (Aghbashlo et al., 2009; Buzrul, 2022; Onwude et al., 2016; Raponi et al., 2021). In this context, linear regressions can offer a simplistic solution considering the spatial changes of the product to provide models that are more robust and not solely time dependent. This hypothesis was based on our recent study on modelling apple drying for which the AS changed proportionally to the MC_{db} loss (Raponi et al., 2021). However, in the case of carrot slices, this linearity might have deviated considering the observation that a sharp decrease along the drying time was observed at 8 h for AS values, whereas at 11 h for the drying rate. In other words, it can be speculated that the AS was proportional to the MC_{db} loss for most of the falling-rate period and registered deviation after the MC_{db} reached approx. 1.40 (CNT) to 0.80 (BL) g g^{-1}. This observation can be visualized in figure 4.6b which shows both the general linearity between AS and MC_{db} as well as the breakpoint corresponding to the threshold value at which the linearity deviated. Subsequently, the linear segmented model seemed to fit precisely to the experimental values, with no observable under and/or over-estimation for CNT samples (Fig. 4.6c) as well as BL samples (figure not shown) for which different regression equations were used. The MR thus predicted using the linear-segmented model was further visually projected in the drying rate curve in figure 4.6d. This visualization was tested as it can be of interest for developing user interfaces that can allow for multiple projections of the real-time data within the scope of a unified query thereby allowing for optimal monitoring and decision flow by the operator.

As for the model behaviors, they can be further described by the regression parameters presented in table 4.2 and 4.3. As stated, separate regression equations were used for CNT and BL samples as the model parameters like model constants (k, a, c, m and q) differed significantly for CNT and BL samples. This can be attributed to the fact that drying rates were higher in BL due to improved cell permeability by surface microcracks, as previously observed in drying rates (section 3.1) resulting in higher values of rate constant k (t^{-1}) for non-linear models and slope (m) for linear models, respectively. An exception observed was the linear segmented model, wherein the model parameters (m_1, q_1) were statistically non-significant when AS > BP. Whereas, when AS ≤ BP after an AS value of approx. 0.47, the intercept (q_2) values differed significantly between the segments of the model indicating two non-intersecting regression lines for CNT and BL samples. In other words, an averaged model can be used for MC_{db} prediction irrespective of pre-treatment until AS > BP; after which i.e., AS ≤ BP the MC_{db} changes should be predicted based on individual equations considering the significant effect of pre-treatments on the AS behavior. Also, due consideration must be given to the fact that in the present study, the utilized BP was observed beyond 9 h of drying in the carrot slices, which can be stated as prolonged drying at MC_{db} approx. 2.022 (CNT) to 1.22 (BL) g g^{-1} in CNT and BL samples respectively. However, the proposed linear segmented model and in general the use of BP can be of practical significance in cases of monitoring vegetal matrices wherein prolonged drying times and variable pre-treatments that can affect the shrinkage and drying rates are utilized.

Further, in terms of comparison of prediction performances between the time-dependent and shrinkage-dependent models, the selected performance metrics i.e., RMSE, MAE, BIAS, and red. χ^2 are presented in Table 4.4. In general, all the fitted models registered an adj. R^2 of approx. 0.99 and reduced χ^2 approaching to zero indicating excellent prediction capability for the drying behavior of carrot slices. As for the other performance metrics i.e., RMSE, MAE, and BIAS, the values for each model were significantly affected by the model as well as the treatment i.e., CNT or BL. The RMSE values ranged from 0.007 to 0.174 in CNT comparable to those of 0.005 to 0.115 in BL samples. Among the evaluated models, the linear model registered significantly higher RMSE values (CNT, 0.174; BL, 0.115), whereas other models had comparable values and the lowest values were observed in logarithmic (CNT, 0.008; BL, 0.013) and linear-segmented models (CNT, 0.007; BL, 0.005). In fact, it was of interest to note that the error of the linear-segmented model based on relative area shrinkage was superior to the 3-parameter logarithmic model, indicating a good fit and performance in moisture prediction for the carrot slices. As the RMSE is sensitive to outliers, the MAE metric was also considered for evaluation. However, MAE showed a similar pattern to that of RMSE with significantly higher error for the linear model and the lowest error noted for logarithmic and linear-segmented models in both CNT and BL samples. Further, the BIAS values (systematic error) were found to be in the range of 2.23 x 10^{-16} (segmented-linear) to 2.07 x 10^{-02} (simple linear) for CNT samples and 1.35 x 10^{-16} (segmented-linear) to 1.06 x 10^{-01} (simple linear) for BL samples, respectively. The lowest values were noted for logarithmic and linear-segmented models, whereas other models were highly impacted by systematic error indicative of the consideration that the improvement of model performance will be limited even when replicates are increased (Bellon-Maurel et al., 2010). In fact, the significant higher bias of the simple linear model in both CNT and BL samples indicative of an overestimation of the moisture along drying was concurrent with the poor fit observed from red. χ^2 and RMSE values.

Finally, evaluating the presented performance metrics it can be highlighted that the linear-segmented model showed the best performance metrics that can be benchmarked to the best performing thin layer model i.e., logarithmic model for moisture prediction.

Remarks on the SMCS implementation

Thanks to the CV system and the load cells integrated in the dryer as SMCS, the attributes of product i.e., weight loss, color, and shrinkage as well as the pre-defined operation variables (Section - temperature, relative humidity, and airflow) were successfully recorded in real-time i.e., during the product drying for the 36 h of drying period. The use of reverse-engineering approach as part of quality strategy allowed to pre-define and select the said product attributes within carrot drying. Consequently, the acquired in-line spatial changes i.e., shrinkage of carrot slices were successful in prediction of the product moisture changes through use of simplistic linear regression models as explained in the previous section. The evaluated shrinkage dependent linear models when benchmarked against conventional thin-layer models, have shown promising prediction accuracy.

To visualize the model performance, the predicted moisture values from the best performing linear-segmented model for pre-defined thresholds of shrinkage were mapped onto the images of individual carrot slices using an interpolated color palette (purple to white). The resultant images for 36 h were time-lapsed into a video (suppl. Video 4.1) which allows the observer to visualize the potential of the smart system for process-product monitoring as well as the inherent heterogeneity of the process on a hypothetical segment of dryer bed. In the video, the changes in the original carrot slices on the dryer tray (Panel A), the segmented image changes (Panel B) and the color-mapped slices using moisture prediction from linear segmented model (Panel C) are represented. When played, the video clearly shows the following: (i) the change in the shape of the carrot slices measured as area shrinkage (AS) with respect to the drying time; (ii) the change in color indicative of the loss in MC_{db} with respect to the changes in AS; and (iii) the heterogeneity among the samples within the same drying tray owing to the natural variation in the diameter and drying behavior.

Based on the experimental results it can be said that the use of CV and load cell system supplemented with validated shrinkage-dependent model can enable continuous monitoring and risk assessment through prediction and visualization of a specific process-product space. Moreover, adapting a quality strategy can allow for systematic pre-definition of the specific process parameters and target product characteristics. To conclude, the tools and approaches adapted in this work form the basis for a QbD-ready smart dryer that can allow for proactive risk assessment through predictive monitoring for improved operability and continuous learning.

CONCLUSIONS

The computer vision (CV) system and load cells were successfully implemented for in-line monitoring of carrot slices during drying within a convective dryer. Further, shrinkage-dependent models were evaluated to identify best models that include spatial data for predicting the process flow with scope for proactive risk assessment. The study lays foundation for a practical instrument capable of real-time monitoring and control based in QbD strategy. However, further studies are being performed to integrate the SMCS, predictive models and process automation by use of AI based algorithms (like neural networks) as well as multiple product-process spaces for real-time monitoring and prediction of product changes and process-flow, which is beyond the scope of the present study.

The salient findings of this study can be outlined as below:

(i) the CV system successfully tracked the shrinkage and colour changes of carrot slices during drying irrespective of pre-treatments;

(ii) the moisture evolution during drying can be effectively predicted by linear-segmented model considering deviations of shrinkage linearity along the drying period by use of the breakpoint (BP);

(iii) the CV system enabled with shrinkage-based modelling and proactive quality strategy can be an appropriate and feasible approach for a ‘Smart dryer’ capable of real-time monitoring for better process and product control.

Table 4.1

Time-dependent and time-independent models tested for the drying of carrot slices.

Model type	**Model**	**Equations**
Time-dependent	Newton-Lewis	$y = \exp(-kt)$
(Thin layer)	Page	$y = \exp(-(kt^n))$
	Handerson & Pabis	$y = a \exp(-kt^n)$
	Logarithmic	$y = a \exp(-kt)+c$
Time-independent	Simple linear	$y = mx + q$
	Linear segmented	$x > BP$, $y = m_1x + q_1$
		$x \leq BP$, $y = m_2x + q_2$

***MR**, Moisture Ratio; **k**, drying constant (h^{-1}); **t**, drying time (h); **n**, **a** and **c** model constant (dimensionless); **m**, **m_1** and **m_2**, slope; **q**, **q_1** and **q_2**, intercept; **AS**, relative area shrinkage; **BP**, break point.*

Table 4.2

Model parameters and ANOVA for the fitted time-dependent models.

Model Name	**Treatment**	**Model Parameters**							
		k		**n**		**a**		**c**	
Newton-Lewis	Control	0.163	b	-	-	-	-	-	-
	Blanched	0.186	a	-	-	-	-	-	-
Page	Control	0.158	ns	1.015	b	-	-	-	-
	Blanched	0.186	ns	1.136	a	-	-	-	-
Handerson &	Control	0.166	b	-	-	1.020	b	-	-
Pabis	Blanched	0.196	a	-	-	1.057	a	-	-
Logarithmic	Control	0.179	ns	-	-	1.018	b	0.020	a
	Blanched	0.200	ns	-	-	1.056	a	0.006	b

**ns, no significant differences (P > 0.05).*

Table 4.3

Model parameters and ANOVA for the fitted time-independent models.

Model name	Treatment	Model parameters									
		m1		**q1**		**m2**		**q2**		**BP**	
Linear	Control	-0.320	b	1.254	a	-	-	-	-	-	-
	Blanched	-0.243	a	1.186	b	-	-	-	-	-	-
Linear segmented	Control	-0.432	ns	1.410	ns	-0.257	ns	0.900	b	0.430	ns
	Blanched	-0.401	ns	1.393	ns	-0.207	ns	1.041	a	0.510	ns

**ns, no significant differences (P > 0.05).*

Table 4.4

Model performance metrics analyzed by ANOVA for the time-dependent and time-independent models fitted to predict MR changes in Control and Blanched carrot slices.

Model type	Model name	Sample	RMSE		MAE		BIAS		red. χ^2	
Time-dependent (Thin layer)	Newton-Lewis	Control	0.016	abc	0.014	abc	7.61E-03	a	2.53E-04	bc
		Blanched	0.018	ab	0.014	abc	2.67E-03	bc	3.45E-04	ab
	Page	Control	0.015	abc	0.013	abc	8.03E-03	a	2.35E-04	bc
		Blanched	0.010	cde	0.009	cde	5.58E-03	ab	1.14E-04	cde
	Henderson-Pabis	Control	0.015	abc	0.013	bc	7.56E-03	a	2.31E-04	bc
		Blanched	0.015	abc	0.011	bc	2.25E-03	bc	2.17E-04	bcd
	Logarithmic	Control	0.008	de	0.006	de	1.97E-11	c	5.87E-05	de
		Blanched	0.013	bcd	0.009	bcd	1.28E-09	c	1.82E-04	bcde
Time-independent	Linear	Control	0.174	a	0.170	a	2.07E-02	c	3.09E-02	a
		Blanched	0.115	abc	0.106	bc	-1.06E-01	c	1.33E-02	bc
	Linear Segmented	Control	0.007	de	0.006	de	2.23E-16	c	5.69E-05	de
		Blanched	0.005	e	0.003	e	1.35E-16	c	2.86E-05	e

RMSE – Root mean square error; MAE - Mean average error; BIAS - Systematic error; red. $\chi2$ - reduced chi-square; Mean performance metrics with different letters indicate significant differences (p<0.05).

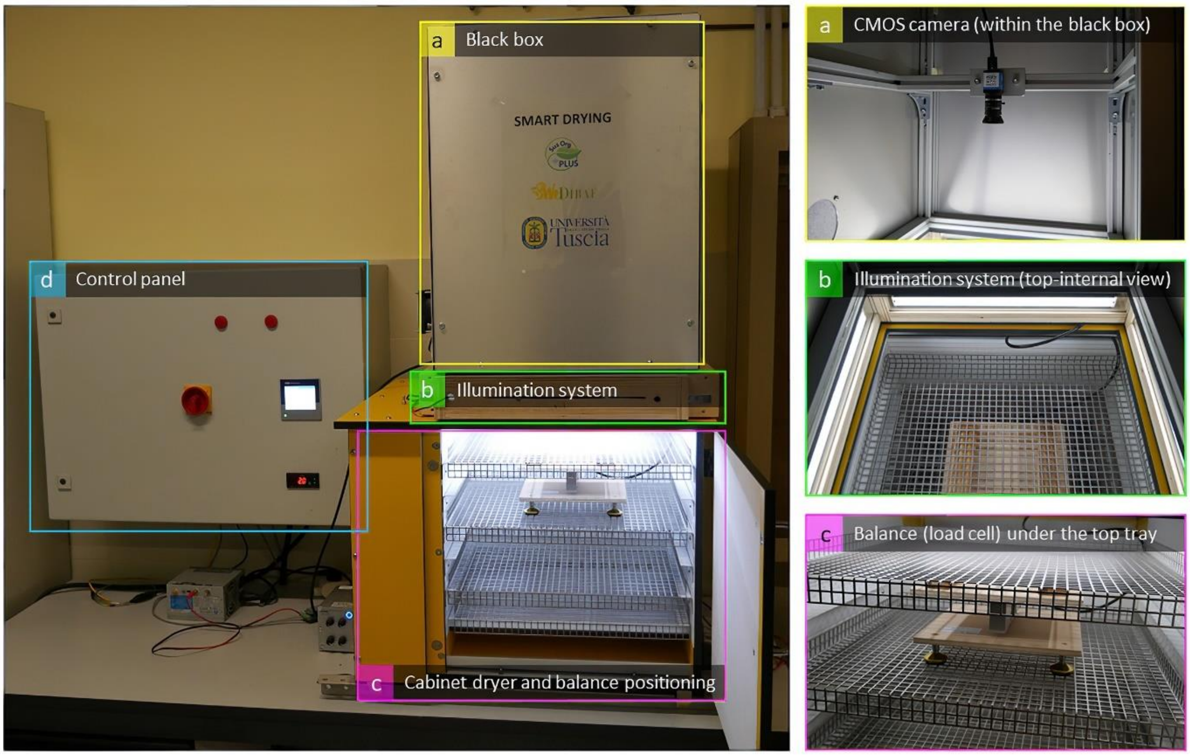

Figure 4.1

Convection-based cabinet dryer prototype set-up embedded with PAT tools for real-time monitoring of drying: a) black box with camera, b) illumination system, c) cabinet dryer and balance positioning, with respective insets on the right side and d) control panel.

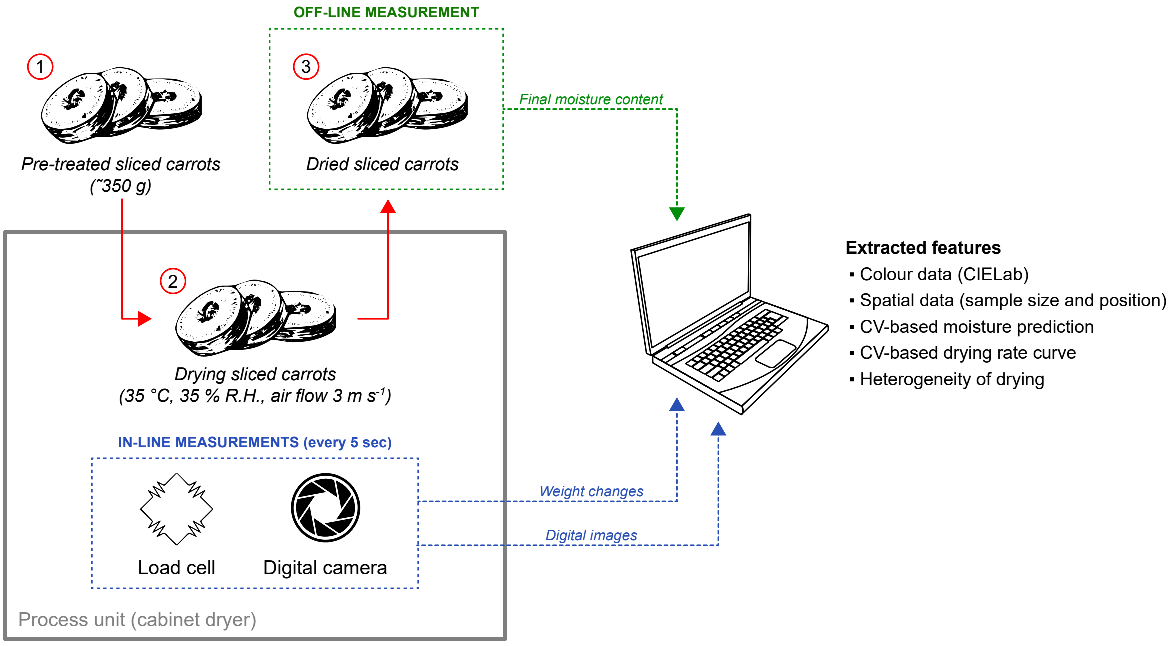

Figure 4.2

Schematic of smart dryer prototype embedded with in-line PAT tools - Load cell and digital camera for QbD-based real-time monitoring of carrot slice drying (steps 1, 2 and 3).

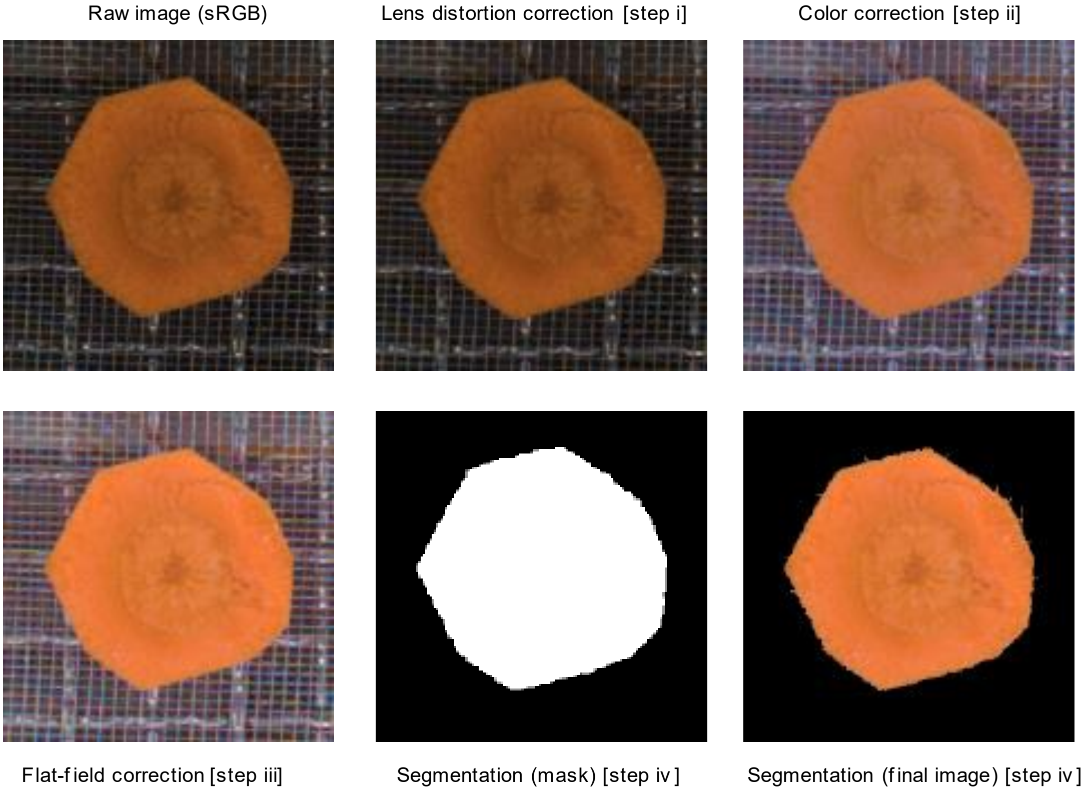

Figure 4.3

Sequential steps in image correction and segmentation from raw image (sRGB) to the final corrected and segmented image.

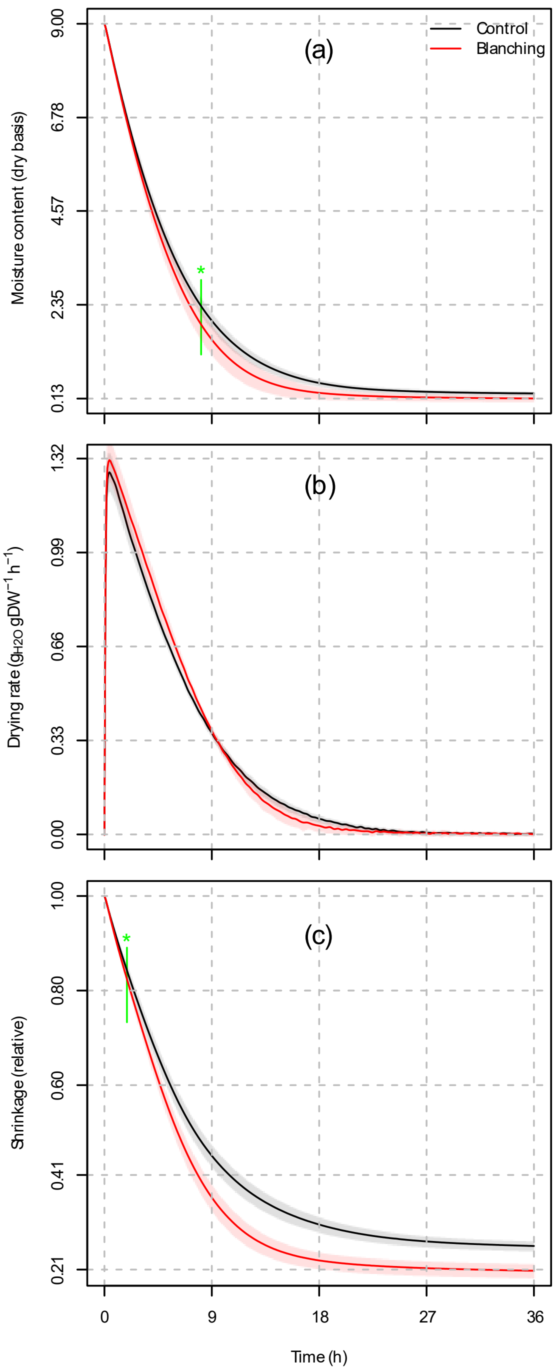

Figure 4.4

*In-line monitoring of a) dry basis moisture content, MC_{db}; b) drying rate, DR; and c) relative area shrinkage, AS along 36 h of drying of control (CNT) and blanched (BL) carrot slices dried at 35 °C, 35 % R.H. and ~3 m s^{-1} air velocity. Results are reported as mean and standard deviation of the mean. The vertical green line with the * symbol at the top represents the initial moment at which the CNT and BL values become statistically different ($p \leq 0.05$).*

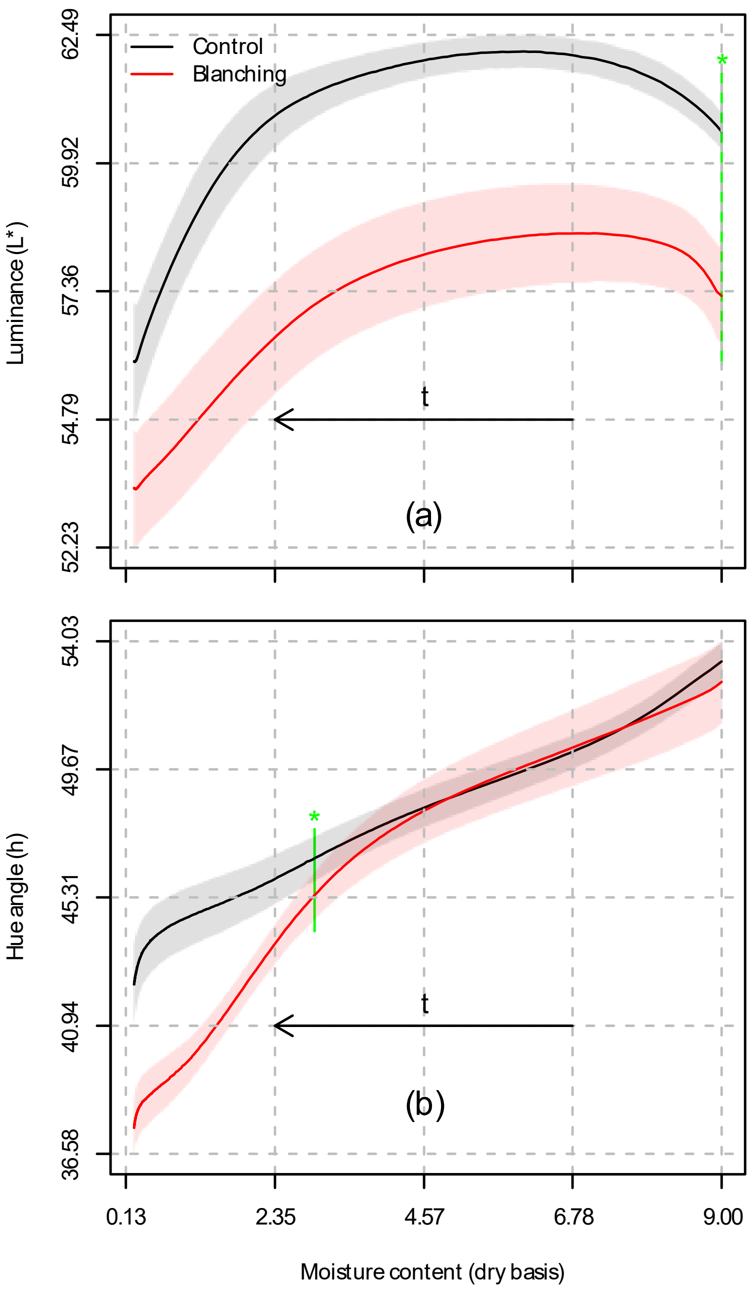

Figure 4.5

In-line monitoring of color changes a) luminance (L) and b) hue angle (h) with respect to dry basis moisture content (MC_{db}) along 36 h of drying for control (CNT) and blanched (BL) carrot slices dried at 35 °C, 35 % R.H. and ~3 m s^{-1} air velocity. The arrow (in black, from right to left) denotes the time flow for both L* and h. Results are reported as mean and standard deviation of the mean. The vertical green line with the * symbol at the top represents the initial moment at which the CNT and BL values become statistically different ($p \leq 0.05$).*

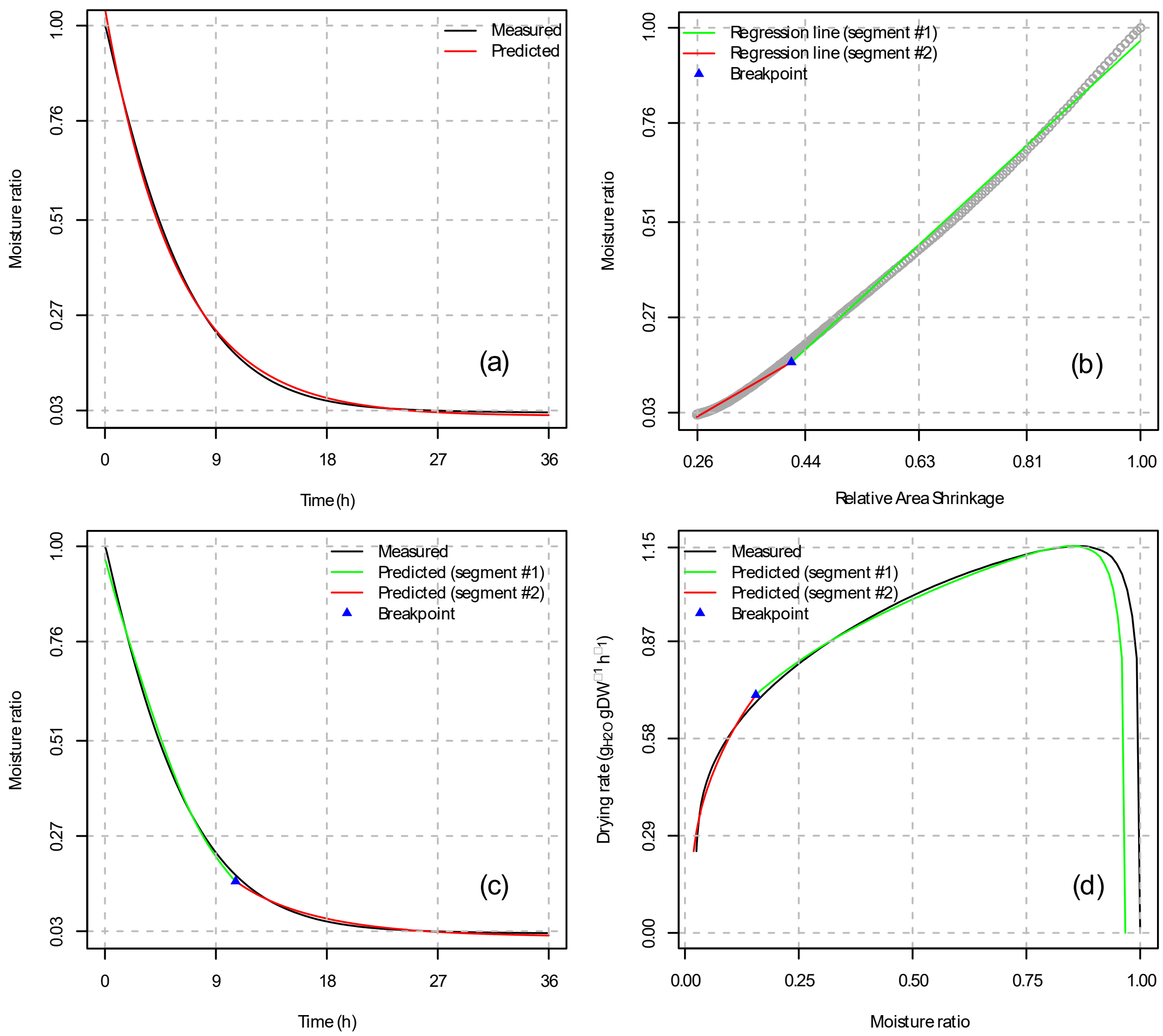

Figure 4.6

Plots depicting a replication of a) MR prediction using the logarithmic model wit; b) model fit of the linear segmented model, MR vs AS; c) MR prediction using the linear segmented model; d) drying rate curve as a function of the MR predicted based using the linear segmented model.

Supplementary video 4.1

Time-lapse video of 36 h of drying representing the variable shrinkage of the carrot slices on the dryer tray (Panel A), the segmented images (Panel B) and the colour-mapped slices using moisture prediction from results of the linear segmented model (Panel C). The change in color from purple to white gradients in panel C shows the heterogenous change in the moisture content proportional to the degree of shrinkage within sample set.

Please see the link below:

https://drive.google.com/file/d/1Yq_C37vTJEW5UgO2Oudiv1QS_ETfSbYJ/view

REFERENCES

Aghbashlo, M., Hosseinpour, S., Ghasemi-Varnamkhasti, M., 2014. Computer vision technology for real-time food quality assurance during drying process. Trends Food Sci. Technol. https://doi.org/10.1016/j.tifs.2014.06.003

Aghbashlo, M., Kianmehr, M.H., Arabhosseini, A., 2009. Performance analysis of drying of carrot slices in a semi-industrial continuous band dryer. J. Food Eng. 91, 99–108. https://doi.org/10.1016/j.jfoodeng.2008.08.020

Aprajeeta, J., Gopirajah, R., Anandharamakrishnan, C., 2015. Shrinkage and porosity effects on heat and mass transfer during potato drying. J. Food Eng. 144, 119–128. https://doi.org/10.1016/j.jfoodeng.2014.08.004

Bedini, G., Nallan Chakravartula, S.S., Bastianelli, G., Caccia, R., Contarini, M., Morales-Rodríguez, C., Rossini, L., Speranza, S., Vannini, A., Moscetti, R., Massantini, R., 2020. Feasibility of ft-nir spectroscopy and vis/nir hyperspectral imaging for sorting unsound chestnuts. Italus Hortus 27, 3–18. https://doi.org/10.26353/j.itahort/2020.1.0318

Buzrul, S., 2022a. processes Reassessment of Thin-Layer Drying Models for Foods: A Critical Short Communication. https://doi.org/10.3390/pr10010118

Crippa, M., Solazzo, E., Guizzardi, D., Monforti-Ferrario, F., Tubiello, F.N., Leip, A., 2021. Food systems are responsible for a third of global anthropogenic GHG emissions. Nat. Food 2, 198–209. https://doi.org/10.1038/s43016-021-00225-9

Defraeye, T., 2014. Advanced computational modelling for drying processes - A review. Appl. Energy. https://doi.org/10.1016/j.apenergy.2014.06.027

Dhall, A., Datta, A.K., 2011. Transport in deformable food materials: A poromechanics approach. Chem. Eng. Sci. 66, 6482–6497. https://doi.org/10.1016/j.ces.2011.09.001

Erbay, Z., Icier, F., 2010. A review of thin layer drying of foods: Theory, modeling, and experimental results. Crit. Rev. Food Sci. Nutr. 50, 441–464. https://doi.org/10.1080/10408390802437063

Erenturk, S., Erenturk, K., 2007. Comparison of genetic algorithm and neural network approaches for the drying process of carrot. J. Food Eng. 78, 905–912. https://doi.org/10.1016/j.jfoodeng.2005.11.031

Fellows, P.J., Fellows, P.J., 2017. Blanching, in: Food Processing Technology. pp. 525–538.

https://doi.org/10.1016/B978-0-08-100522-4.00009-2

Ghasemi-Varnamkhasti, M.G., Aghbashlo, M., 2014. Electronic nose and electronic mucosa as innovative instruments for real-time monitoring of food dryers. Trends Food Sci. Technol. https://doi.org/10.1016/j.tifs.2014.05.004

González-Fésler, M., Salvatori, D., Gómez, P., Alzamora, S.M., 2008. Convective air drying of apples as affected by blanching and calcium impregnation. J. Food Eng. 87, 323–332. https://doi.org/10.1016/j.jfoodeng.2007.12.007

Gulati, T., Datta, A.K., 2015. Mechanistic understanding of case-hardening and texture development during drying of food materials. J. Food Eng. 166, 119–138. https://doi.org/10.1016/J.JFOODENG.2015.05.031

Khan, M.I.H., Sablani, S.S., Joardder, M.U.H., Karim, M.A., 2020. Application of machine learning-based approach in food drying: opportunities and challenges. Dry. Technol. 0, 1–17. https://doi.org/10.1080/07373937.2020.1853152

Krokida, M.K., Karathanos, V.T., Maroulis, Z.B., Marinos-Kouris, D., 2003. Drying kinetics of some vegetables. J. Food Eng. 59, 391–403. https://doi.org/10.1016/S0260-8774(02)00498-3

Lahsasni, S., Kouhila, M., Mahrouz, M., Jaouhari, J.T., 2004. Drying kinetics of prickly pear fruit (Opuntia ficus indica). J. Food Eng. 61, 173–179. https://doi.org/10.1016/S0260-8774(03)00084-0

Lemmens, L., Tibäck, E., Svelander, C., Smout, C., Ahrné, L., Langton, M., Alminger, M., Van Loey, A., Hendrickx, M., 2009. Thermal pretreatments of carrot pieces using different heating techniques: Effect on quality related aspects. Innov. Food Sci. Emerg. Technol. 10, 522–529. https://doi.org/10.1016/j.ifset.2009.05.004

Liu, C., Liu, W., Lu, X., Chen, W., Yang, J., Zheng, L., 2016. Potential of multispectral imaging for real-time determination of colour change and moisture distribution in carrot slices during hot air dehydration. Food Chem. 195, 110–116. https://doi.org/10.1016/j.foodchem.2015.04.145

Liu, Y., Pu, H., Sun, D.W., 2017. Hyperspectral imaging technique for evaluating food quality and safety during various processes: A review of recent applications. Trends Food Sci. Technol. https://doi.org/10.1016/j.tifs.2017.08.013

Lyndgaard, C.B., Engelsen, S.B., Van Den Berg, F.W.J., 2012. Real-time modeling of milk coagulation using in-line near infrared spectroscopy. J. Food Eng. 108, 345–352. https://doi.org/10.1016/J.JFOODENG.2011.07.029

Madiouli, J., Sghaier, J., Lecomte, D., Sammouda, H., 2012. Determination of porosity change from shrinkage curves during drying of food material. Food Bioprod. Process. 90, 43–51. https://doi.org/10.1016/j.fbp.2010.12.002

Mayor, L., Sereno, A.M., 2004. Modelling shrinkage during convective drying of food materials: A review. J. Food Eng. 61, 373–386. https://doi.org/10.1016/S0260-8774(03)00144-4

Menon, A., Stojceska, V., Tassou, S.A., 2020. A systematic review on the recent advances of the energy efficiency improvements in non-conventional food drying technologies. Trends Food Sci. Technol. https://doi.org/10.1016/j.tifs.2020.03.014

Moscetti, R., Berhe, D.H., Agrimi, M., Haff, R.P., Liang, P., Ferri, S., Monarca, D., Massantini, R., 2021. Pine nut species recognition using NIR spectroscopy and image analysis. J. Food Eng. 292, 110357. https://doi.org/10.1016/j.jfoodeng.2020.110357

Moscetti, R., Haff, R.P., Ferri, S., Raponi, F., Monarca, D., Liang, P., Massantini, R., 2017. Real-Time Monitoring of Organic Carrot (var. Romance) During Hot-Air Drying Using Near-Infrared Spectroscopy. Food Bioprocess Technol. 10, 2046–2059. https://doi.org/10.1007/s11947-017-1975-3

Moscetti, R., Massantini, R., Fidaleo, M., 2019. Application on-line NIR spectroscopy and other process analytical technology tools to the characterization of soy sauce desalting by electrodialysis. J. Food Eng. 263, 243–252. https://doi.org/10.1016/j.jfoodeng.2019.06.022

Moscetti, R., Sturm, B., Crichton, S.O.J.O., Amjad, W., Massantini, R., 2018. Postharvest monitoring of organic potato (cv. Anuschka) during hot-air drying using visible–NIR hyperspectral imaging. J. Sci. Food Agric. 98, 2507–2517. https://doi.org/10.1002/jsfa.8737

Moses, J.A., Alagusundaram, K., Tiwari, B.K., 2014. Novel Drying Techniques for the Food Industry ´ 43–55. https://doi.org/10.1007/s12393-014-9078-7

Nguyen, T.K., Mondor, M., Ratti, C., 2018. Shrinkage of cellular food during air drying. J.

Food Eng. 230, 8–17. https://doi.org/10.1016/j.jfoodeng.2018.02.017

Onwude, D.I., Hashim, N., Abdan, K., Janius, R., Chen, G., 2018. The potential of computer vision, optical backscattering parameters and artificial neural network modelling in monitoring the shrinkage of sweet potato (Ipomoea batatas L.) during drying. J. Sci. Food Agric. 98, 1310–1324. https://doi.org/10.1002/jsfa.8595

Onwude, D.I., Hashim, N., Janius, R.B., Nawi, N.M., Abdan, K., 2016. Modelling the Thin-Layer Drying of Fruits and Vegetables: A Review. Compr. Rev. Food Sci. Food Saf. 15, 599–618. https://doi.org/10.1111/1541-4337.12196

Planinić, M., Velić, D., Tomas, S., Bilić, M., Bucić, A., 2005. Modelling of drying and rehydration of carrots using Peleg's model. Eur. Food Res. Technol. 221, 446–451. https://doi.org/10.1007/s00217-005-1200-x

Purlis, E., Cevoli, C., Fabbri, A., 2021. Modelling Volume Change and Deformation in Food Products/Processes: An Overview. Foods 2021, Vol. 10, Page 778 10, 778. https://doi.org/10.3390/FOODS10040778

Raponi, F., Moscetti, R., Monarca, D., Colantoni, A., Massantini, R., 2017. Monitoring and optimization of the process of drying fruits and vegetables using computer vision: A review. Sustain. 9. https://doi.org/10.3390/su9112009

Raponi, F., Moscetti, R., Nallan Chakravartula, S.S., Fidaleo, M., Massantini, R., 2021. Monitoring the hot-air drying process of organically grown apples (cv. Gala) using computer vision. Biosyst. Eng. https://doi.org/10.1016/j.biosystemseng.2021.07.005

Rathore, A.S., Kapoor, G., 2016. Implementation of Quality by Design for processing of food products and biotherapeutics. Food Bioprod. Process. https://doi.org/10.1016/j.fbp.2016.05.009

Rocha, A.M., Ferreira, J.F., Silva, Â.M., Almeida, G.N., Morais, A.M., 2007. Quality of grated carrot (var. Nantes) packed under vacuum. J. Sci. Food Agric. 87, 447–451. https://doi.org/10.1002/jsfa.2723

Rocha, A.M.C.N., Mota, C.C.A.R., Morais, A.M.M.B., 2007. Physico-chemical qualities of minimally processed carrot stored under vacuum. J. Foodserv. 18, 23–30. https://doi.org/10.1111/j.1745-4506.2007.00043.x

Seyedabadi, E., Khojastehpour, M., Abbaspour-Fard, M.H., 2019. Online measuring of quality changes of banana slabs during convective drying. Eng. Agric. Environ. Food 12, 111–117. https://doi.org/10.1016/j.eaef.2018.10.004

Simões, A. do N., Ventrella, M.C., Moretti, C.L., Carnelossi, M.A.G., Puschmann, R., 2010. Anatomical and physiological evidence of white blush on baby carrot surfaces. Postharvest Biol. Technol. 55, 45–52. https://doi.org/10.1016/J.POSTHARVBIO.2009.07.007

Toğrul, H., 2006. Suitable drying model for infrared drying of carrot. J. Food Eng. 77, 610–619. https://doi.org/10.1016/j.jfoodeng.2005.07.020

van den Berg, F., Lyndgaard, C.B., Sørensen, K.M., Engelsen, S.B., 2013. Process Analytical Technology in the food industry. Trends Food Sci. Technol. https://doi.org/10.1016/j.tifs.2012.04.007

Wu, B., Pan, Z., Qu, W., Wang, B., Wang, J., Ma, H., 2014. Effect of simultaneous infrared dry-blanching and dehydration on quality characteristics of carrot slices. LWT - Food Sci. Technol. 57, 90–98. https://doi.org/10.1016/j.lwt.2013.11.035

Zhang, M., Chen, H., Mujumdar, A.S., Tang, J., Miao, S., Wang, Y., 2017. Recent developments in high-quality drying of vegetables, fruits, and aquatic products. Crit. Rev. Food Sci. Nutr. 57, 1239–1255. https://doi.org/10.1080/10408398.2014.979280

4.2 PRELIMINARY SEMI-DRYING TESTS ON POTATO SLICES

This section describes a preliminary study performed on potato slices using the same prototype smart-enabled cabinet dryer set-up described in previous section 4.1. The data reported represents the results a preliminary study performed as a part a master thesis. Following further investigation, these data may be considered as a part of a publication in the near future.

INDEX

KEYWORDS: *Process Analytical Technology; Quality-by-Design; computer vision; Solanum tuberosum L.; segmented-linear model.*

ABSTRACT

The semi-drying process was tested at 35 °C, 35 % R.H. and 2.98 m/s air velocity using a convective dryer embedded with computer vision (CV) system and load cell. The potato slices were 6-mm thick (cv. Fontane). The product was dried to a final moisture content of 60 % (wet basis). In order to reduce the occurrence of oxidative browning development, four treatments were tested: (i) control; dipping in solutions of (ii) citric acid at 3 % (w/v) and (iii) sodium metabisulphite at 0.1 % (w/v) and (iv) blanching at 90 °C. The convection-based cabinet dryer prototype set-up embedded with Process Analytical Technology tools allowed i) to monitor the product features (i.e., weight, color, and size); and ii) to develop shrinkage-dependent moisture prediction models using linear regression. No treatment affected the drying kinetics of the potato slices, except for blanching which slightly accelerated the drying rate. The use of citric acid effectively controlled the browning development of the potato slices during the process. Even the blanching reduced the oxidative phenomena occurrence but rarely showed dark areas at the cortex of tuber, due to the well-known "after cooking darkening" phenomenon.

The evaluated shrinkage-dependent linear models showed good performances (RMSE, 0.006-0.020). This preliminary study showed promising results and future developments will concern

the optimization of the process and the evaluation of important quality parameters (e.g., shelf-life, culinary aspects, oil uptake during frying, etc.).

MATERIALS AND METHODS

Sample preparation

Potato tubers (*Solanum tuberosum* L.) of the cultivar selected trough the activity reported in chapter 4 (cv. Fontane) were provided by the "Patata dell'Alto Viterbese PGI" consortium (C.C.OR.A.V.). Tubers were stored at 5 ± 1 °C until further processing. Potatoes free of blemishes and defects were tempered to room temperature for 12 h, washed, and cut into 6-mm thick slices. Samples were split into batches of ~350 g of fresh weight before processing (~30 carrot slices). One batch of samples (BL) were blanched in water at 90 °C for 5 min (Klarstein Slowcooker 550W, Germany) to reduce the residual polyphenol oxidase (PPO) activity to less than 10 % based on our previous study (Moscetti et al., 2019). Other two batches were pre-treated by (i) dipping in citric acid (CA) and (ii) sodium metabisulphite (SMB) solutions (3 % and 0.1 % w/v, respectively) for 5 min. The product:solution ratio was 1:5 (w/v). The control (CNT) batch was dipped in water at room temperature for 5 min. Immediately after the treatment, the samples were cooled using an ice bath, rested on a cotton cloth for 2 min to remove excess surface moisture, re-weighed, and subjected to drying tests.

'Smart cabinet dryer' set-up

The prototype smart-enabled cabinet dryer set-up used in the drying tests is described in section 4.1 (Materials and Methods).

Semi-Drying process and real-time data acquisition

The hot-air drying experiments were performed at 35 °C, 35 % R.H and ~3 m s^{-1} air flow based on preliminary trials. Each drying trial consisted of about 350 g of potato slices. The semi-drying process was stopped at a wet-basis moisture content of 60 % (~6 h). Each treatment was replicated 2 times. The samples were subjected to offline analysis of moisture content at the end of the drying process according to AOAC 934.06 official method.

Regarding real-time acquisitions and recordings the procedures and tools used are described in section 4.1 (Materials and Methods).

Data handling and features extraction

The changes in dry-basis moisture content (MC_{db}) during drying were computed following the approach described in section 4.1 (Materials and Methods).

As for the in-line images acquired, they were utilized for features extraction (i.e., color and size information over time from samples). Prior to feature extraction, the camera was (i) calibrated, to remove the lens distortion on the image; (ii) profiled, to correct color distortion due to the camera sensor; and the images were (iii) flat-field corrected, to remove shading distortion due to uneven illumination; (iv) and segmented, to separate the true image of each sample (i.e., foreground) from its background (i.e., non-sample data) (Figure 4.7).

The camera calibration, the color and flat-field correction of the images, the image segmentation and the features extraction were performed using procedures, software, functions and scripts described in section 4.1 – Materials and Methods.

Computer Vision-based moisture prediction models

Moisture ratio (MR) prediction models were computed for each treatment (i.e., CNT, BL, CA and SMB), evaluating two different shrinkage-dependent models i.e., the linear and segmented-linear models, using changes in MR as a function of area shrinkage (AS). The breakpoint (BP) was identified using the *segmented()* function of the Segmented R-package to fit the standard linear model with segmented relationships between MR and AS; for the intended purpose, the ‘npsi’ attribute of function (i.e., number of BR to be identified) was set equal to 1.

The model’s goodness of fit was evaluated in terms of Root Mean Square Error (RMSE), systematic error (BIAS) and reduced chi-square (red. χ^2).

Data handling and statistical analysis

One-way analysis of variance was performed to evaluate and compare the effects of the different pre-treatments tested on the drying process and their effectiveness in preventing enzymatic browning and after-cooking darkening.

Two-way analysis of variance (ANOVA) was performed to evaluate and compare the main effect of the (i) treatment (TRT) factor (CNT, BL, CA and SMB), (ii) the model (MD) factor (linear and segmented-linear) and their interaction (TRT x MD) on the metrics of each model, as well as to identify the best model in terms of performances.

Tukey's pairwise comparison method was performed, and the Honestly Significant Difference (HSD) was calculated for an appropriate level of interaction ($P \leq 0.05$). Scripts for data handling, breakpoint identification for the development of linear-segmented models, modelling and ANOVA were prepared using the R software v3.6.9 in combination with ‘dplyr’, ‘segment’, and ‘Agricolae’ R-packages.

RESULTS AND DISCUSSION

In-line quality parameters

Moisture content and drying rates

Data acquired from the load cell during the process were used to monitor the change in moisture on a dry basis and the drying rate of the samples. The trend of moisture loss is presented in Figure 4.8a. The trend is quite linear, likely because the duration of the process was very short (6 hours, approx.) and a temperature of 35°C is not sufficient to show a moisture loss in the product describable by first-order kinetics. The initial MC_{db} for all treatments ranged from 3.52 to 3.88 g g^{-1}. Figure 4.8b shows the relationship between the drying rate and the MC_{db} of the product. The average drying rates increased rapidly as expected to 0.37-0.42 g H_2O g DW^{-1} h^{-1} due to the initial warm-up period and consequent increase in the product's surface temperature. Interestingly, a tendentially higher drying rate was observed for BL and this can be attributed to damage of the cell membranes caused by the high temperature (90 °C). In support of this statement, the ANOVA results (Table 4.5) showed significant differences in the drying rate among the different pre-drying treatments. Specifically, BL reported a statistically higher drying rate than CNT. The chemical treatments (CA and SMB) showed intermediate values, not statistically different from both BL and CNT.

Shrinkage

Figure 4.8c shows the general tendency of the relative area shrinkage (AS) of potato slices along the drying time without significant differences between pre-drying treatments at the end of the process. Also in this case, all samples exhibited pseudo linear trend, similar to that of MC_{db} (Fig. 4.8a) with rapid decrease in AS from an initial value of 1.00 to about 0.60-0.70 in within 6 h of drying time. The results confirm what has already showed for carrots, namely that potatoes had ideal shrinkage behavior, with shrinkage linearly related to that of moisture loss.

In contrast with the results obtained for carrot slices, the ANOVA test revealed no statistical differences between the tested pre-treatments concerning the shrinkage behavior after 6 h of drying (data not shown). Thus, in this case, the effect of blanching was irrelevant.

Surface color changes

Colorimetric parameters (CIELab), as an important visual aspect also dried potato critically impacting the purchase decisions, were monitored along the drying process by the CV system. The samples as expected exhibited changes in the CIELab coordinates (L^*, luminance; a^*, redness; b^*, yellowness) along the drying time represented by luminance (L^*), hue angle (*h*) and chroma (*C**) in figures 4.9a, 4.9b and 4.9c, respectively.

In terms of luminance (*L**), the values were observed to linearly decrease concurrent to the loss of MC_{db} along the drying time (*t*, shown in Fig. 4.9a) for all samples. Within the tested samples, BL evidenced significantly lower *L** values than CNT and chemical treatments (i.e., CA and SMB) both at the beginning and at the end of semi-drying process (Table 4.6). As already reported for carrot, this can be attributed to blanching which could have limited the stated enzyme activity as well as improved the surface homogeneity by gas expulsion as observed in other studies on drying (Moscetti et al., 2017). As for the general decrease in the *L** value, it can be considered as a direct consequence of moisture loss during drying which resulted in lower refractive indices similar to dried apple, carrot and potato slices (Moscetti et al., 2017; Onwude et al., 2018; Raponi et al., 2021).

Regarding the hue angle (*h*), a continuous decrease in values was observed (Fig. 4.9b) for all samples during 6 h of drying. The BL samples registered the statistically highest hue values and continued to be significantly higher than other samples all through the drying. These values corresponded to a more intense yellow coloring of the product. However, the BL samples showed blackening in the cortex tissue. This negative process is named after-cooking darkening (ACD) and it is due to the oxidation of the ferri-chlorogenic acid in the blanched potato slices (Wang-Pruski and Nowak, 2004). The ACD was evident also for CNT samples, demonstrating a predisposition of cv. Fontane to this process. Regarding chemical pre-drying treatments (i.e., CA and SMB), the well-known effectiveness in preventing both enzymatic browning and ACD was confirmed. Specifically, the dipping in CA solution stabilized the hue angle to a value statistically higher than the control, demonstrating greater efficacy than SMB, which reported no statistical differences from CNT samples (Table 4.6).

Figure 4.9c reports the results of chroma (*C**). For all samples, color saturation decreased except for blanched potato slices, where, after an initial decrease, it tended to increase in concomitance with the loss of MC_{db}. The statistical analysis showed no significant difference between chemical treatments and control, but it reported the highest color saturation for BL samples (Table 4.6).

Computer Vision-based moisture prediction models

As explained in the methodology section, two types of shrinkage-dependent models (i.e., linear and segmented-linear model) using relative area shrinkage (AS) as predictor were fitted. This choice was based on our studies on modelling apple and carrot drying for which the AS changed proportionally to the MC_{db} loss (Raponi et al., 2021; Sirisha et al., 2023). The study was performed for all tested pre-treatments (i.e., BL, CA, SMB and CNT).

As already reported for carrot slices, the segmented-linear model seemed to fit precisely to the experimental values, with no observable under and/or over-estimation for samples treated with CA (Figure 4.10) and for all other samples (figures not shown). In fact, just by observing at the figure 4.10, it is possible to understand how the segmented linear model (Fig. 4.10b) better describes the relationship between shrinkage and moisture than simple linear model (Fig. 4.10a), limiting prediction errors to a minimum. The linear models shows both the general linearity between AS and MC_{db} as well as the breakpoint corresponding to the threshold value at which the linearity deviated. Specifically, the algorithm identified the breakpoint (BP) at a shrinkage of 0.94. This means that as soon as the product shrunk by 6% of its initial size, the linear relationship between AS and MC_{db} changed to remain constant until the desired MC_{db} was reached.

Figure 4.11 compared the trend of MC_{db} measured and predicted for both linear and segmented-linear model (Fig. 4.11a and 4.11b , respectively). Specifically, in the simple linear model, an underestimation in the first hour of the process, an overestimation between the first and fourth hours, and an underestimation again in the last hour of the process were observed. Differently, for segmented-linear model, the lines are largely overlapping, graphically showing a low effect of the systematic error of measurements, thereby a better ability of the model to correctly estimate the MC_{db}.

Further, thought the two-way ANOVA was evaluated the impact of treatment, models and of their interaction on the metrics of models. In addition, the comparison in terms of prediction performances between the two shrinkage-dependent models (i.e., linear and segmented linear) was performed and the selected metrics i.e., RMSE, BIAS, and red. χ^2, are presented in Table 4.7. Regarding RMSE, no significant interaction was observed between treatments and model (TRT x MD), while the effect of individual factors was significant. As an effect of the treatments (TRT), the control presented a tendentially higher estimation error, reporting a RMSE value statistically different from SMB, but comparable with CA and BL. Concerning the model factor (MD), as already noted observing the regression plots, the segmented-linear model reported a statistically lower prediction error than the simple linear model (0.006 and 0.020, respectively). No significant differences related to the BIAS were found due to the interaction of factors or the effect of individual factors. In each model, the BIAS tended to zero, meaning that the impact of systematic error in the measurements was very low and almost completely irrelevant for the prediction. For the red. $\chi2$, the ANOVA test revealed a significant interaction between factors (TRT x MD), highlighting a lower effectiveness of the simple linear model in predicting the MCdb of the control based on product shrinkage.

CONCLUSIONS

The implementation of a computer vision (CV) system and load cells for in-line monitoring of potato slices during drying within a convective dryer allowed to perform color analysis and to select the dipping in citric acid solution (3 % w/v) as the best pre-drying treatment. This chemical treatment was effective in preventing both enzymatic browning and after-cooking darkening. The shrinkage-dependent models already tested in the previous study performed on carrot slices demonstrated their accuracy in predicting the residual moisture content of potato slices. In particular, the segmented-linear regression approach reported the best prediction performance irrespective of treatments. These models will have to be validated, but the preliminary results confirm that the smart monitoring and control systems (SMCS) for real-time monitoring of food drying can allow to obtain a high-quality final product, reducing the energy consumption and environmental impact. However, to make this process feasible in a company, further studies are needed. In particular, further investigations will be performed (i) to integrate the SMCS, predictive models and process automation by use of Artificial Intelligence-based algorithms (like neural networks), and (ii) to asses some important quality parameters such as shelf-life and oil uptake during frying.

Table 4.5

Initial MC_{db} and drying rate measured during 6 h of drying of pre-treated (SMB, CA and BL) and control (CNT) potato slices dried at 35 °C, 35 % R.H. and ~3 m s^{-1} air velocity. Results are reported as mean. Within-column values followed by the same letter are not significantly different, $p \leq 0.05$.

Treatment	**Initial MC_{db}**	**Drying rate ($g\ H_2O\ g\ DW^{-1}h^{-1}$)**	
Control (CNT)	3,52	0,37	b
Sodium Metabisulphite (SMB)	3,58	0,38	ab
Critic Acid (CA)	3,53	0,40	ab
Blanching (BL)	3,88	0,42	a
p-value	0.20	< 0.01	

Table 4.6

CIELab colorimetric parameters of pre-treated potato slices (var. Fontane) at the beginning of semi-drying process at 35 °C, 35 % R.H. and ~3 m s^{-1} air velocity. Results are reported as mean. Within-column values followed by the same letter are not significantly different, $p \leq 0.05$.

Treatment	**Initial CIELab Color parameters**							
	L*		***a****		***b****	***h***		***C****
Control (CNT)	76,24	a	2,05	a	35,91	86,55	b	36,00
Sodium Metabisulphite (SMB)	75,70	a	2,50	a	33,95	85,70	c	34,06
Citric Acid (CA)	76,36	a	2,54	a	32,76	85,47	c	32,88
Blanching (BL)	70,43	b	-1,01	b	32,70	91,67	a	32,73
p-value	< 0.001		< 0.001		0,32	< 0.001		0,32

Table 4.7

CIELab colorimetric parameters of pre-treated potato slices (var. Fontane) at the end of the semi-drying process at 35 °C, 35 % R.H. and ~3 m s^{-1} air velocity. Results are reported as mean. Within-column values followed by the same letter are not significantly different, $p \leq 0.05$.

Treatment	**Final CIELab Color parameters**				
	L*	***a****	***b****	***h***	***C****
Control (CNT)	70,81 a	4,25 a	28,54 b	80,78 c	27,15 b
Sodium Metabisulphite (SMB)	72,85 a	4,04 a	29,57 a	81,36 bc	27,37 b
Citric Acid (CA)	73,14 a	3,74 a	30,13 a	81,92 b	27,22 b
Blanching (BL)	65,62 b	0,67 b	29,99 a	88,76 a	32,81 a
p-value	< 0.01	< 0.001	< 0.01	< 0.001	< 0.01

Table 4.8

The interaction of pretreatment (TRT) and model (MD) on the metrics of the MC predictive models on potato slices dried at 35 °C, 35 % R.H. and ~3 m s^{-1} air velocity. Results are reported as mean. Within-column values followed by the same letter are not significantly different according to the Honestly Significant Difference or HSD ($p \leq 0.05$).

Factors		RMSE		BIAS	Reduced $\chi 2$	
Treatment (TRT)						
Control (CNT)		0,021	a	-1,30E-16	6,17E-04	
Sodium Metabisulphite (SMB)		0,008	b	6,38E-07	1,47E-04	
Citric Acid (CA)		0,010	ab	2,31E-16	1,42E-04	
Blanching (BL)		0,014	ab	-9,75E-17	2,36E-04	
p-value		< 0.05		0,38	< 0.05	
Model (MD)						
Linear		0,020	a	2,94E-07	5,24E-04	
Segmented-linear		0,006	b	2,50E-08	4,77E-05	
p-value		< 0.01		0,39	< 0.01	
TRT x MD						
Control	Linear	0,033		-3,23E-16	1,14E-03	a
Control	Segmented	0,010		6,19E-17	9,29E-05	b
Metabisulphite	Linear	0,012		1,18E-06	2,72E-04	b
Metabisulphite	Segmented	0,004		1,00E-07	2,30E-05	b
Citric Acid	Linear	0,016		6,17E-16	2,61E-04	b
Citric Acid	Segmented	0,005		-1,55E-16	2,30E-05	b
Blanching	Linear	0,020		3,93E-17	4,21E-04	b
Blanching	Segmented	0,007		-2,34E-16	5,20E-05	b
p-value		0,34		0,51	< 0.05	

Raw image (sRGB)

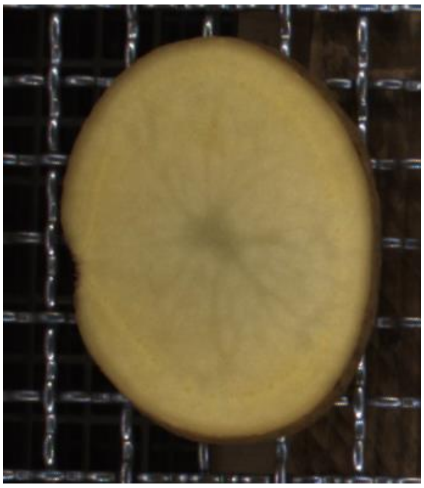

Corrected and segmented final image

Figure 4.7

Image correction and segmentation: raw image (sRGB) and the final corrected and segmented image.

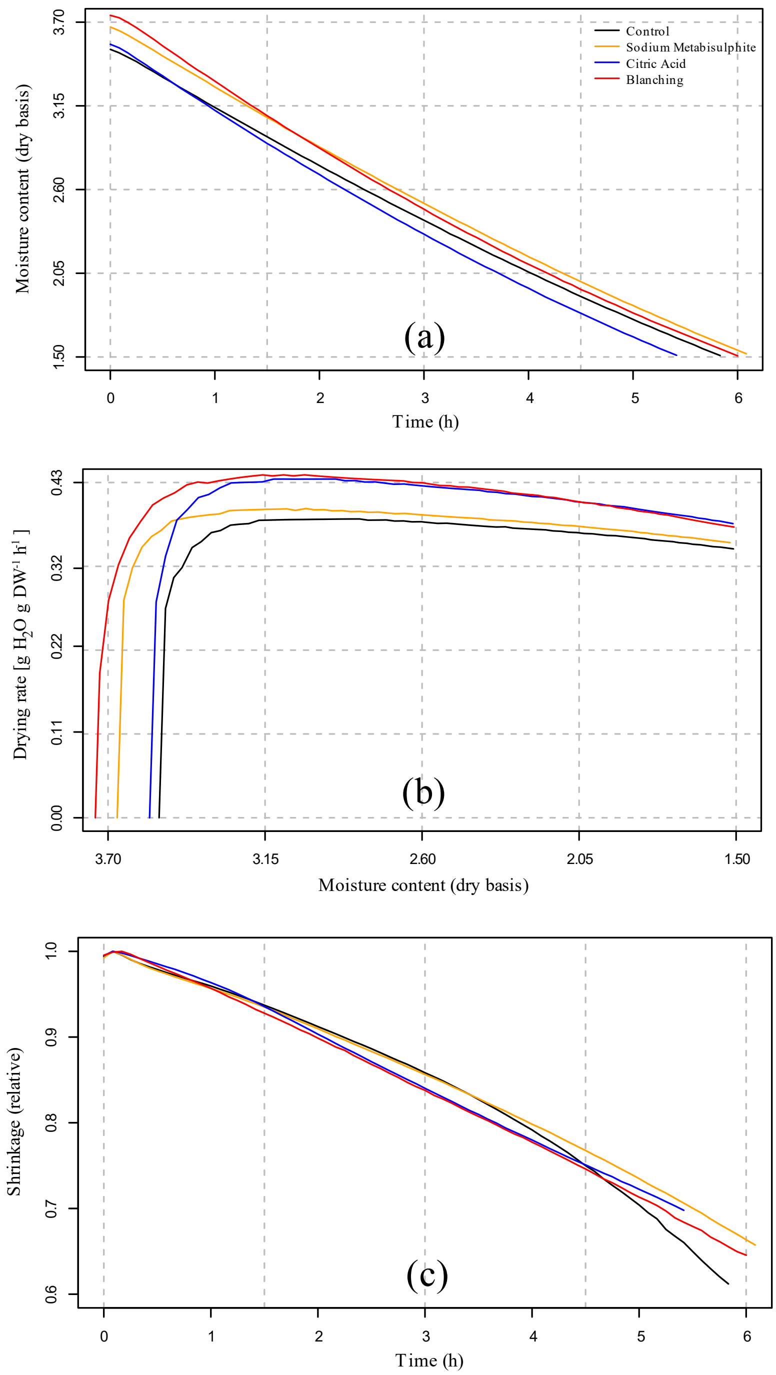

Figure 4.8

In-line monitoring of a) dry basis moisture content, MCdb; b) drying rate, DR; and c) relative area shrinkage, AS, along 6 h of semi-drying of pre-treated and control potato slices dried at 35 °C, 35 % R.H. and ~3 m s^{-1} air velocity up to 1.5 of dry basis moisture content. Results are reported as mean.

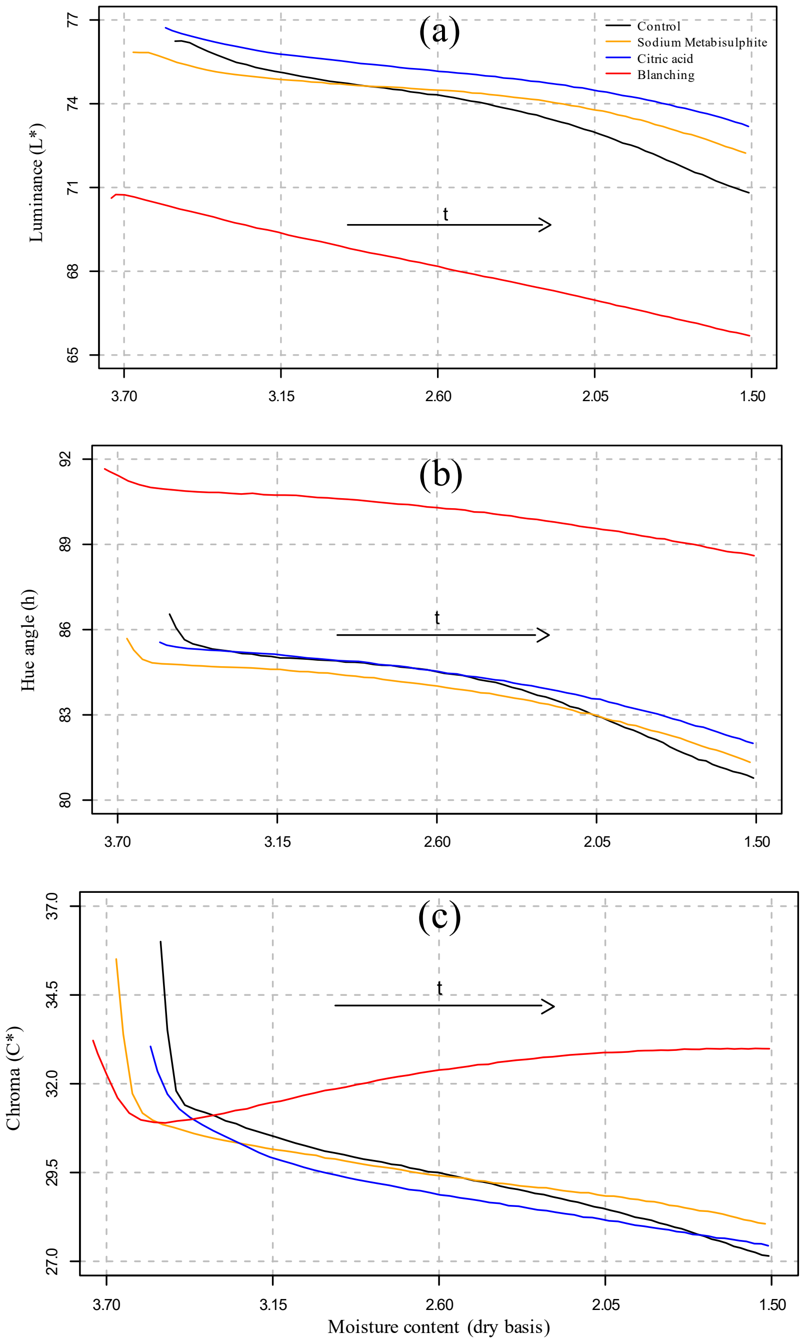

Figure 4.9

In-line monitoring of color changes a) luminance (L), b) hue angle (h) and c) Chroma (C*) with respect to dry basis moisture content (MCdb) along 6 h of semi-drying of pre-treated and control potato slices dried at 35 °C, 35 % R.H. and ~3 m s^{-1} air velocity up to 1.5 of dry basis moisture content. Results are reported as mean.*

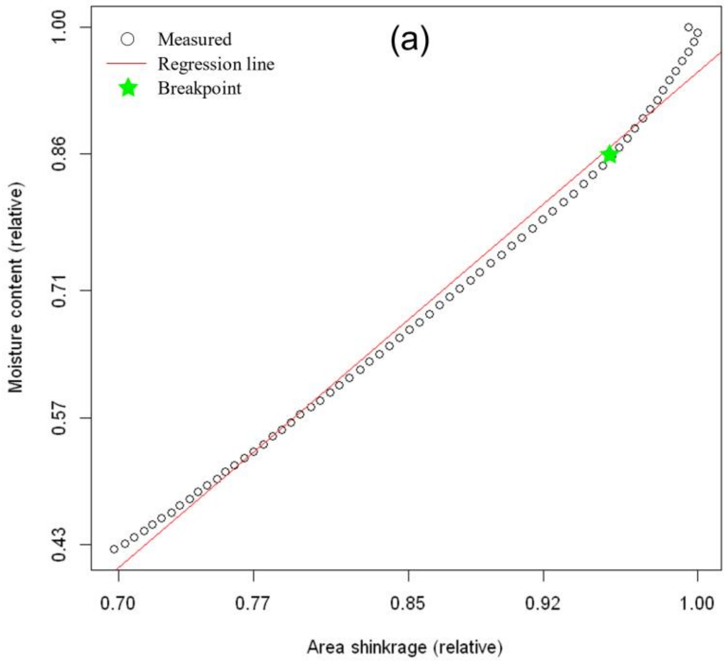

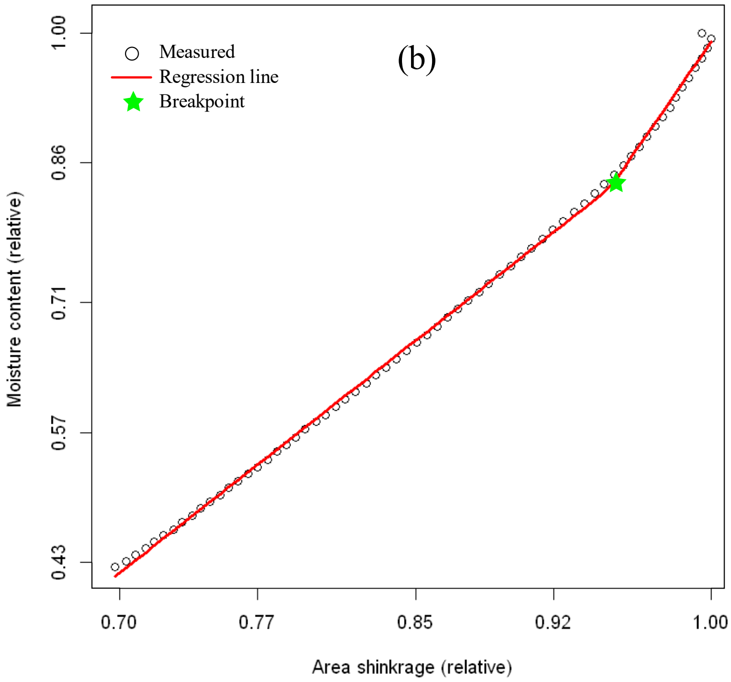

Figure 4.10

Example of model fit of the linear (a) and segmented-linear (b) model, MR vs AS, along 6 h of semi-drying of potato slices pre-treated by dipping in citric acid solution (3 % w/v) and dried at 35 °C, 35 % R.H. and ~3 m s-1 air velocity up to 1.5 of dry basis moisture content.

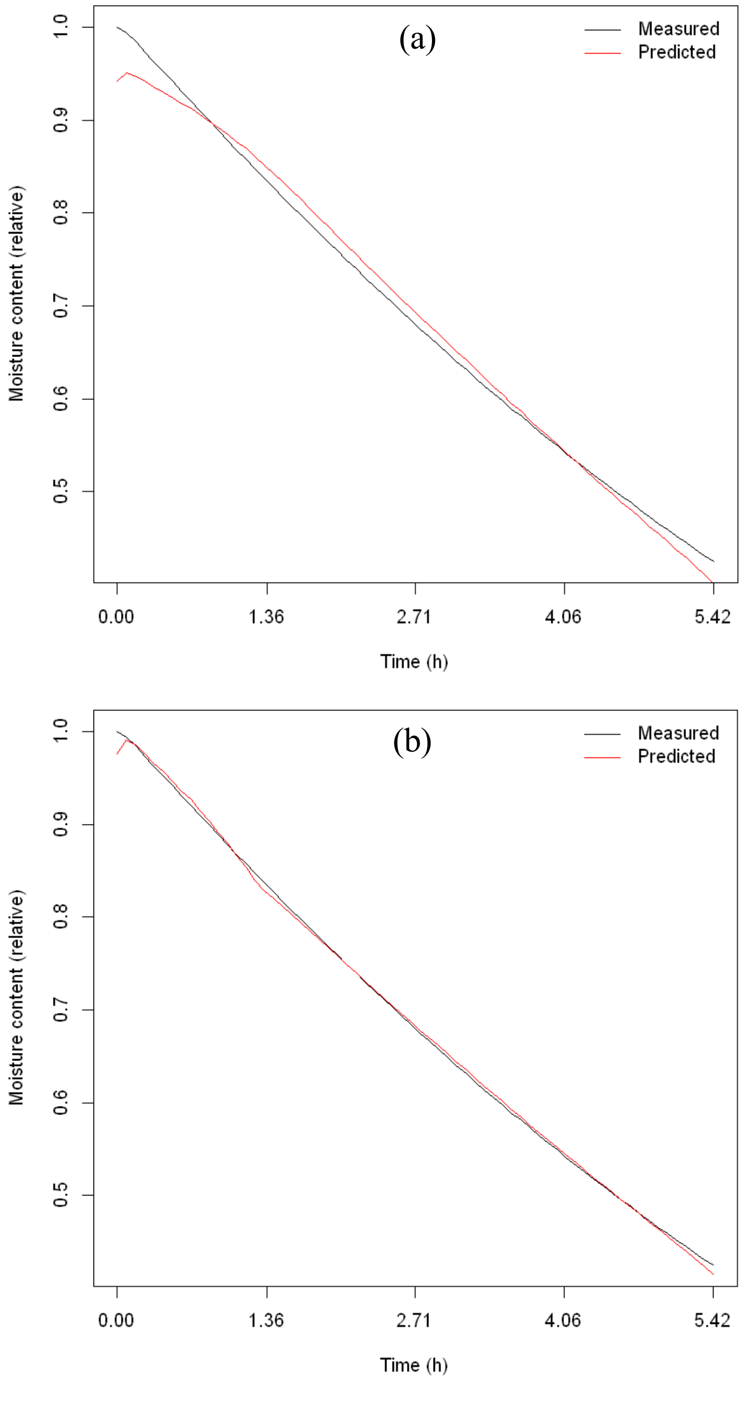

Figure 4.11

Example of MR prediction using the linear (a) and segmented-linear (b) model along 6 h of semi-drying of potato slices pre-treated by dipping in citric acid solution (3 % w/v) and dried at 35 °C, 35 % R.H. and ~3 m s-1 air velocity up to 1.5 of dry basis moisture content.

REFERENCES

Moscetti, R., Haff, R.P., Ferri, S., Raponi, F., Monarca, D., Liang, P., Massantini, R., 2017. Real-Time Monitoring of Organic Carrot (var. Romance) During Hot-Air Drying Using Near-Infrared Spectroscopy. Food Bioprocess Technol. 10, 2046–2059. https://doi.org/10.1007/s11947-017-1975-3

Moscetti, R., Raponi, F., Monarca, D., Bedini, G., Ferri, S., Massantini, R., 2019. Effects of hot-water and steam blanching of sliced potato on polyphenol oxidase activity. Int. J. Food Sci. Technol. 54, 403–411. https://doi.org/10.1111/ijfs.13951

Onwude, D.I., Hashim, N., Abdan, K., Janius, R., Chen, G., 2018. The potential of computer vision, optical backscattering parameters and artificial neural network modelling in monitoring the shrinkage of sweet potato (Ipomoea batatas L.) during drying. J. Sci. Food Agric. 98, 1310–1324. https://doi.org/10.1002/jsfa.8595

Raponi, F., Moscetti, R., Nallan Chakravartula, S.S., Fidaleo, M., Massantini, R., 2021. Monitoring the hot-air drying process of organically grown apples (cv. Gala) using computer vision. Biosyst. Eng. https://doi.org/10.1016/j.biosystemseng.2021.07.005

Sirisha, S., Chakravartula, N., Bandiera, A., Nardella, M., Bedini, G., Ibba, P., Massantini, R., Moscetti, R. (2023). Computer vision-based smart monitoring and control system for food drying: a study on carrot slices. https://ssrn.com/abstract=4234123

Wang-Pruski, G., Nowak, J., 2004. Potato after-cooking darkening. Am. J. Potato Res. 81, 7–16. https://doi.org/10.1007/BF02853831

CHAPTER 5

DEVELOPMENT OF NIR-BASED PREDICTIVE MODELS FOR DRY MATTER DETERMINATION

5.1 PREDICTION OF POTATO DRY MATTER CONTENT BY FT-NIR SPECTROSCOPY: IMPACT OF TUBER TISSUE ON MODEL PERFORMANCE

Giacomo Bedini, Swathi Sirisha Nallan Chakravartula, Marco Nardella,
Andrea Bandiera, Riccardo Massantini, Roberto Moscetti*
Department of Innovation in Biology, Agri-food and Forest systems,
University of Tuscia, Italy
** Corresponding author*

INDEX

KEYWORDS: *Solanum tuberosum L., post-harvest losses, near-infrared spectroscopy, chemometrics, PLS algorithm.*

ABSTRACT

Potato, an important cash crop, is critically affected by supply chain losses that require attention of both research and industry to ensure sustainable production (SDG 12.3). Within potato supply chain management, dry matter (DM) determination is a key factor affecting the harvest quality, storability, food losses, designated user and tuber prices. Even though rapid methods like near-infrared spectroscopy (NIR) enable operators to carry out fast, reliable in situ measurements, the prediction results are often unsatisfactory due to inherent variability of tuber's composition. Thus, this study aims to evaluate Fourier Transformed-NIR based DM prediction in different potato tissues: i) periderm, ii) cortex, iii) outer medulla and iv) inner medulla of 12 different cultivars. The DM prediction models developed using standard

chemometrics approaches (i.e., partial least squares, PLS; and interval-PLS, iPLS) showed that features selection by iPLS allowed for better performances. Among the evaluated tissues, the inner medulla had more precise and reliable measurements with RMSE and R^2 prediction values of 0.93 % and 0.90, respectively. This information can be used to develop more advanced systems inclusive of portable tools and advanced technologies for in situ evaluation to support operators and ensure better pre- and post-harvest management of potatoes.

INTRODUCTION

Potato (*Solanum tuberosum* L.), one of the most widely grown crops in the world, is a staple food in many developed and developing countries with a total production of 359 million tonnes in 2020 (FAOSTAT, 2022). Being a cash crop, the harvest maturity and the post-harvest storage are the most critical factors that determine the quality and shelf life of potato tubers. In fact, measuring maturity of potato tuber, at or shortly before harvest, is considered useful for the purpose of selecting potato lots for long-term storage. This is due to the complexity of potato tuber maturation as described by Heltoft et al. (2017), involving a variety of processes that include skin set (physical maturation), accumulation of dry matter (physiological maturation) and lowering of sucrose content (chemical maturation).

Commercially, potatoes are harvested after reaching their physiological maturity to preserve the quality, maximize the storability as well as to reduce risks of mechanical damage during harvesting and handling procedures. For mid and late-season potato varieties, the physiological maturity sets in when the peak of dry matter (DM) is attained which usually coincides with the minimum sucrose content (chemical maturation) and maximum starch content (Iritani, 1981). The maturity of potato has also been reported to be related to the respiration rate, water loss, pests and diseases development, dormancy and Low-Temperature Sweetening (LTS). Specifically, water loss is of focal interest as it compromises the marketability of the tubers when it is higher than 10 % of initial weight. Also, the tubers with high water losses succumb to bruising and blue or black discoloration, as well as greater peeling losses and reduction in culinary quality (Pinhero and Yada, 2016). Thus, monitoring the DM content during potato storage could provide information about the water loss and physiological status of tubers, allowing post-harvest losses to be reduced through a proper storage control. Moreover, DM measurements can also allow operators to make guided decisions on the length of storage and the order of crop processing (Heltoft et al., 2017). This can avoid food losses within the potato production and supply chain thereby pursuing the target 12.03 of the Sustainable Development Goals of the United Nations (United Nations, 2022).

DM content also is a fundamental quality parameter for the potato processing industry, wherein the varieties used for processing must have a DM content greater than 20 %, which allows for improved textural quality of crisps and fries as well as increased yields of processing (Scanlon et al., 1999). DM content in potatoes at-harvest and/or at-delivery is commonly measured by oven or gravimetric methods. The gravimetric method is industrially accepted for the measurement of DM, owing to the lesser time requirement compared to oven methods. Both oven and gravimetric methods are accurate, repeatable, and simple, but are frequently criticized for disadvantages like: i) time intensiveness, ii) invasive nature and, most importantly, iii) requirement of a laboratory. Thus, developing novel and handy methods to enable operators to carry out fast and reliable in situ measurements is important for choosing the optimal harvesting time for potatoes as well as for continuously monitoring and predicting the DM content during storage, thereby circumventing food losses by timely facing possible storability issues.

In this regard, López et al. (2013) described several applications of Near-Infrared (NIR) spectroscopy for major and minor components determination in potatoes. Specifically, many authors focused on the DM content measurements on different states of potato like whole (Helgerud et al., 2015), mashed (Haase, 2003) and fried (Shiroma and Rodriguez-Saona, 2009) samples. However, these results are not immediately comparable owing to the different NIR acquisition approaches and sample preparations. As for the resultant predictive models reported in literature, the performance metrics are often acceptable but not satisfactory, especially when developed on whole potato tubers, with a determination coefficient (R^2) lower than 0.90 (López et al. 2013). In fact, some authors reported that the best results were observed when the sample was mashed and homogenized (Brunt and Drost, 2010; Haase, 2011), owing to the heterogeneous distribution of moisture among periderm, cortex and medulla tissues as evidenced by Pritchard and Scanlon (1997) and Peiris et al. (1999). Consequently, mashing and homogenizing potato samples can boost the prediction accuracy of DM, however sacrificing two of the strengths of NIR spectroscopy: minimum sample preparation and the possibility of in situ measurement (or portability of measure).

Although many authors have tested the suitability of NIR spectroscopy for the determination of DM content in potatoes, to the best of our knowledge, there are no studies that tried to boost the prediction performance of models considering the impact of the scanned area, i.e. the tissue type of potato on the signal quality. The present study proposes a novel approach for the prediction of potato DM content through the development and validation of NIR-based models specific for tuber periderm, cortex and medulla tissues. The study will form the basis for the design of a portable NIR solution, and an end-user-friendly protocol for in situ analysis of potatoes.

MATERIAL AND METHODS

Sample preparation

Potato (*Solanum tuberosum* L.) tubers were provided by the "Patata dell'Alto Viterbese" PGI consortia (C.C.OR.A.V. and Coop. Centro Agricolo Alto Viterbese, Viterbo, Italy). Of the available cultivars, twelve cultivars were selected on the basis of a preliminary study focused on ensuring the widest DM data range (approx. 8-22 %) for regression model development: Actrice, Ambra, Avanti, Constance, El Mundo, Finka, Fontane, Gaudi, Jelly, Monalisa, Universa and Vitalia (Fig. 5.1a). The potatoes were collected immediately after harvesting and stored at 4 ± 1 °C until analysis. Tubers were analyzed by randomly sampling 5 tubers per cultivar from 5 kg bags (each bag contained 25-30 potato tubers). The potato tubers were selected to be of uniform size, without damage, defects or blemishes. Samples were tempered to room temperature for 16 h prior to spectral acquisition.

NIR spectral acquisition

The spectra of the potato tubers were acquired using the Antaris II Fourier-transform NIR (FT-NIR) spectrophotometer (Thermo Fisher Scientific, Madison, WI, USA) equipped with a fiber-optic probe and was warmed-up for at least 1 h prior to spectral acquisition. The Fourier's transformed spectra were acquired at room temperature (20 ± 1 °C) in the spectral range of 10000-4000 cm^{-1} (1000-2500 nm) with a 4 cm^{-1} scan resolution. The spectra were acquired in diffuse reflectance mode and directly converted to absorbance (abs) by means of the RESULT 3 software (Thermo Scientific, Madison, WI, USA). A total of 984 spectra were acquired performing the scans on four different types of tissues as classified by Faridnia et al. (2015) obtained by cutting the tuber transversally in sub-samples (Fig. 5.1b): (i) periderm (whole and unpeeled tuber); (ii) cortex (peeled tuber); (iii) outer medulla and (iv) inner medulla. In detail, 246 spectra per tissue were scanned. The spectrum of each sub-sample had an average of 32 scans (technical replications), with the internal instrument standard as reference. Immediately after the spectral acquisition, the potato samples were subjected to the conventional DM determination as described in the next section.

Dry matter determination

Each scanned area from the previous step was cored (8-mm diameter, 5-mm depth) and dried in an electric oven at 105 °C for 72 h. Dry matter (DM) was expressed as percentage by mass (grams per 100 grams) (Fig. 5.1c). The data obtained was tested for normality and homoscedasticity for each cultivar using the Shapiro-Wilk and the Levene tests, respectively. Results indicated that no premises of normality and homoscedasticity were violated. Consequently, the descriptive statistics for DM content distribution and statistical differences among DM content of potato tissues by one-way analysis of variance (ANOVA) were evaluated for each potato cultivar. Tukey's pairwise comparison method was performed, and the Honestly Significant Difference (HSD) was calculated for an appropriate level of interaction ($P \leq 0.05$). Finally, Pearson's linear correlation test was computed to detect significant bivariate correlations among potato tissues in terms of DM content (Fig. 5.1d). Data handling, descriptive statistics, ANOVA and the Pearson's linear correlation test were performed using R software 4.0.3 coupled with 'Agricolae' package v1.3-3.

Further, to better understand the heterogeneous distribution of the DM content in the potato tissue, an example graphical representation was used. For the intended purpose, a potato tuber from randomly selected cultivar (Fontane) was sampled into a 1-mm thick slice, cut transversely at the midpoint. The slice was further cut into 20 cubes of approximately equal size. Each cube was labeled for its position in the slice (x,y) and analyzed to determine its DM content. The graphical representation was computed by defining a surface by the z-coordinates of points (the DM content) above an ideal circular grid in the x-y plane (the position of each sample cube in the potato slice). The surface plot was generated using the 'geom_contour_filled()' function as part of the 'ggplot2' R-package (Wickham, 2016).

Chemometrics

FT-NIR-based models were individually developed for each tissue and compared for their performance in predicting the DM content in potato tuber (Fig. 5.1d), with the final objective of identifying the most reliable method of spectral acquisition regardless of potato cultivar. Chemometrics was performed using Matlab environment R2017b (Mathworks Inc., USA) coupled with PLS Toolbox software v8.6.2 (Eigenvector research Inc., USA).

Spectral pre-treatments

As the first step, the spectra were subjected to spectral preprocessing to reduce non-linearities, scattering effects and noise. For the intended purpose, the following preprocessing treatments were applied and tested for their effectiveness: (i) Standard Normal Variate (SNV), (ii) Multiplicative Scatter Correction (MSC), and (iii) Savitzky-Golay algorithm as smoothing and/or differentiation filter. Each smoothing/derivative pre-treatment was applied with a second or third order polynomial fitted over a window of 11, 13 or 15 features. Finally, data normalization through mean centering (MC) or autoscaling (AS) was performed. Every possible combination of spectral pre-treatments was tested and only those that improved the performance of the model were retained.

Model development

For the model development within this study two extensively used algorithms namely, Partial Least Squares (PLS) and Interval-PLS (iPLS) were applied. Prediction models were individually developed based on the linear combinations of independent variables for each potato tissue from all cultivars, using pre-processed spectra as X-matrix and dry matter content as Y-vector. The spectral dataset of each tissue was split into calibration and prediction sets: i.e., ~70 % (172) and ~30 % (74) of spectra, respectively. Equal representativeness of each cultivar and tissue in both calibration and prediction sets was ensured to guarantee a comparable DM range between the two. For PLS models the whole spectral range was utilized whereas the iPLS models were built on the spectral range with feature subsets selection to potentially improve the prediction results. The iPLS algorithm for the feature selection was set to stepwise forward mode with a maximum of 10 waveband intervals of 10 features (wavelengths) each. Models were developed using a Venetian blinds cross-validation with 10 data splits to find the correct number of latent variables (LVs) with an optimal trade-off between underfitting and overfitting. The optimal number of LVs was also chosen by estimating the signal-to-noise ratio for each LV and only those with a ratio greater than 2 were selected as described by Henry et al. (1999).

Model performances were evaluated in terms of Root Mean Square Error, BIAS and coefficient of determination for calibration (RMSEC, BIASC and R^2C, respectively), cross-validation (RMSECV, BIASCV and R^2CV, respectively), and prediction (RMSEP, BIASP and R^2P, respectively) (Moscetti et al., 2019). The Hotelling's t-squared and Q-residuals tests were used in combination to identify potential outliers of each given model.

RESULTS AND DISCUSSION

Dry matter content: trends in potato tissue

The DM content within a tuber was observed to be heterogeneously distributed with clear demarcation among tissues (Fig. 5.2). In general, the DM content decreased from the periphery towards the center of the tuber: i.e., the outer periderm to inner medulla as also observed by Pritchard and Scanlon (1997).

This pattern of inter-tissue variability for DM content was observed for all the evaluated cultivars as presented in Figure 5.3. In general, the DM content distribution among tissues was approximately similar among cultivars with external tissues registering higher DM contents than the internal tissues. Specifically, the inner medulla always had the lowest DM content followed by the outer medulla, periderm and cortex. These differences for each cultivar were significant, except for Universa which however showed a similar trend. Among the tissues, the DM contents of periderm and cortex had no significant differences for cultivars Actrice, Ambra, Constance, Finka, Fontane, Gaudi, Jelly, Monalisa and Vitalia. As for the outer and inner medulla, no significant differences were observed for cultivars Actrice, Constance, Monalisa and Vitalia. Interestingly, in the case of Avanti, Fontane, Gaudi and Monalisa cultivars, outer medulla reported DM contents as high as their periderm and cortex. These observed variations among cultivars are in agreement with those of Thybo et al. (2003) on tuber slices from four different potato cultivars.

Considering the similarities in trends of DM distribution, the DM values of all cultivars were averaged for each tissue investigated and the relevant statistical parameters are presented in Table 5.1. Further, the use of 12 varieties with high, medium, and low DM content provided for a wider value range which can allow for building more representative prediction models. As observed for each individual cultivar, also in this case the externally placed potato tissues registered higher mean DM content than the internally placed tissues in the order of cortex (20.41 %), periderm (19.45 %), outer medulla (18.64 %) and inner medulla (14.32 %). Also, the min and max values were higher for external tissues than internal tissues; however, the standard deviation among tissues was similar. The observed results were in agreement with Pritchard and Scanlon (1997) and Riza et al. (2017), with the inner tissues (outer and inner medulla) having a lower DM content as a consequence of their vascular structure retaining higher moisture.

Further, the existence of linear relationships between DM content of different potato tissues were evaluated. The results showed positive relationships between tissues ($P < 0.05$) (Tab. 5.2). The highest correlation coefficient values were reported between periderm and cortex, and between cortex and outer medulla ($r = 0.96$ and 0.91, respectively). The weakest relationships were observed between periderm and inner medulla and between cortex and inner medulla ($r = 0.76$ and 0.68, respectively). These results might be of potential interest for the indirect determination of DM of one tissue based on the DM content of another tissue and thus, in other words, to get an approximation of the overall DM content of the tuber from the compositional analysis of one tissue. However, it is important to consider that the variation in tuber size may alter i) the perceptual distribution of the various tissues in the tuber (larger tubers have more medulla tissue and, thus, a lower DM content); and ii) the cell size of tuber (a smaller cell has more cell wall and therefore a higher DM content) (Gancarz, 2016).

Spectral features

Figure 5.4 shows the representative absorbance spectra for each type of potato tissue (periderm, cortex, outer medulla, and inner medulla) averaged from the spectral data of the twelve selected cultivars. As can be observed, the spectra exhibited visually appreciable differences in the absorbance values but had similar spectral profiles for all tissues, except for the periderm. These spectral variations, as in the case in other fruits and vegetables, can be attributed to their variable DM content as previously observed and the scattering effect related to the microstructure of the tissue (Nicolaï et al., 2007).

In terms of spectral intensity (abs), periderm registered the lowest range (~0.50-0.85), whereas inner medulla had the highest values ranging between ~0.85 and 2.95. The cortex and outer medulla exhibited similar spectral profiles (~0.60-2.50 intensity range) except for slight shifts in two specific spectral bands of 10000-7500 cm^{-1} and 6250-5500 cm^{-1}. These observed differences are mainly due to the differences in chemical composition among tissues; it is particularly evident for the periderm (potato skin) with its lower moisture and starch content compared to the tissues forming the potato flesh (cortex, inner and outer medulla). The lower absorbance in periderm can also be attributed to the barrier function of the skin causing higher reflectance in the NIR region as observed by Riza et al. (2017). The authors noted that the presence of surface impurities (such as soil or dirt) and irregularities may be responsible for multiplicative scattering patterns and longer scattering paths thus resulting in spectra with a lower signal-to-noise ratio (Riza et al., 2017). On the other hand, the inner medulla is the most vascularized tissue of the tuber, therefore rich in moisture and with higher spectral intensity values.

Considering the absorption bands, irrespective of the type of tissue evaluated, peaks that can be associated with water were observed at 5160-5220, 6880-7020 and 10210-10340 cm^{-1} in agreement with the observations of Riza et al. (2017). Further, the small peaks around 5665-5555 cm^{-1} and 8500-8300 cm^{-1} can be related to the first and second overtone of C–H stretching of starch, respectively, whereas the band close to 4000 cm^{-1}, characterized by a low signal-to-noise ratio during all measurements, may be attributed to the combinations of C–H and C–C stretching of starch (Workman and Weyer, 2012). Based on the chemical composition of raw potatoes, it was not surprising that the absorption bands of water and starch were dominant ones in the acquired spectra.

To summarize, the average spectral profiles highlight the differences in the microstructure and chemical composition (i.e., the heterogeneous distribution of moisture and starch) within each tissue of the tuber. This is in good compliance with the findings of Helgerud et al. (2015) and Peiris et al. (1999). Consequently, each of these tissues may have considerable effect on the performance and robustness of DM prediction models based on FT-NIR spectroscopy.

Dry matter prediction model

DM prediction (PLS and iPLS) models were subsequently built based on the obtained DM content values and the spectra for different tissues. The results of predictive models showed that the full spectrum PLS models exhibited poor performances irrespective of the tissue, with RMSE > 2 % and $R^2 < 0.60$ regardless of the pre-processing method used (Table 5.3). Whereas the iPLS algorithm produced accurate and reliable models with better metrics for DM prediction (Table 5.3) by simply removing unnecessary spectral regions. As for the spectral pre-treatments among all the tested combinations only Savitzky-Golay smoothing filter over a window of 15 features combined with mean centering (MC) was retained for further evaluation and discussion as it was observed to effectively remove the noise and, thus, improve the signal-to-noise ratio.

Considering the PLS models, all the evaluated tissues had poor performances and overfit the DM content despite the optimally low number of LVs (3-6). This can be also evidenced from the BIAS values and the observed discrepancy between the R^2 values for calibration and prediction (< 0.60). Whereas for the iPLS models, the inner tissues (outer and inner medulla) in general exhibited better performance metrics than external tissues, with the best results being shown by inner medulla among all the evaluated tissues (Table 5.3). Among the evaluated external tissues, models developed using spectra from periderm resulted in very poor performance metrics as shown in Table 5.3. This was consistent with the results reported by Han et al. (2021) for soluble solid content prediction in potatoes. These authors observed that the presence of surface impurities, spectral drift and light scattering can lead to an excessive presence of irrelevant and redundant information in the spectra which negatively affects the prediction performances. Similarly, the cortex-based models also reported poor performances with a RMSE and R^2 values of 1.66 % and 0.60 for prediction, respectively. This may be attributed to the lowest moisture content and, thus, the highest density of the cortex tissue (Pritchard and Scanlon, 1997), which may have negatively affected the depth of light penetration during the NIR measurement. However, further investigation is required for a better understanding of this phenomenon.

As for the internal tissues, both outer and inner medulla iPLS models exhibited good performance metrics for prediction with RMSE and R^2 values of 1.12 % and 0.86, and 0.93 % and 0.90, respectively, better to that of PLS models (RMSE = 1.78 % and 2.30 %; R^2 = 0.56 and 0.45). Specifically, the iPLS model of inner medulla was observed to be the best model considering not only the lowest RMSE but also the better BIAS values that tended towards zero. The iPLS models reported in Figure 5.5 for the inner (Fig. 5.5a) and outer medulla (Fig. 5.5b) further enable the visual understanding of the ideal regression from the largely overlapping regression lines confirming a low effect of the systematic error on measurements, and thereby a better ability of the model to accurately estimate the dry matter values.

In comparison, the performances of the inner medulla-based prediction models were found to be better than the results reported by Camps and Camps (2019) on entire and peeled potatoes (RMSEP = 1.2 % and R^2 = 0.84), whereas similar to the results achieved by Helgerud et al. (2015) for on-line measurements on whole potatoes (RMSECV = 1.06 % and R^2 = 0.92). Further, the number of latent variables utilized for the models was similar to both Helgerud et al. (2015) (6 latent variables) and Camps and Camps (2019) (5 latent variables). However, the results were found to be slightly worse than those reported by Subedi and Walsh (2009) on sliced tubers by using short-wavelength NIR spectroscopy (RMSEP = 0.5 % and R^2P = 0.95), which can be attributed to the differential sampling techniques used. Overall, the generally superior performances of the models for the inner medulla compared to the other tissues can be speculated as a direct consequence of higher moisture content as observed previously from the DM content distribution, spectral absorbances and positioning of peaks (Fig. 5.1).

To verify the contribution of moisture content, the spectral bands selected by the iPLS algorithm were also evaluated. As highlighted in Figure 5.6, two spectral bands each were selected and used by the iPLS models namely, Band #1 (10000-9425 cm^{-1}) for inner medulla, Band #3 (6144-5377 cm^{-1}) for outer medulla and commonly Band #2 (8458-7690 cm^{-1}) for both the internal tissues. The band #1 region (10000-9425 cm^{-1}) corresponds to the 2nd overtone of O-H and N-H groups and of the 3rd overtone of C-H group. Approximately, Subedi and Walsh (2009) identified the same NIR region, highlighting the importance of absorbance at about 10900 cm^{-1} to predict the DM content in potatoes. The band #2 (8458-7690 cm^{-1}) was selected both for inner and outer medulla models. It was associated with the 2nd overtone of C-H and N-H groups. Finally, the band #3 (6144-5377 cm^{-1}) selected for the outer medulla model was related to the 1st overtone of C-H as previously stated in spectral features (section 3.1). Similarly, Camps and Camps (2019) identified band #2 and band #3 to develop a good model acquiring the spectra on peeled potatoes. Moreover, the three selected wavelength regions by iPLS algorithm in this study were related to starch and moisture content which are the major components of potatoes (Workman and Weyer, 2012) and have subsequently contributed to superior model performances.

CONCLUSIONS

Potato being a cash crop requires rapid and reliable measures for determination of dry matter content both during harvest and post-harvest for better management of potato storage, processing and distribution. The determination of DM content in potato using NIR spectroscopy in destructive and/or non-destructive manner has been extensively studied in the literature. However, although the performance of models appears to be strongly affected by the sampling methodology used, to the best of our knowledge there are no studies investigating this aspect. Consequently, the present study contributes to the body of knowledge by providing novel insight into the impact of potato tissue on the performance of NIR-based models.

The results showed that iPLS algorithms with selected features performed better than the full spectrum PLS models. Further, the importance of the scanning area on the quality of performance metrics was evident in the iPLS models developed. In fact, the prediction models for the DM of the internal tissues (i.e., outer and inner medulla) exhibited better performance metrics than the external tissue (i.e., periderm and cortex). In particular, the best prediction performances were obtained for the inner medulla with BIAS tending towards zero, and RMSEP and R^2P equal to 0.93 % and 0.90, respectively. The iPLS prediction models for internal tissues were built based on the wavebands of 10000-9425, 8458-7690 and 6144-5377 cm^{-1}, related to the moisture and starch content. The identification of specific bands enable the transferability of the models to portable handheld instruments that could be very useful to i) define the optimal potato harvesting time; ii) monitor quality parameters during storage; iii) ensuring optimal quality of potatoes for each processing segment, thereby reducing food losses and allowing for better potato supply chain management. However, further studies should be carried out to i) make the model usable with additional cultivars and verify the effects of agricultural conditions on its robustness; ii) make the model usable for in situ measurements by robustness to product temperature variations through the exploitation of correcting strategies, e.g. external parameters orthogonalisation; iii) minimize, or possible remove, error propagation in the model due to moisture loss during the sampling procedure; iv) test the use of linear/non-linear algorithms alternative to PLS and deep chemometrics solutions like convolutional neural networks for improving model accuracy; v) test the development of data-fusion-based models by combining NIR spectroscopy with other portable-ready technologies with a history of success in predicting fruit and vegetables dry matter (e.g. bioimpedance); vi) develop an end-user-friendly analysis protocol for in situ applications; vii) render the models efficient to allow the continuous instrumental and computational developments and thereby support the work of even the non-expert user community (Industry 5.0).

Table 5.1

Descriptive statistics of the DM content (%) for each potato tissue.

Potato tissue	**Min.[a]**	**1st Qu.[b]**	**Mean[c]**	**SD[d]**	**3rd Qu.[e]**	**Max[f]**
Periderm	11.73	17.26	19.45	3.13	21.77	29.23
Cortex	9.36	18.18	20.41	3.19	22.68	28.47
Outer medulla	9.87	15.81	18.64	3.46	21.48	25.43
Inner medulla	8.82	11.73	14.32	3.29	16.54	21.84

[a] minimum value; [b] first quartile (Q1); [c] mean value; [d] standard deviation; [e] third quartile (Q3); [f] maximum value.

Table 5.2

Pearson's product-moment correlation coefficients (r) between DM contents of potato tissues.

	Periderm	**Cortex**	**Outer medulla**	**Inner medulla**
Periderm	-	-	-	-
Cortex	0.960***	-	-	-
Outer medulla	0.895***	0.913***	-	-
Inner medulla	0.757**	0.675*	0.807**	-

****, **, * significant correlations at $P \leq 0.001$, $P \leq 0.01$ and $P \leq 0.05$, respectively (two–tailed)*

Table 5.3

Summary of the performance metrics for iPLS models that performed best in predicting dry matter content in potato tissues.

Potato tissue	LVs[a]	RMSE[b] (%)		BIAS (%)		R^{2c}	
		Cal[d]	*Pred[e]*	*Cal*	*Pred*	*Cal*	*Pred*
Cortex	5	1.36	1.66	$-2.78\ 10^{-16}$	$2.69\ 10^{-3}$	0.75	0.60
Outer medulla	5	1.08	1.12	$1.11\ 10^{-16}$	$-2.60\ 10^{-3}$	0.87	0.86
Inner medulla	6	0.79	0.93	$7.77\ 10^{-16}$	$-3.03\ 10^{-4}$	0.93	0.90

[a]LVs, latent variables; [b]RMSE, Root Mean Square Error; [c]R^2, coefficient of determination; Cal, calibration; Pred, prediction.

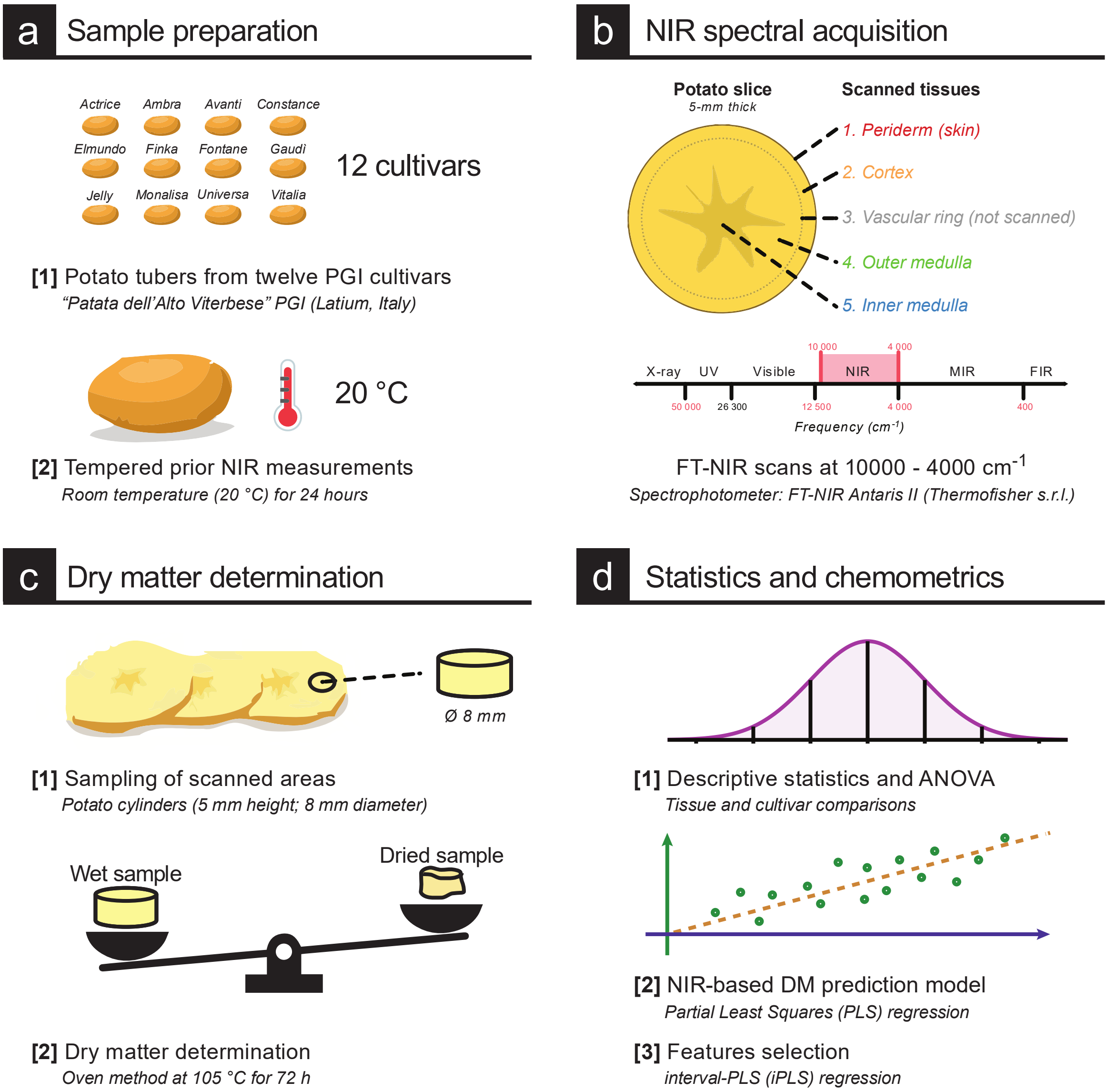

Figure 5.1

Simplified step-by-step representation of the experimental procedure.

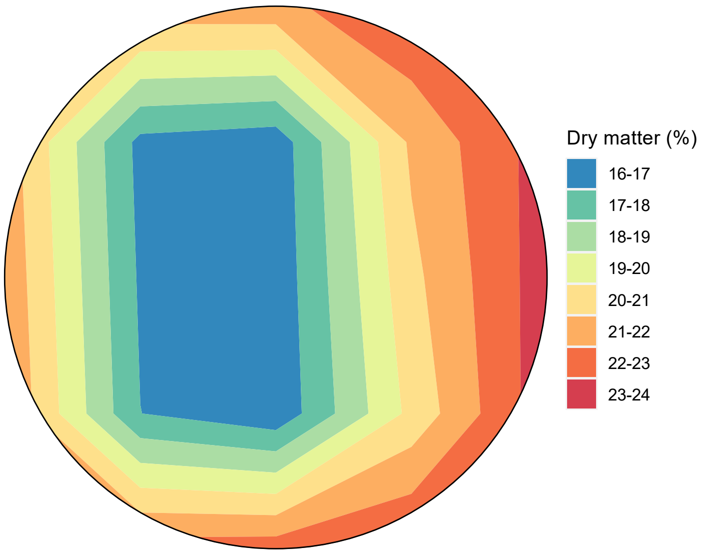

Figure 5.2

Example of dry matter distribution in the cross-section of a tuber (cv. Fontane).

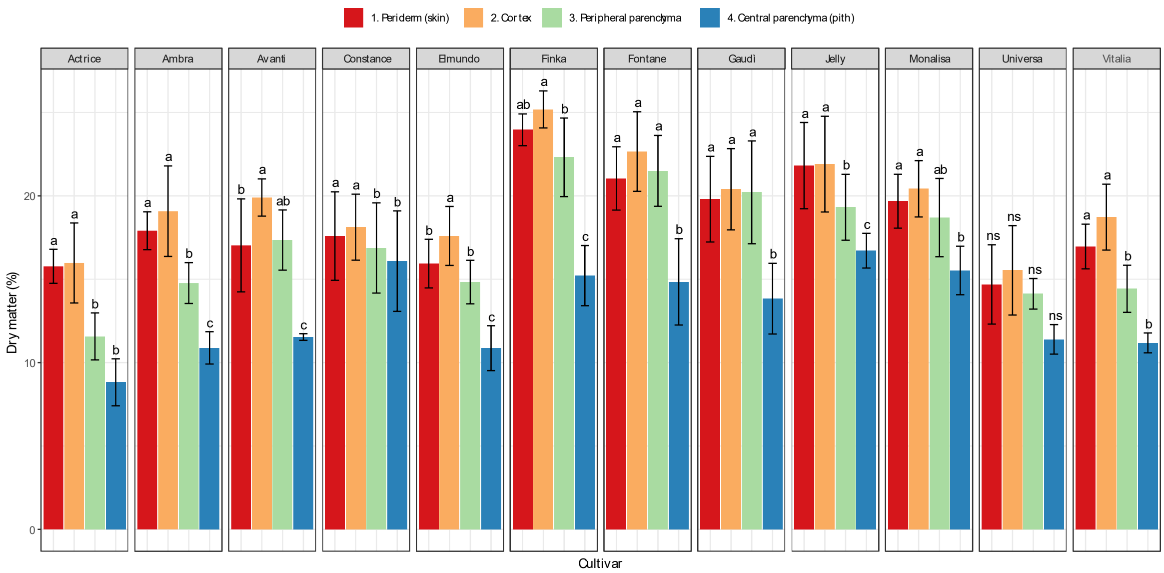

Figure 5.3

Bar plot showing the main effect of potato tissues on the dry matter content in each of the 12 cultivars used in the experimentation. Mean values with no common letters are statistically different according to HSD ($P \leq 0.05$). ns, no significant differences.

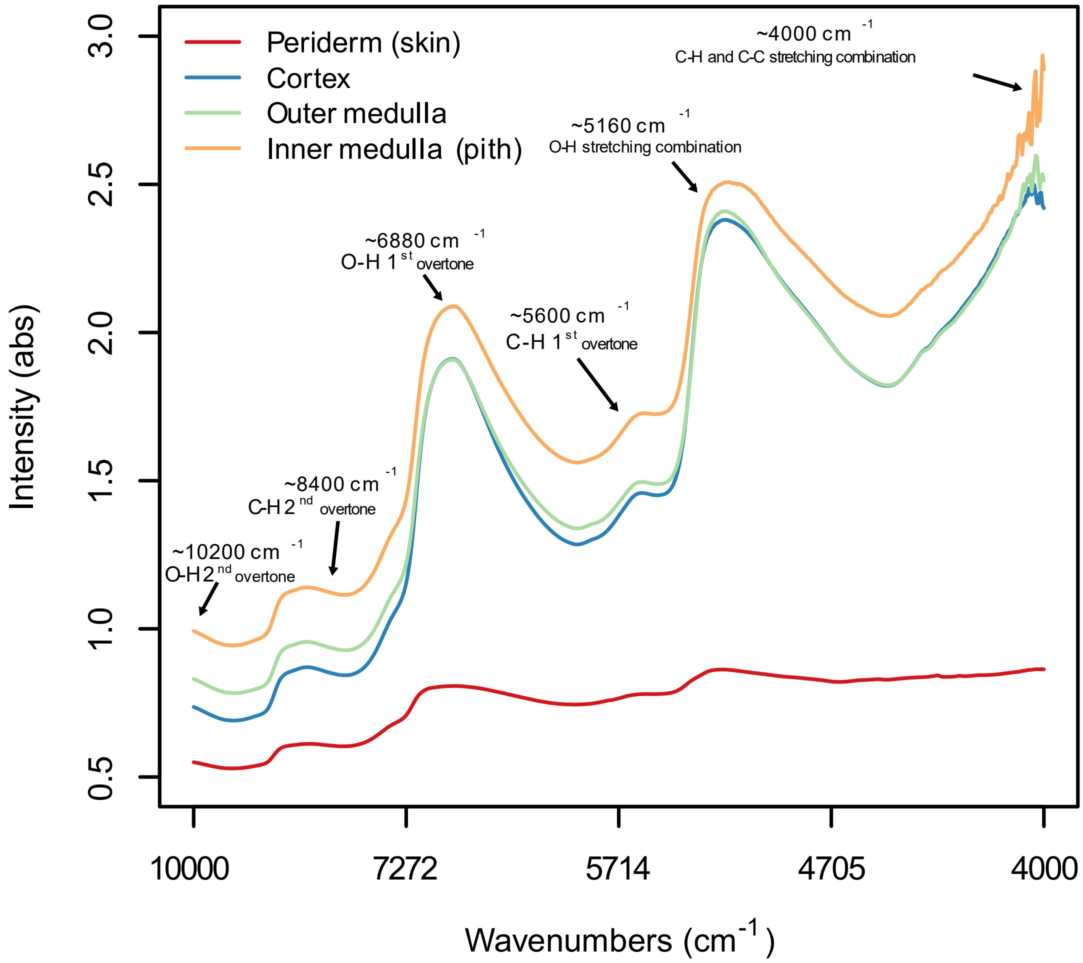

Figure 5.4

Mean absorbance spectra acquired on the four potato tissues (i.e., periderm, cortex, outer medulla and inner medulla).

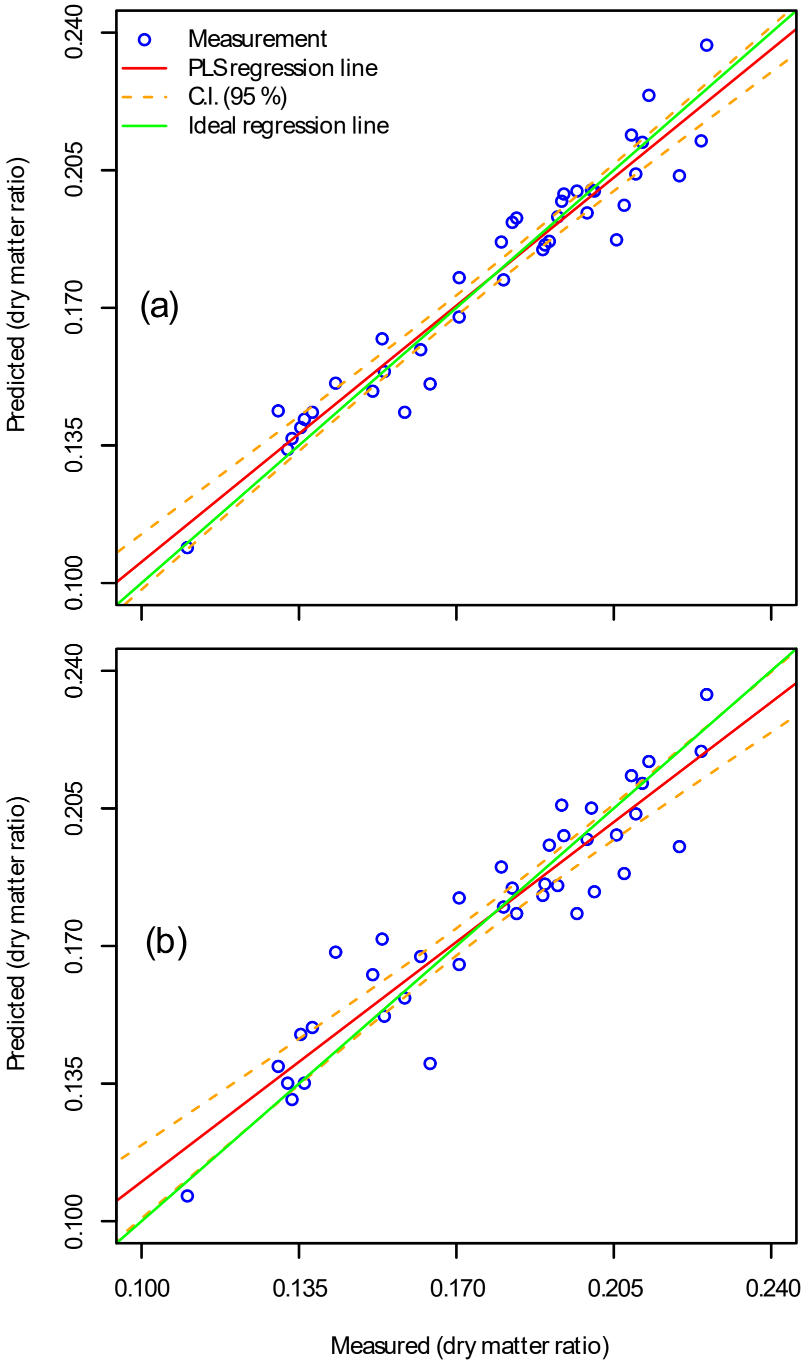

Figure 5.5

iPLS regression plots for measured (reference) and predicted (NIR) values for dry matter in (a) inner medulla and (b) outer medulla tissues.

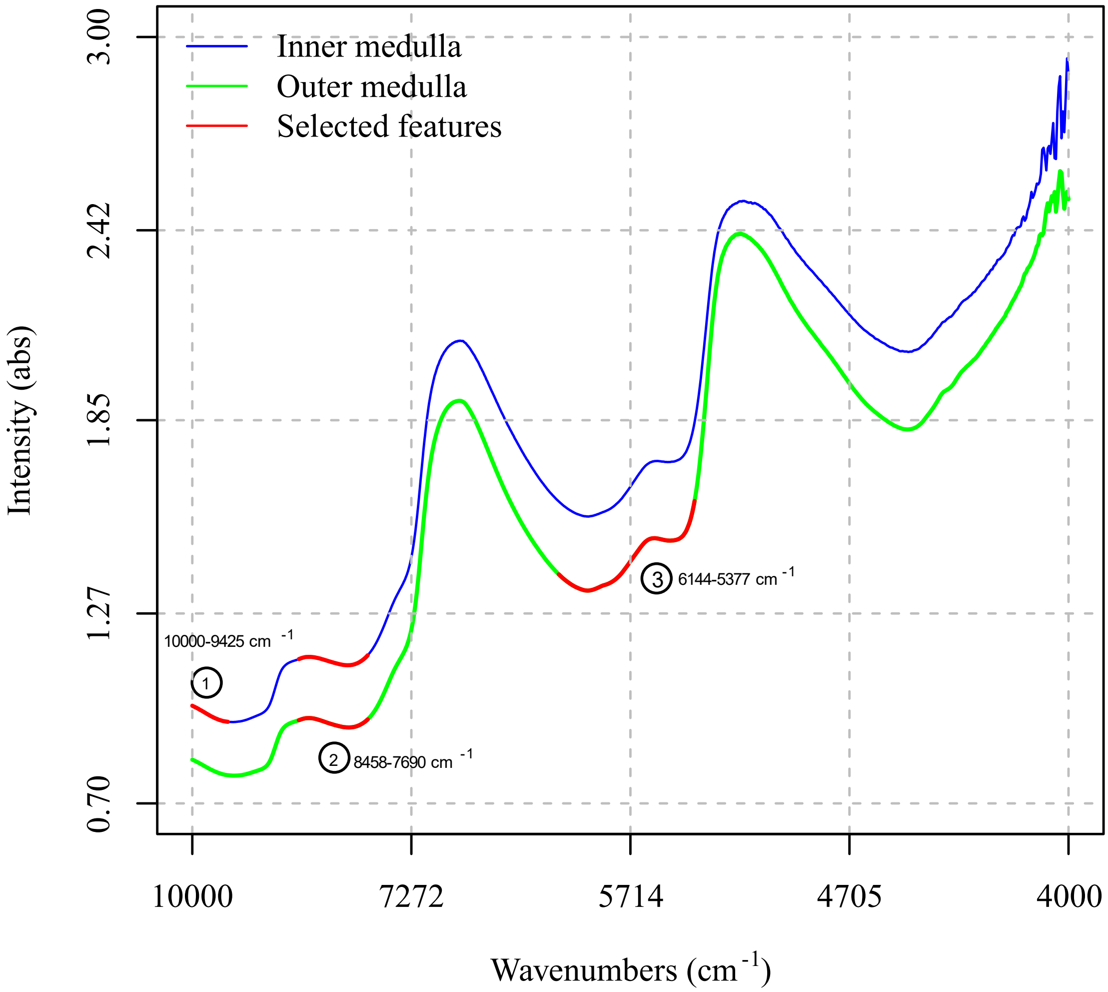

Figure 5.6

NIR features (cyan bands) selected using the iPLS algorithm for the dry matter prediction in inner and outer medulla tissues.

REFERENCES

Brunt K, Drost WC (2010) Design, construction, and testing of an automated NIR in-line analysis system for potatoes. Part I: Off-line NIR feasibility study for the characterization of potato composition. Potato Res 53:25–39. doi: 10.1007/s11540-010-9149-y

Camps C, Camps ZN (2019) Optimized prediction of reducing sugars and dry matter of potato frying by FT-NIR spectroscopy on peeled tubers. Molecules 24:. doi: 10.3390/molecules24050967

FAOSTAT (2022) Food and Agriculture Organization of the United Nations. https://www.fao.org/faostat/en/#data/QCL/visualize. Accessed 14 Apr 2022

Faridnia F, Burritt DJ, Bremer PJ, Oey I (2015) Innovative approach to determine the effect of pulsed electric fields on the microstructure of whole potato tubers: Use of cell viability, microscopic images and ionic leakage measurements. Food Res Int 77:556–564. doi: 10.1016/j.foodres.2015.08.028

Gancarz M (2016) Correlation between cell size and blackspot of potato tuber parenchyma tissue after storage. Postharvest Biol Technol 117:161–167. doi: 10.1016/j.postharvbio.2016.03.004

Haase NU (2003) Estimation of dry matter and starch concentration in potatoes by determination of under-water weight and near infrared spectroscopy. Potato Res 46:117–127. doi: 10.1007/BF02736081

Haase NU (2011) Prediction of potato processing quality by near infrared reflectance spectroscopy of ground raw tubers. J Near Infrared Spectrosc 19:37–45. doi: 10.1255/jnirs.919

Han M, Wang X, Xu Y, et al (2021) Variable selection for the determination of the soluble solid content of potatoes with surface impurities in the visible/near-infrared range. Biosyst Eng 209:170–179. doi: 10.1016/j.biosystemseng.2021.06.019

Helgerud T, Wold JP, Pedersen MB, et al (2015) Towards on-line prediction of dry matter content in whole unpeeled potatoes using near-infrared spectroscopy. Talanta 143:138–144. doi: 10.1016/j.talanta.2015.05.037

Heltoft P, Wold AB, Molteberg EL (2017) Maturity indicators for prediction of potato

(Solanum tuberosum L.) quality during storage. Postharvest Biol Technol 129:97–106. doi: 10.1016/j.postharvbio.2017.03.011

Henry RC, Park ES, Spiegelman CH (1999) Comparing a new algorithm with the classic methods for estimating the number of factors. Chemom Intell Lab Syst 48:91–97. doi: 10.1016/S0169-7439(99)00015-5

Iritani WM (1981) Growth and preharvest stress and processing quality of potatoes. Am Potato J 58:71–80. doi: 10.1007/BF02855381

López-Maestresalas A, Aernouts B, Van Beers R, et al (2016) Bulk Optical Properties of Potato Flesh in the 500–1900 nm Range. Food Bioprocess Technol 9:463–470. doi: 10.1007/s11947-015-1639-0

López A, Arazuri S, García I, et al (2013) A review of the application of near-infrared spectroscopy for the analysis of potatoes. J Agric Food Chem 61:5413–5424. doi: 10.1021/jf401292j

Moscetti R, Massantini R, Fidaleo M (2019) Application on-line NIR spectroscopy and other process analytical technology tools to the characterization of soy sauce desalting by electrodialysis. J Food Eng 263:243–252. doi: 10.1016/j.jfoodeng.2019.06.022

Nicolaï BM, Beullens K, Bobelyn E, et al (2007) Nondestructive measurement of fruit and vegetable quality by means of NIR spectroscopy: A review. Postharvest Biol Technol 46:99–118. doi: 10.1016/j.postharvbio.2007.06.024

Peiris KHS, Dull GG, Leffler RG, Kays SJ (1999) Spatial variability of soluble solids or dry-matter content within individual fruits, bulbs, or tubers: Implications for the development and use of NIR spectrometric techniques. HortScience 34:114–118. doi: 10.21273/hortsci.34.1.114

Pinhero RG, Yada RY (2016) Postharvest Storage of Potatoes. In: Singh J, Kaur L (eds) Advances in potato chemistry and technology, Second edi. pp 283–309

Pissard A, Marques EJN, Dardenne P, et al (2021) Evaluation of a handheld ultra-compact NIR spectrometer for rapid and non-destructive determination of apple fruit quality. Postharvest Biol Technol 172:. doi: 10.1016/j.postharvbio.2020.111375

Pritchard MK, Scanlon MG (1997) Mapping dry matter and sugars in potato tubers for prediction of whole tuber process quality. Can J Plant Sci 77:461–467. doi: 10.4141/P96-111

Riza DF Al, Suzuki T, Ogawa Y, Kondo N (2017) Diffuse reflectance characteristic of potato surface for external defects discrimination. Postharvest Biol Technol 133:12–19. doi: 10.1016/j.postharvbio.2017.07.006

Scanlon MG, Pritchard MK, Adam LR (1999) Quality evaluation of processing potatoes by near infrared reflectance. J Sci Food Agric 79:763–771. doi: 10.1002/(SICI)1097-0010(199904)79:5<763::AID-JSFA250>3.0.CO;2-O

Shiroma C, Rodriguez-Saona L (2009) Application of NIR and MIR spectroscopy in quality control of potato chips. J Food Compos Anal 22:596–605. doi: 10.1016/j.jfca.2008.09.003

Subedi PP, Walsh KB (2009) Assessment of potato dry matter concentration using short-wave near-infrared spectroscopy. Potato Res 52:67–77. doi: 10.1007/s11540-008-9122-1

Thybo AK, Andersen HJ, Karlsson AH, et al (2003) Low-field NMR relaxation and NMR-imaging as tools in differentiation between potato sample and determination of dry matter content in potatoes. LWT - Food Sci Technol 36:315–322. doi: 10.1016/S0023-6438(02)00210-4

United nations (2022) Sustainable Development Goals. https://sdgs.un.org/goals. Accessed 14 Apr 2022

USDA (2022) Food data central – Potatoes, flesh and skin, raw. https://fdc.nal.usda.gov/fdc-app.html#/food-details/170026/nutrients. Accessed 14 Apr 2022

Workman JJ, Weyer L (2012) Practical giude and spectral atlas for interpretive near-infrared spectroscopy, Second. New York

5.2 FURTHER STUDIES IN PROGRESS

Starting from the good results obtained using samples collected during season 2020 and described in previous section 5.1, the measurements were repeated on tubers collected in season 2021 slightly changing the acquisition procedure of NIR spectra. The results reported in this section refers to a study performed as a part of a master thesis.

INDEX

ABSTRACT

This study aimed to develop NIR-based predictive models for DM determination by acquiring spectra with two different spectrophotometers: a bench-top FT-NIR and a portable NIR instruments. Seven points of a central slice of potato tuber were selected to acquire spectra, each one representing one of the four tuber tissues (periderm, cortex, outer and inner medulla). Spectral data (X-matrix) were associated with DM values (Y-vector) obtained from oven method. Six datasets were obtained also combining data from different tissues, following a low-level data fusion method. Every possible combination of spectral preprocessing was tested in further chemometrics steps and only the best results, in terms of their predictive ability, were retained. PLS and iPLS algorithms were tested for developing DM predictive models. The models obtained scanning periderm tissue showed the worst prediction performances. Feature selection by the iPLS algorithm compared to PLS revealed a not-significant decrease in prediction ability. Moreover, the lower resolution as well as the reduced spectral range of the handled NIR instrument appeared to negatively influence the metrics.

The best two models obtained using the bench-top FT-NIR spectrophotometer reported the following metrics in prediction: RMSE equal to 1.076 and 1.333; R^2 equal to 0.809 and 0.819.

MATERIALS AND METHODS

Sample preparation

Potato (*Solanum tuberosum* L.) tubers were provided by the “Patata dell’Alto Viterbese" PGI consortia (C.C.OR.A.V. and Coop. Centro Agricolo Alto Viterbese, Viterbo, Italy). A total of 81 tubers from nine different cultivars were analyzed: i.e., Agata (7 tubers), Annalena (11 tubers), Ambra (11 tubers), Concordia (11 tubers), Constance (9 tubers), Fontane (9 tubers), Gaudi (8 tubers), Jelly (9 tubers), Levante (6 tubers). The potatoes were collected immediately after harvesting and stored at 4 ± 1 °C until analysis. The potato tubers were selected to be of uniform size, without damage, defects or blemishes. Samples were washed in tap water to remove soil and dirty, and tempered to room temperature for 16 h prior to spectral acquisition.

NIR spectral acquisition

The spectra of the potato tubers were acquired using both the mod. Antaris II Fourier-transform NIR (FT-NIR) spectrophotometer (Thermo Fisher Scientific, Madison, WI, USA) equipped with a sample-cup spinner and the portable NIR spectrophotometer mod. microPHAZIR™ RX Analyzer (Thermo Fisher Scientific, Madison, WI, USA). Instruments were warmed-up for at least 1 h prior to spectral acquisition. The spectra were acquired at room temperature (20 ± 1 °C). The Antaris II spectrophotometer allowed to acquire in the spectral range of 10000-4000 cm^{-1} (1000-2500 nm) with a 4 cm^{-1} scan resolution. Differently, the portable spectrophotometer mod. microPHAZIR™ RX Analyzer acquired spectra in the range of 6250-4170 cm^{-1} with a ~38 cm^{-1} scan resolution. The spectra were acquired in diffuse reflectance mode and directly converted to absorbance (abs). The scans were performed on four different types of tissues as classified by Faridnia et al. (2015) obtained by cutting the central slice as showed in Figure 5.7. Specifically, INT1 and INT2 corresponded to the periderm tissue (whole and unpeeled tuber); TA1 and TA5 corresponded to the cortex tissue (peeled tuber); TA2 and TA4 corresponded to the outer medulla (or outer parenchyma) tissue and TA3 corresponded to the inner medulla (or inner parenchyma) tissue. The spectrum of each sub-sample had an average of 32, for Antaris II, and 10 scans for microPHAZIR™ RX Analyzer (technical replications), with the internal instrument standard as reference.

Dry matter determination

Each scanned cube from the previous step was dried in an electric oven at 105 °C for 72 h. Dry matter (DM) was expressed as percentage by mass (grams per 100 grams).

Chemometrics

Spectral pre-treatments

Prior to chemometrics, the spectra were subjected to spectral pre-processing to reduce nonlinearities, scattering effects and noise. For the intended purpose, 441 and 345 combinations (for benchtop and portable NIR, respectively) of the pre-processing treatments listed in the Table 5.4 were tested using an ad-hoc Matlab script. The only combinations that improved the performance of the models were retained.

Model development

Within this study two extensively used algorithms, i.e., Partial Least Squares (PLS) and intervalPLS (iPLS), were applied. Six datasets were obtained also combining data from different internal tissues, following a low-level data fusion approach (Table 5.5). Prediction models were developed for each dataset using pre-processed spectra as X-matrix and dry matter content as Y-vector. PLS was used for prediction of the dry matter content based on linear combinations of independent variables. PLS models were computed by splitting data into calibration and prediction sets (60 and 40 % of samples, respectively) using the Kennard-Stone algorithm. Moreover, the prediction set was split into three subsets to allow statistical comparison of the prediction metrics obtained for each model. Subsequently, iPLS was tested to select subsets of features from the spectra to potentially improve the prediction results. The iPLS algorithm was set to stepwise-forward mode with a selection of a maximum of 10 waveband intervals of 10 features (wavelengths) each. Models were cross validated for the correct number of latent variables (LVs) to find the optimal trade-off between under-fitting and over-fitting. For the intended purpose, a venetian blinds cross-validation with 10 data splits was used. Model performances were evaluated in terms of Root Mean Square Error, BIAS and coefficient of determination (R^2) for calibration (RMSEC, BIASC and R^2C, respectively), cross-validation (RMSECV, BIASCV and R^2CV, respectively), and prediction (RMSEP, BIASP and R^2P).

Data handling and statistical analysis

Descriptive statistics for the distribution of DM content in potato tissues were computed. Further, statistical differences among predictive models in terms preformance metrics were evaluated one-way analysis of variance (ANOVA). Tukey's pairwise comparison method was performed, and the Honestly Significant Difference (HSD) was calculated for an appropriate level of interaction ($P \leq 0.05$). Data handling, descriptive statistics and ANOVA test were performed using R software 4.0.3 coupled with ‘Agricolae’ package v1.3-3. Chemometrics was performed using Matlab environment R2017b (Mathworks Inc., USA) coupled with PLS Toolbox software v8.6.2 (Eigenvector research Inc., USA).

RESULTS AND DISCUSSION

Dry matter content: trends in potato tissue

The results obtained in season 2021 confirmed that the external tissues of potato (i.e., periderm and cortex) had a DM content higher than internal tissues (i.e., outer and inner medulla). Specifically, the cortex tended to have a higher mean value than periderm. The medulla tissue was characterized by a lower DM content. In fact, internal tissues are more vascularized and then richer in moisture (Fig. 5.8).

Spectral features

As already reported in previous section 5.1, the heterogenous distrubution of dry matter content among potato tissue has an impact on NIR acquisitions. In fact, an effect of the scan area was observed on the NIR spectral profile obtained from both instruments.

Figure 5.9 shows the representative absorbance spectra for each type of potato tissue (periderm, cortex and parenchyma) averaged from the spectral data acquired using benchtop (a) and portable (b) NIR spectrophotometer. As can be observed, the spectra exhibited visually appreciable differences in the absorbance values but had similar spectral profiles for all tissues, except for the periderm.

Dry matter prediction model

The best twelve models obtained for both instruments were selected and compared computing ANOVA and post hoc Tukey’s test (data not shown). Both PLS and iPLS developed using spectra from periderm revealed unacceptable metrics (data not shown), not comparable with the metrics of other datasets. For this reason, the ANOVA test was performed not including the models of periderm, and the metrics were not considered in the discussion.

Without performing features selection, the best PLS model obtained by scanning the inner medulla reported a Root Mean Square Error in prediction (RMSEP) close to 1%. This result could be related to the most accurate acquisition procedure performed. However, in contrast with the results of previous season, features selection by the iPLS algorithm showed no positive effect on improving metrics. Further investigations will be necessary to understand the reason of these results. In general, the benchtop FT-NIR spectrophotometer performed better than the portable NIR instruments, probably due to its higher resolution and wider spectral acquisition range. Moreover, the performance metrics obtained for portable NIR showed no significant differences, highlighting an insignificant impact of potato tissue and algorithms on DM prediction. The RMSEP values of pre-selected models of the benchtop FT-NIR ranged from 1.076 to 1.527. Whereas, for portable NIR, RMSEP ranged from 1.522 to 1.970. Regarding the BIAS, identifying a tolerable error threshold of 0.5, the values were lower than this threshold in every pre-selected models, demonstrating a poor impact of systematic. Regarding the tissue, the RSMEP values of inner medulla (p_3) tending to be lower for both instruments, confirming the results obtained in the last season (2020). Specifically, the best results in terms of RMSEP was obtained for benchtop FT-NIR, reporting a RMSEP statistically lower than the other models (1.076). This model also showed a good robustness, reporting the lowest difference of RMSEP ratio (1.011) to the unit value. Comparing the best models obtained for both instruments, the p_3 model revealed a lower R^2 than the others, but without showing significant differences. Considering all above-mentioned metrics, p_3 PLS and p_All iPLS models of benchtop FT-NIR spectrophotometer were considered the best.

Figure 5.10 reports the scatterplots related to the best models for DM prediction obtained by acquiring spectra using the benchtop FT-NIR spectrophotometer: p_3 PLS (a) and p_All iPLS (b). Both plots show the good ability of the models to correctly estimate the dry matter values. The intersection point between the ideal regression line (green) and the PLS regression line (red) delineates two regions where the models tended to underestimate or overestimate DM content.

Figure 5.11 shows the selected features by iPLS algorithm for model p_All developed in the season 2021 (Fig. 5.11b) and for model developed using spectra of inner and outer medulla during season 2020 (Fig. 5.11a). The identification of specific bands is a crucial aspect for transferability of the models to portable handheld instruments. Comparing the wavebands selected, it’s notable that a spectral band from 8458 to 7690 cm^{-1} approximately, was selected in both studies. This peak is associated with water and starch which are the major components of potatoes. Specifically, in NIR range, many authors reported an important peak associated with water at 8333 cm^{-1}. Moreover, the 2nd overtone C-H stretch vibration around 8097 cm^{-1} of a specific CH_2 group in amylopectin, the branched glucan of starch, was reported.

CONCLUSIONS

During NIR 2019 conference (Gold Coast, Australia) various aspects were raised connected with the emerged new generation of near-infrared instrumentation, with many individuals expressing their point-of-view on the merits and pitfalls of the miniaturized spectrometers. The community remains concerned about the applicability of such devices. That concern reflects the still relatively shallowly explored miniaturization versus performance factor, which can only be dismissed by focused feasibility studies with comparative analyses carried out on scientific-grade benchtop spectrometers (Beć et al., 2020). In accordance with what was reiterated at this conference, this study compared the performance of a bench-top NIR spectrophotometer and a handled NIR spectrophotometer for predicting the dry matter content of potato tubers. The results achieved confirmed the effectiveness of NIR spectroscopy for potato DM prediction. However, further investigations are needed to understand the reasons for obtaining sub-optimal metrics from the portable NIR spectrophotometer, increasing the reliability of this technology. For this intended purpose, further studies should be carried out to i) make the model usable with additional cultivars and verify the effects of agricultural conditions on its robustness; ii) make the model usable for in situ measurements by robustness to product temperature variations; iii) test the use of deep chemometrics solutions like convolutional neural networks for improving prediction accuracy; iv) test the development of data-fusion-based models by combining NIR spectroscopy with other portable technologies with a history of success in predicting fruit and vegetables dry matter (e.g., bioimpedance); v) develop an end-user-friendly analysis protocol for in situ applications.

Parallel activity

In collaboration with the University of Bolzano, the combination of electrical impedance spectroscopy (EIS) and Near-Infrared Spectroscopy (NIRS) was tested.

Electrical Impedance Spectroscopy (EIS) has gained popularity as a reliable alternative to the classical non-destructive techniques. EIS quantitatively characterizes the interaction between the dielectric dipole moment of a sample under test and an externally applied electric field. In particular, the impedance value output of the EIS measurement is dependent on the frequency of the applied signal. The choice of the input frequency range is typically dependent on the structure and chemical composition of the studied sample, as the correlation of quality parameters with the measured impedance appears at specific frequencies for different types of materials. EIS techniques are applied for multiple applications, such as food products screening, solid materials properties characterization and human body analysis (Ibba et al., 2020).

The hypothesis behind this research activity is that the combination of the information resulting from an interaction at different frequency of the EM spectrum (i.e., EIS and NIRS) has the potential to give a better understanding, and thus modeling, of the potato quality. This will be achieved through novel data science approaches, spectral data fusion (i.e., the combination of sensor data at different levels) and deep learning algorithms (i.e., a branch of machine learning where brain-inspired neural networks automatically learn from large amounts of data), to produce more precise, consistent, and fast quality prediction models. Specifically, spectral data from nine potato cultivars provided by "Patata dell'Alto Viterbese PGI" were acquired using both EIS and NIRS. NIR acquisitions were performed through the portable spectrophotometer microPHAZIR™ RX Analyzer. Data analysis is ongoing in order to develop reliable predictive models for DM determination. Figure 5.12 shows an overview of EIS spectra acquired on nine potato cultivars.

Table 5.4

List of pre-treatments tested in combination.

Pre-treatments	Antaris II FT-NIR				microPHAZIR™ RX			
Normalization area = 1	absent		present		absent		present	
Multiplicative Scatter Correction (MSC)	absent		present		absent		present	
Standard Normal Variate (SNV)	absent		present		absent		present	
Derivative	*D0f*	*D1f*	*D2f*	*D3f*	*D0f*	*D1f*	*D2f*	*D3f*
Savitzky-Golay algorithm (2nd order polynomial)	0 15 17 19 21 23 25 27 29 31				0 3 5 7 9 11 13 15			
Data normalization	AS		MC		AS		MC	

AS: Autoscaling; MC: Mean Centering

Table 5.5

Data splitting into six different datasets using a low-level data fusion approach.

POTATO TISSUE	MODEL ID	TUBER SECTION ID						
		INT1	INT2	TA1	TA2	TA3	TA4	TA5
Skin	Periderm	✓	✓					
All internal tissue	pAll			✓	✓	✓	✓	✓
Inner medulla	p3					✓		
Cortex	p15			✓				✓
Whole medulla	p234				✓	✓	✓	
Cortex and Outer medulla	p1245			✓	✓		✓	✓

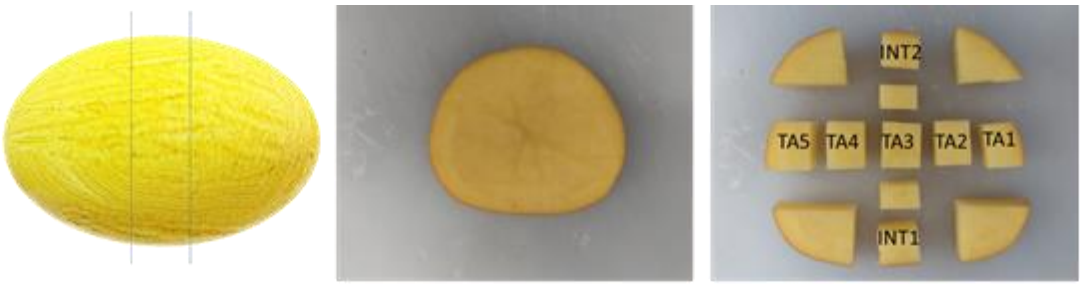

Figure 5.7

Tuber sectioning and spectral acquisition points.

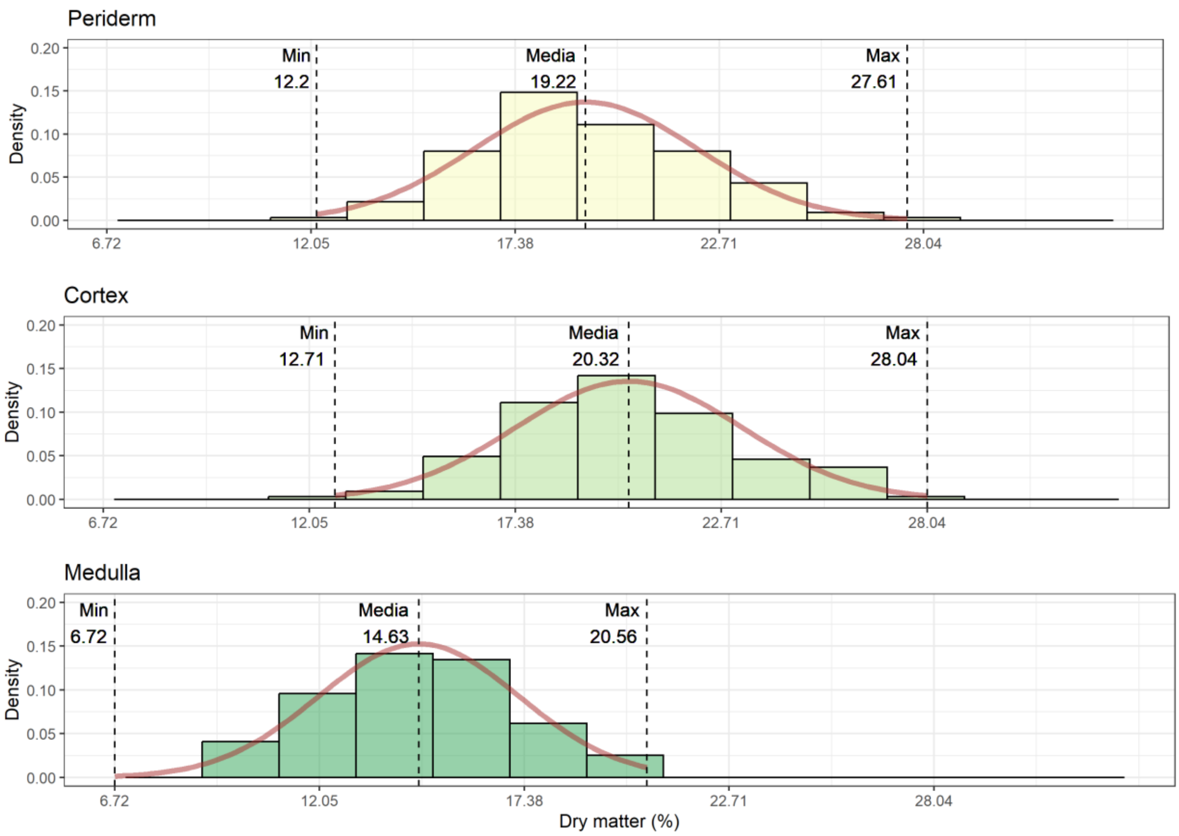

Figure 5.8

Descriptive statistics of the DM content of each potato tissue.

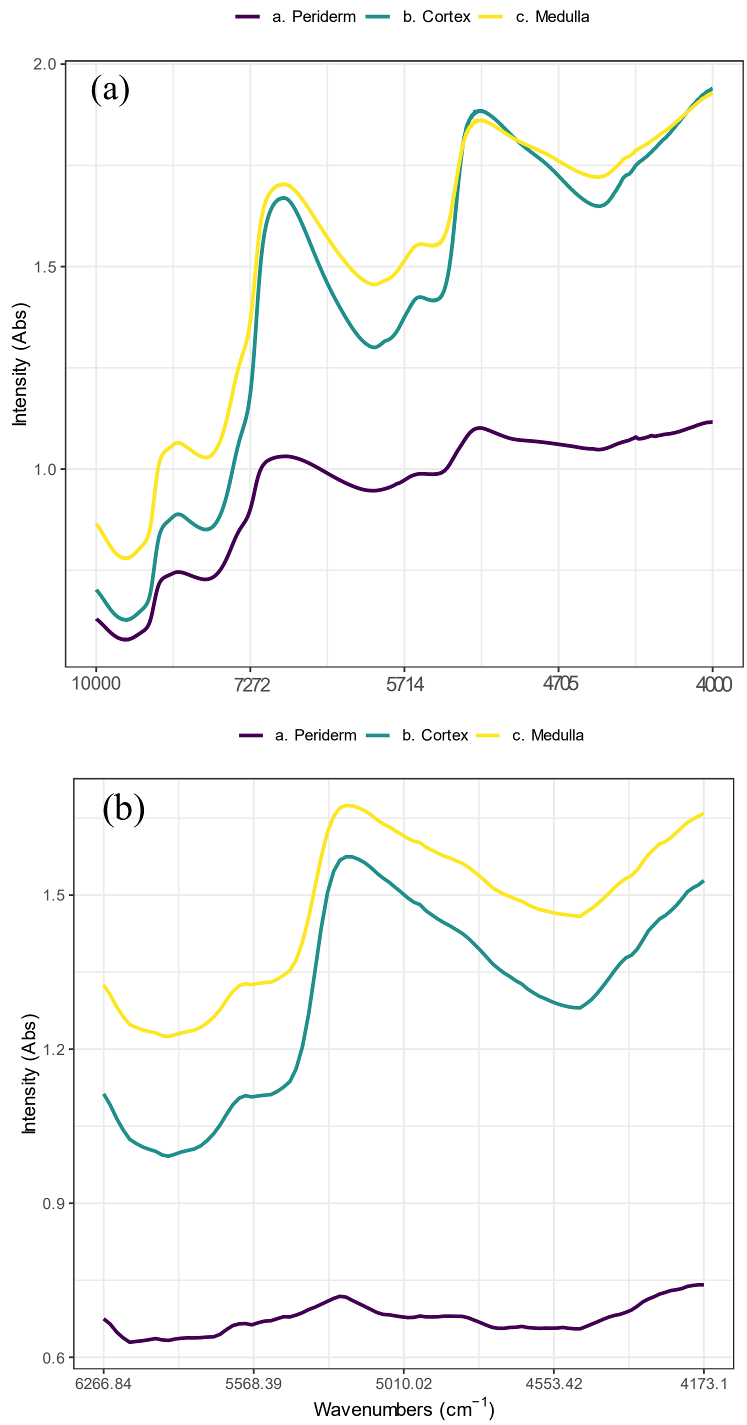

Figure 5.9

Representative mean absorbance spectra acquired on periderm (purple line), cortex (teal line) and parenchyma (yellow line) using benchtop FT-NIR (a) and portable (b) NIR spectrophotometer.

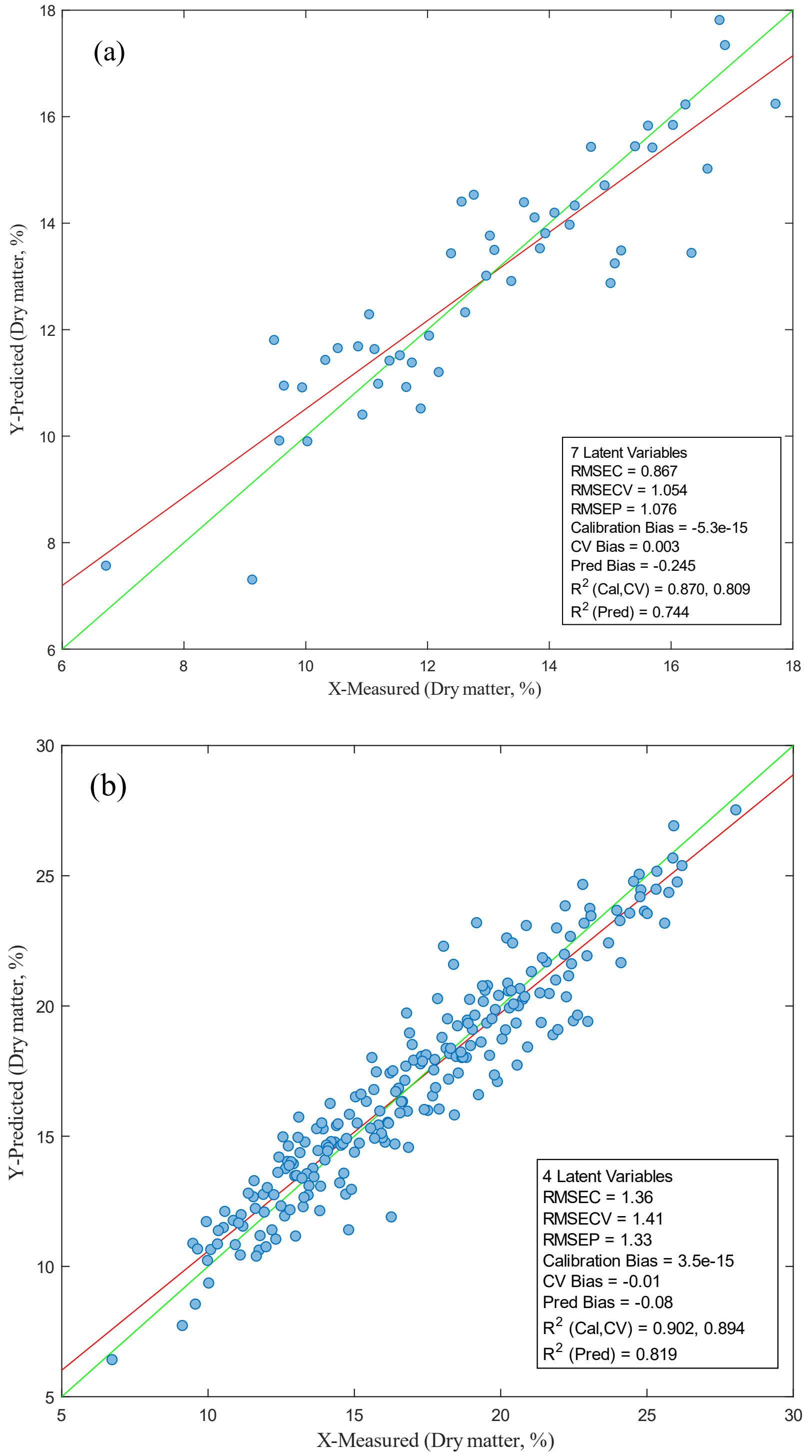

Figure 5.10

PLS (a) and iPLS (b) model for DM prediction through the scan of the inner medulla (p_3) and combining the dataset of internal tissue (p_All), respectively. The results refer to spectra acquired by using benchtop FT-NIR spectrophotometer.

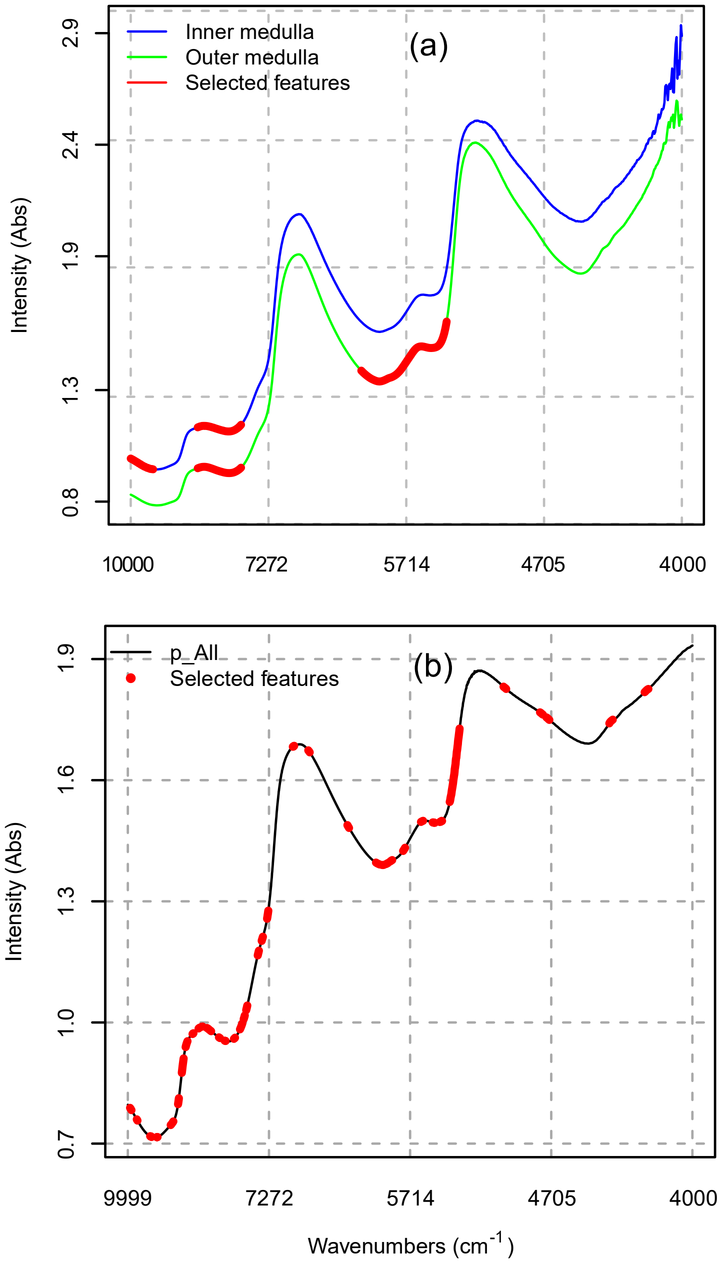

Figure 5.11

Mean spectrums (black line) with the features (wavebands) selected by the iPLS algorithms (red points/lines). The plot on the top (a) refers to the analysis during season 2020 computing the iPLS algorithm on the dataset of outer and inner medulla while the plot on the bottom (b) refers to analysis conducted along the season 2021 computing iPLS on dataset from all internal tissue (cortex, outer and inner medulla, p_All).

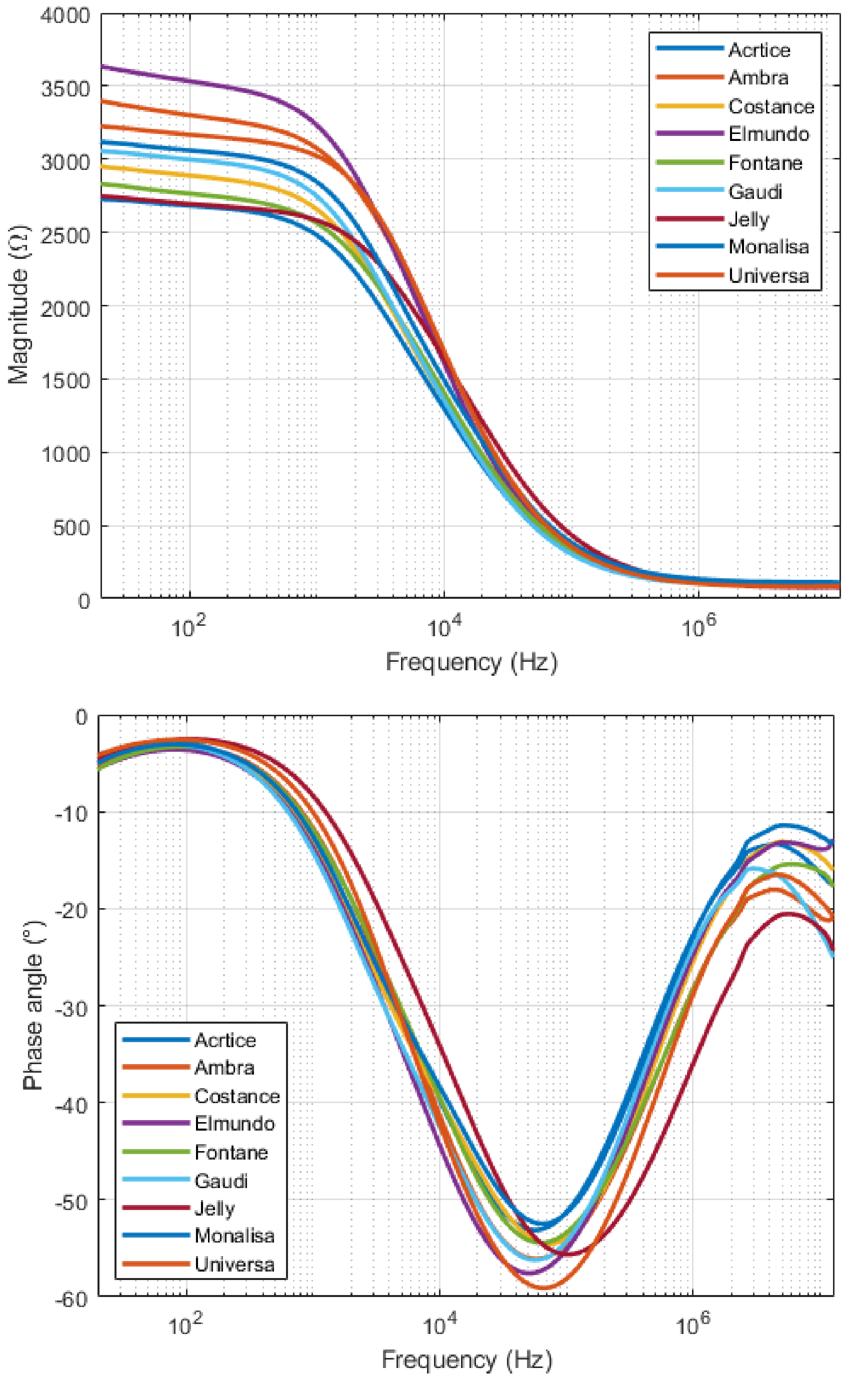

Figure 5.12

Overview of the training set of bioimpedance magnitude (a) and phase (b) spectra for all potato cultivars analyzed.

REFERENCES

Beć, K.B., Grabska, J., Siesler, H.W., Huck, C.W., 2020. Handheld near-infrared spectrometers: Where are we heading? NIR news 31, 28–35. https://doi.org/10.1177/0960336020916815

Ibba, P., Falco, A., Abera, B.D., Cantarella, G., Petti, L., Lugli, P., 2020. Bio-impedance and circuit parameters: An analysis for tracking fruit ripening. Postharvest Biol Technol 159. https://doi.org/10.1016/j.postharvbio.2019.110978

CHAPTER 6

CONCLUSIONS AND FUTURE PERSPECTIVES

The general objective of the thesis was to improve the competitiveness of the 'Patata dell'Alto Viterbese' PGI supply chain. Several research activities have been performed to solve some specific issues and criticalities and new emerging technologies have been proposed to help operators to make guided decisions.

The results of the experimentation highlighted the importance of cultivar characterization for the potato processing industry, but also for domestic culinary use. Each variety differs from the others in terms of physical-chemical and enzymatic composition and in terms of storability. A thorough knowledge of the quality characteristics of each cultivar grown and how these change during the storage is important to select suitable varieties for processing, planning production and sales.

In order to provide local consortiums with a tool to perform fast and *in-situ* analysis of quality parameters, the Near Infrared Spectroscopy was tested to develop an easily applicable method for dry matter determination. The results confirm the reliability of the NIR technology for the prediction of this quality attribute (RMSE ~ 1 % and R^2 ~ 0.9), but the results were strongly influenced by the potato tissue scanned and by the type of instrument employed. In fact, the portable spectrophotometer reported unsatisfactory results.

The other research activity was carried out to propose to the consortiums a semi-dried potato product obtained by an innovative drying method. Specifically, a computer vision (CV) system and load cells were successfully implemented inside a cabinet convective dryer for in-line monitoring of potato slices during the drying process. In addition, shrinkage-dependent models were evaluated to identify the best models including spatial data for predicting the residual moisture content of the product. The accuracy of these models (RMSE ~ 0.006) allows to continuously monitor the water loss of the product making possible to stop the drying process at the optimal time avoiding quality deterioration and reducing energy consumption.

Despite the promising results obtained, it is important to evaluate some limitations of the thesis work. For the first activity (i.e., cultivar characterization), the experimental design included the analysis of the main quality parameters of only 4 of the more than 15 potato cultivars grown in the 'Patata dell'Alto Viterbese' PGI area. For the smart semi-drying test, the data reported for potato slices represent the results of a preliminary study performed on one variety (i.e. Fontane) evaluating only two different shrinkage-dependent models. Regarding the third activity (i.e., development of NIR-based predictive models for dry matter determination), the number of samples acquired using NIR spectrophotometers is not sufficient to make the model usable for in situ measurements. Moreover, PLS and iPLS models should be compared with other commonly used algorithms or with novel emerging chemometrics algorithms.

Considering the results achieved and the thesis work limitations, the future perspectives concern:

i. The analysis of other important potato cultivars grown in the "Patata dell'Alto Viterbese" PGI area including analysis of other relevant parameters (e.g., phenol composition)
ii. Test the use of other linear/non-linear algorithms and Artificial Intelligence-based algorithms (like neural networks) to improve NIR model accuracy and to integrate the smart monitoring and control system (SMCS), predictive models and process automation;
iii. The assessment of some important quality parameters of dried potato slices such as shelf-life and oil uptake during frying.
iv. Test the application of data-fusion approach and deep chemometrics solutions on spectral data acquired combining NIR spectroscopy with the Electrical Impedance Spectroscopy

CHAPTER 7

OTHER SCIENTIFIC PUBLICATIONS

NALLAN CHAKRAVARTULA, S. S., BANDIERA A., NARDELLA M., **BEDINI G.**, IBBA P., MASSANTINI R., MOSCETTI R. (2023). Computer Vision-based Smart Monitoring and Control System for Food Drying: A Study on Carrot. Computers and Electronics in Agriculture. (Accepted)

NARDELLA M., MOSCETTI R., **BEDINI G.,** BANDIERA A., NALLAN CHAKRAVARTULA S. S., MASSANTINI R. (2023). Impact of traditional and innovative malaxation techniques and technologies on nutritional and sensory quality of virgin olive oil – A review. Food Chemistry Advances.

BANDIERA, A., **BEDINI, G.**, NALLAN CHAKRAVARTULA, S. S., MASSANTINI, R., MOSCETTI, R. (2022). Computer vision for the development of smart drying processes - Impiego della visione artificiale per lo sviluppo di processi di disidratazione smart. Industrie Alimentari, 61(633), pp. 22–29.

NALLAN CHAKRAVARTULA, S. S., MOSCETTI R., **BEDINI G.**, NARDELLA M., MASSANTINI R. (2022). Use of convolutional neural network (CNN) combined with FT-NIR spectroscopy to predict food adulteration: A case study on coffee. Food Control, Volume 135, 2022.

NARDELLA M., MOSCETTI R., NALLAN CHAKRAVARTULA S. S., **BEDINI G.**, MASSANTINI R. (2021). A review on high-power ultrasound-assisted extraction of olive oils: effect on oil yield, quality, and consumer perception. Foods, 10(11), 2743.

CIMINI, A., **BEDINI, G.**, & MORESI, M. (2021). Rough Beer Filterability in Industrial Powder-Filters and Lab-Scale Dead-End and Crossflow Filtration Apparatuses. Chemical Engineering Transactions, 87, 247-252.

MORALES-RODRIGUEZ, C., BASTIANELLI, G., CACCIA, R., **BEDINI, G.**, MASSANTINI, R., MOSCETTI, R., & VANNINI, A. (2021). Impact of brown rot caused by Gnomoniopsis castanea on chestnut fruits during the postharvest process: critical phases and proposed solutions. Journal of the Science of Food and Agriculture.

NALLAN CHAKRAVARTULA, S. S., MOSCETTI, R., FARINON, B., VINCIGUERRA, V., MERENDINO, N., **BEDINI, G.**, NERI L., PITTIA P., MASSANTINI, R. (2021). Stinging Nettles as Potential Food Additive: Effect of Drying Processes on Quality Characteristics of Leaf Powders. Foods, 10(6), 1152.

MOSCETTI, R., NALLAN CHAKRAVARTULA, S.S., BANDIERA, A., **BEDINI, G.**, MASSANTINI, R. (2020). Computer Vision Technology for Quality Monitoring in Smart Drying System. 2020 IEEE International Workshop on Metrology for Agriculture and Forestry, MetroAgriFor 2020 - Proceedings, 2020, pp. 134–138, 9277543

BEDINI G., NALLAN CHAKRAVARTULA. S.S., BASTIANELLI. G., CACCIA. R., CONTARINI. M., MORALES-RODRÍGUEZ. C., ROSSINI. L., SPERANZA. S., VANNINI. A., MOSCETTI. R., MASSANTINI. R. (2020). Feasibility of FT-NIR spectroscopy and Vis / NIR hyperspectral imaging for sorting unsound chestnuts, 27 pp. 3–18.